

Late Holocene Geomorphic Development of Coastal Barriers Around Lake Hamana and in Hamamatsu Strand Plain

佐藤, 善輝

<https://doi.org/10.15017/1398313>

出版情報：九州大学, 2013, 博士（理学）, 課程博士
バージョン：
権利関係：全文ファイル公表済



**Late Holocene Geomorphic Development of Coastal Barriers Around
Lake Hamana and in Hamamatsu Strand Plain**

完新世後期における浜名湖周辺および浜松平野における
砂州地形の地形発達過程

by

YOSHIKI SATO

Late Holocene Geomorphic Development of Coastal Barriers Around Lake Hamana and in Hamamatsu Strand Plain

YOSHIKI SATO

Abstract

This study discussed the geomorphological development of coastal sand barriers around the lake Hamana and western Hamamatsu strand plain during the middle to late Holocene. The Holocene geology of lake bed at the central part of the lake and the alluvial lowland were presumed by coring survey and previous studies. Chronologies of the core samples were determined by accelerator mass spectrometry (AMS) radiocarbon measurements and tephra layers. The lacustrine and sedimentary environments were reconstructed mainly by diatom fossil assemblages with molluscan fossils and depositional facies.

In order to reconstruct lacustrine environmental change of the Lake Hamana during the middle to late Holocene, diatom assemblages in a lake bed core (HMN08-7) were investigated. Six diatom zones were identified based on major species composition changes in the diatom assemblages. Diatom zones V and VI in the upper part of the core were subdivided into 3 sub-zones respectively. Stepwise development of the lacustrine environment in the Lake Hamana was suggested: Vigorous seawater inflow inferred by marine diatoms (Stage I, 4600-4700 cal BP); A closed inner bay environment with laminated sediments due to rapid formation of sand barriers (Stage II, 4500-4600 cal BP); A circulative brackish lacustrine environment by active mixture of riverine fresh water with enhanced inflow of seawater since 3500 cal BP (Stage III, 2650-4500 cal

BP); Gradual salinity decrease of the lake water by reduced seawater inflow (Stage IV, 2250-2650 cal BP); Lake water from brackish to fresh since 2250 cal BP with intermittent salinity increase in the middle of this period, water depth of the lake getting deeper (Stage V, 1498 AD-2250 cal BP); Re-development of an inner bay environment after the Meio earthquake in 1498 AD with temporal salinity increase during 1600 AD to 1750 AD (Stage VI, after 1498 AD).

Analyses on diatom assemblages of sediment cores taken from alluvial lowlands around the Lake Hamana, Rokkengawa Lowland, Higashi-Kandagawa Lowland, Miyakodagawa Lowland and Shinjo Lowland indicated stepwise environmental changes from a shallow marine (intertidal zone of a bay) to a fresh water ponds or marsh, which occurred during the middle to late Holocene. In particular, fresh water ponds and/or marshes were formed around 5000 cal BP and during 3200-3500 cal BP. During 3200-4500 cal BP, seawater flowed into the lowlands overlying the peaty deposits of fresh water marshes. In the Miyakodagawa Lowland, seawater inflow was expanded in ca. 6800 cal BP. With riverine inputs of sediments, fresh water marsh was formed in the central part of the lowland in ca. 3500 cal BP. Before formation of the fresh water marsh, episodic salinity increase was suggested by brackish to marine diatom species.

Well-developed six beach ridges (BR) are in the western Hamamatsu Strand Plain, called BR I to VI from landward to seaward. Diatom assemblages in sediment cores in the inter-ridge marshes were investigated. Timings of development of fresh water pond/marsh at the two inter-ridge marshes were estimated from radiocarbon ages and tephra layers and indicate that they occurred almost simultaneously. Tidal area changed to fresh water marsh/pond at ca. 3200 cal BP in two drowned lowlands and synchronous with those in the inter-ridge marshes. Formation of the fresh water pond at the inter-ridge marsh between BR III and IV and wide distribution of the BRs

suggests that emergence of the BR IV caused this environmental change. In addition, salinity presumably increased before ca. 3200 cal BP in both lowlands. Timings of fresh water pond/marsh formation of the inter-ridge marshes were at ca. 3200 cal BP based on radiocarbon ages and tephra chronologies. This suggests that emergence of the BR IV was occurred at ca. 3200 cal BP.

Paleo-geographical changes during the middle to late Holocene in the study area were reconstructed. After the Last Glacial Maximum, sea area expanded associated with relative sea-level rise (the Jomon Transgression). Because the BR I had not developed enough to prevent seawater inflow, inner bay in the incised valleys were formed around the lake. During 6500-5000 cal BP, fresh water pond and/or marshes started to form in the alluvial lowlands associated with the BR I development. However, repeated seawater inflow into the lowlands due to vulnerability of the BRs was suggested in this period. During 4500-5000 cal BP, BRs I, II and III were developed and emerged to form fresh water ponds/marshes in the alluvial lowlands and strongly closed inner bay in the lake. However, obstruction by the BRs became weaker after 4500 cal BP resulting in re-formation of brackish to marine water environment in the alluvial lowlands. In particular, active seawater inflow into the lake became vigorous since 3500 cal BP. After 3200 cal BP, fresh water pond and/or marshes formed in the alluvial lowlands around the lake and the western Hamamatsu Strand Plain, presumably associated with the BR IV emergence. Limited seawater inflow since 2650 cal BP led gradual salinity decline and stable fresh water environment formed after 2250 cal BP.

Geomorphologic development of coastal sand barriers around the Lake Hamana and in western Hamamatsu Strand Plain during the middle to late Holocene was generally categorized into two periods, one was transient period between ca. 6500 to ca. 3200 cal BP and the other was stable

period since ca. 3200 cal BP. Before 3200 cal BP, development process of sand barriers in the study area was characterized by temporal fresh water environment, related to co-seismic subsidence (i.e., abrupt relative sea-level rise). On the other hand, after 3200 cal BP, the developing process was characterized by stable fresh water environment. Assuming that the seismic activities have been constant throughout the late Holocene, trend shift of geomorphological developing processes at ca. 3200 cal BP was due to faster sedimentation to form BRs than that before. Fast enough sedimentation made the BRs less affected by co-seismic subsidence. Because most of sandy deposits composing BRs were supplied by the Tenryugawa River, enhanced sediment discharge by the Tenryugawa River may have been increased since 3200 cal BP. Such enhanced sediment discharge around 3200 cal BP was reported in the lower Yahagigawa Lowland, relating to the Yayoi Regression.

Table of Contents

Abstract	ii
Table of Contents	vi
List of Tables	xii
List of Figures	xiii
CHAPTER I Introduction	1
1-1. Holocene alluvial lowlands	
1-2. Coastal sand barriers	
1-3. purpose of this study	
CHAPTER II Methodology and Study Area	6
2-1. Methodology	
2-1-1. Observation of lowland and lake bed sediments	
2-1-2. ¹⁴ C dating	
2-1-3. Tephra chronology	
2-1-4. Diatom analysis	
2-2. Study area	
2-2-1. Geological and Geomorphological setting	
2-2-2. Tectonic setting	
2-3. Paleo-environmental change in the study area	

- 2-3-1. Lake bed sediments
 - 2-3-1-1. Sedimentological analysis
 - 2-3-1-2. Geochemical analysis
 - 2-3-1-3. Paleontological analysis
- 2-3-2. Coastal sand barriers
- 2-3-3. Alluvial lowlands

CHAPTER III Late Holocene changes in lacustrine environment of the Lake Hamana 20

3-1. Introduction

3-2. Material and methods

- 3-2-1. Core sample (HMN08-7 core)
- 3-2-2. Age model
- 3-2-3. Diatom analyses

3-3. Results of diatom fossil analysis

- 3-3-1. Zone I (Depth: 337-348 cm)
- 3-3-2. Zone II (Depth: 297-336 cm)
- 3-3-3. Zone III (Depth: 261-296 cm)
- 3-3-4. Zone IV (Depth: 222-260 cm)
- 3-3-5. Zone V (Depth: 111-221 cm)
- 3-3-6. Zone VI (Depth: 28-110 cm)

3-4. Transition of lacustrine environment inferred from diatom assemblages

- 3-4-1. Stage I (ca. 4600-4700 cal BP)

- 3-4-2. Stage II (ca. 4500-4600 cal BP)
- 3-4-3. Stage III (ca.2650-4500 cal BP)
- 3-4-4. Stage IV (ca.2250-2650 cal BP)
- 3-4-5. Stage V (1498 AD – ca. 2250 cal BP)
- 3-4-6. Stage VI (after 1498 AD)

CHAPTER IV Middle to late Holocene sedimentary environmental changes of alluvial

lowlands around the Lake Hamana

40

4-1. Introduction

4-2. Geological and Geomorphological backgrounds of the investigated alluvial lowlands

- 4-2-1. Rokkengawa Lowland
- 4-2-2. Higashi-Kandagawa Lowland
- 4-2-3. Miyakodagawa Lowland
- 4-2-4. Shinjo Lowland

4-3. Methods

4-4. Lowland deposits

- 4-4-1. Rokkengawa Lowland
- 4-4-2. Higashi-Kandagawa Lowland
- 4-4-3. Miyakodagawa Lowland
- 4-4-4. Shinjo Lowland

4-5. Result of diatom analysis

- 4-5-1. Rokkengawa Lowland

4-5-1-1. 0511-1 core

4-5-1-2. 0511-2 core

4-5-1-3. 0511-3 core

4-5-2. Higashi-Kandagawa Lowland

4-5-2-1. 0307-1 core

4-5-2-2. 0308-1 core

4-5-3. Miyakodagawa Lowland

4-5-3-1. 0429-1 core

4-5-4. Shinjo Lowland

4-5-4-1. 0512-1 core

4-6. The Middle to Late Holocene sedimentary environmental changes

4-6-1. Paleo-environmental changes of alluvial lowlands

4-6-1-1. Rokkengawa Lowland

4-6-1-2. Higashi-Kandagawa Lowland

4-6-1-3. Miyakodagawa Lowland

4-6-1-4. Shinjo Lowland

4-6-2. Synthesis of environmental changes of alluvial lowlands

CHAPTER V Late Holocene changes in sedimentary-environment of the inter-ridge

marshes in western Hamamatsu strand plain

95

5-1. Introduction

5-2. Methods

5-3. Geomorphological and Geological background of lowlands

5-3-1. Inter-ridges marsh between BRs I and II (Site A)

5-3-2. Inter-ridges marsh between BRs III and IV

5-4. Results of diatom analysis

5-4-1. Inter-ridge marsh between BRs I and II (Site A)

5-4-2. Inter-ridge marsh between BRs III and IV

5-4-2-1. Site B

5-4-2-2. Site C

5-5. Discussions

5-5-1. Environmental change in the inter-ridge marsh between BRs I and II

5-5-2. Environmental change in the inter-ridge marsh between BRs III and IV

5-5-3. Features of geomorphic development of the western Hamamatsu strand plain

CHAPTER VI Synthesis for geomorphic developments of coastal sand barriers around the Lake Hamana during the middle to late Holocene

116

6-1. Paleo-geographical changes around the Lake Hamana

6-1-1. Stage I (ca. 6500 cal BP)

6-1-2. Stage II (from ca. 5000 to ca. 6500 cal BP)

6-1-3. Stage III (from ca. 4500 to ca. 5000 cal BP)

6-1-4. Stage IV (from ca. 4500 to ca. 3200 cal BP)

6-1-5. Stage V (since 3200 cal BP)

6-2. Geomorphic development trends of the Holocene coastal sand barriers

6-2-1. General trends of geomorphic development trend in ca. 3200 cal BP

6-2-2. Trigger of short-term seawater intrusion

6-2-3. Controlling factors for geomorphic developing trends shift in ca. 3200 cal BP

Reference 131

Acknowledgement 146

List of Tables

Table 3-1. AMS radiocarbon ages from the HMN08-7 core were calibrated with CALIB 6.0 (Stuiver *et al.*, 2004) using dataset of IntCal09.14c (Reimer *et al.*, 2009) and Marine09.13c (Reimer *et al.*, 2009). Location map of the core site and geological columnar are shown Fig. 3-1 and Fig. 3-2 respectively.

Table 4-1. AMS radiocarbon ages from study area are calibrated with CALIB 6.0 (Stuiver *et al.*, 2004) using dataset of IntCal09.14c (Reimer *et al.*, 2009) and Marine09.13c (Reimer *et al.*, 2009). Location map of the core sites are shown Fig. 4-1 to Fig. 4-4.

List of Figures

Fig. 2-1. Location and geomorphological classification map of the study area. 2-1A: Location map of the Lake Hamana. 2-1B: geomorphological classification map around the study area based on the observation of aerial photos on a scale of 1/10,000 taken by Geospatial Information Authority of Japan (GSI) in 1962. Bathymetric data is based on the topography map described in 2007 by the GSI. The urban area was changed artificially too much associated with civilization of Hamamatsu city to identify original topography. Locations of the lake bed core analyzed by previous studies (Ikeya *et al.*, 1990; Morita *et al.*, 1998) are described. R, Hk, M and S letters represent investigated alluvial lowlands in the present study, R: Rokkengawa; Hk: Higashi-Kandagawa; M: Miyakodagawa; S: Shinjo Lowlands.

Fig. 2-2. Environmental changes around the Lake Hamana during the Holocene were suggested by previous studies. Depositional facies of the lake bed cores was reported by Ohtsuka and Kimiya (1987). Geochemical analyses (C/N ratio) were performed by Nakai *et al.* (1987). Paleontological analyses were conducted by Kojima (1989), Kashima (1988), Matsubara (1989) and Morita *et al.* (1998). The geomorphic developments of the coastal beach ridges along the Enshu-nada Coast were discussed by Matsubara (2000, 2004 and 2007). Eruption ages of Kg and Os tephra rely on Machida and Arai (2003). According to the historical information, the Meio earthquake (EQ) occurred at 1498 AD.

Fig. 3-1. Location map of the HMN08-7 core, a lake bed core drilled in 2008 by Project Pref. Okamura of Kochi Univ. 3-1A: Location map of the Lake Hamana. 3-1B: Location map

of the HMN08-7 core. Bathymetric map of the Lake Hamana indicates that the core site is located at approximately 1.6km north from the sloop and has about 10 m depth beneath the lake water surface.

Fig. 3-2. Geological columnar and sedimentation curve of the HMN08-7 core. The sedimentation curve estimated from radiocarbon ages and tephra layers assumed that sedimentation rates are constant between each age controlling points. The detail information of AMS radiocarbon ages are shown in Table 3-1. Eruption ages of Kg and Os tephra rely on Machida and Arai (2003).

Fig. 3-3. The diatom assemblage diagram of the HMN08-7 core. The legend of geology is same as that of Fig. 3-2. Diagram of diatom assemblage with exaggeration factor of 3x for lesser taxa.

Fig. 4-1. Location map of the investigated lowlands around the Lake Hamana. 4-1A: location map of the Lake Hamana. 4-1B: Geomorphological classification map and location map of alluvial lowlands.

Fig. 4-2. Location map of coring sites and geological section (A-A' section) in the Rokkengawa Lowland. Black circles represent location of coring sites.

Fig. 4-3. Location map of coring sites and geological section (B-B' section) in the Higashi-Kandagawa Lowland. Black circles represent location of coring sites.

Fig. 4-4. Location map of coring sites and geological sections (C-C', D-D' and E-E' section) in the Miyakodagawa Lowland. Abandoned channel of Miyakodagawa River are distributed around the middle part of the lowland. Black colored squares show location of

archeological remains on natural levees, and black circles represent location of coring site and drilling site.

Fig. 4-5. Location map of coring sites and geological section (E-E' section) in the Shinjo Lowland.

Black colored circles show location of core sites.

Fig. 4-6. Geological section (A-A' section) in the longitudinal direction in the Rokkengawa Lowland. Location of section and coring sites are shown in Fig. 4-2. Information of radiocarbon ages in this figure are shown in Table 4-1.

Fig. 4-7. Geological columnar section (B-B' section) in the longitudinal direction in the Higashi-Kandagawa Lowland. Location of section and coring sites are shown in Fig. 4-3. Information of radiocarbon ages in this figure are shown in Table 4-1.

Fig. 4-8. Content ratio of volcanic glass about the 0307-1 core in the Higashi-Kandagawa Lowland. A Concentrated layer of glass was recognized between -1.91 to -1.93 m T. P. Refractive index and a radiocarbon age taken at the same horizon of the core indicates Kg tephra.

Fig. 4-9. Geological sections (C-C', D-D' and E-E' section) at the Miyakodagawa Lowland. Location of section and coring sites are shown in Fig. 4-4. Information of radiocarbon ages shown in this figure are described in Table 4-1. Classification of the lowland deposit was represented as follow letters, SG: Sand Gravel layer; LSM: Lower sandy mud layer; MM: Middle mud layer; US: Upper sand layer; TS: Top sand layer; TM: Top mud layer; Peat: Peat layer.

Fig. 4-10. Geological section (F-F' section) in the longitudinal direction in the Shinjo Lowland. Location of section and coring sites are shown in Fig. 4-4. Information of radiocarbon ages shown in this figure are described in Table 4-1.

- Fig. 4-11. Diatom assemblage diagram of 0511-1 core taken from the central part of the Rokkengawa Lowland. Location of the core is shown in Fig. 4-2.
- Fig. 4-12. Diatom assemblage diagram of 0511-2 core taken from the central part of the Rokkengawa Lowland. Location of the core is shown in Fig. 4-2.
- Fig. 4-13. Diatom assemblage diagram of 0511-3 core taken from the central part of the Rokkengawa Lowland. Location of the core is shown in Fig. 4-2.
- Fig. 4-14. Diatom assemblage diagram of 0307-1 core taken from the central part of the Higashi-Kandagawa Lowland. Location of the core is shown in Fig. 4-3.
- Fig. 4-15. Diatom assemblage diagram of 0308-1 core taken from the central part of the Higashi-Kandagawa Lowland. Location of the core is shown in Fig. 4-3.
- Fig. 4-16. Diatom assemblage diagram of 0429-3 core taken from the Miyakodagawa Lowland. Location of the core is shown in Fig. 4-4.
- Fig. 4-17. Diatom assemblage diagram of 0512-1 core taken from the central part of the Shinjo Lowland. Location of the core is shown in Fig. 4-5.
- Fig. 4-18. The middle to late Holocene environmental transition of alluvial lowlands around the Lake Hamana based on the results of diatom analyses.
- Fig. 5-1. Geological classification map of the western Hamamatsu Strand Plain and location map of the investigated site and sections. An outcrop site (Site A) of the Holocene lowland deposits was observed by Sato *et al.* (2013) at inter-ridge marsh between BR I and II (IRM I/II). Along two sections, A-A' and B-B' section, in inter-ridge marsh between BR III and IV (IRM III/IV), geological survey was performed by Fujiwara and Sato (2012) and Sato *et al.* (2013).

Fig.5-2. Geological columnar and diatom assemblages diagram of Site A, in the inter-ridge marsh between the BR I and II. Location of site A is shown in Fig.5-1. The radiocarbon ages is based on Sato *et al.* (2013).

Fig. 5-3. Geological columnar sections along the A-A' and B-B' section in the inter-ridge marsh between BR III and IV. These are a part of sections reported by Fujiwara and Sato (2012) and Sato *et al.* (2013). Location of sections is described in Fig. 5-1.

Fig. 5-4. Diatom assemblage diagram of the Site B in the inter-ridge marsh between BR III and IV.

Fig. 5-5. Diatom assemblage diagram of the Site C in the inter-ridge marsh between BR III and IV.

Fig. 6-1. Summary of the reconstructed middle to late Holocene environmental change around the Lake Hamana in the present study. Paleo-environmental changes in the central part of the lake based on results of diatom analysis of the lake bed core (HMT08-7) were shown in the chapter III. Environmental change in the alluvial lowlands are described in the chapter IV and V. Eruption ages of the Kg and Os tephra are based on Machida and Arai (2003). The relative sea level curves around the Ise Bay and the lower Yahagigawa Lowland are referred from Umitsu (1992) and Sato and Masuda (2010) respectively.

Fig.6-2. Paleo-geographic map around the Lake Hamana were reconstructed at total five stages since ca. 6500cal BP based on paleo-environmental changes in the central part of the lake and the alluvial lowlands. A: ca. 6500 cal BP, B: ca. 5000 to ca. 6500 cal BP, C: ca. 4600 to ca. 5000 cal BP, D: ca. 4500 to ca. 3200 cal BP, E: since 3200 cal BP.

Fig. 6-3. The middle to late Holocene coastal sand barriers evolution processes around the Lake Hamana. A: From ca. 6500 to ca. 3200 cal BP; B: since ca. 3200 cal BP.

CHAPTER I

Introduction

1-1. Holocene alluvial lowlands

Coastal alluvial lowlands are one of typical geomorphology distributed along the coastal area in Japan, e.g. Nobi Plain, Kawachi Plain, Nakagawa and Tokyo Lowlands and so on (Iseki 1983, Umitsu 1994). Much of infrastructures and population are distributed on these lowlands. Therefore, understanding of the relationships between natural factors and landform development and deformation is important for disaster mitigation and provision for environmental change in the future.

Alluvial lowlands are defined as the new coastal landform generated by river, wave and/or tidal power after the Last Glacial Maximum (LGM), ca. 20 ka (Umitsu 1994). The alluvial sediments consist of them have filled up “the coastal prism” created by incised rivers ran into the sea during the LGM (Sugai 2012). Abrupt sea-level rising after the LGM, called “the Jomon Transgression”, caused submergence of incised valleys and expansion of sea-area such as inner bay, outer bay and estuary. Since then, sediments have buried whole or part of these sea areas and resulted in formation of alluvial lowlands.

The development of landforms on alluvial lowlands can be changed by environmental changes during the Holocene, e.g. relative sea-level, amount of sediment supply, precipitation and temperature. The relative sea-level curves at many alluvial lowlands in Japanese islands have been reconstructed after the maximum period of the Jomon Transgression around 7 ka (Ota *et al.*, 1990). For example, Ono (2006) showed that depositional amount, area and processes changed by relative

sea-level falling during the Yayoi period (ca.2-3 ka) in the Nobi and Echigo plains. Kawase (1998) and Kawase (2003) also suggested that riverine deltaic evolution had been stimulated during the Yayoi period by active deposition of riverine sediments around the Ise Bay. Yamaguchi *et al.* (2003) indicated regression process in the Nobi Plain (Kiso River delta) showed millennial scale changes based on detail core analyses. Urabe *et al.* (2006) and Ono *et al.* (2006) indicated that transgression and regression processes associated with relative sea-level changes occurred repeatedly at least three times in the Echigo Plain during the Holocene.

Geomorphological development of alluvial lowlands can be reflected Holocene climatic and environmental changes. Therefore, alluvial lowlands are excellent archives recording paleo-environmental changes at centennial to millennial scales (Bond *et al.*, 2001; Mayewski *et al.*, 2004) and local tectonic events.

1-2. Coastal sand barriers

When wave current exceeds riverine or tidal power, coastal sand barriers are well-developed in coastal areas (Matsubara, 1989, 2000; Saito, 2007). Coastal sand barriers are arranged parallel with the coast and consisted of sandy deposit supplied by wave current. Some alluvial lowlands have a number of series of sand barriers called coastal beach ridges (BR). Inner-ridge marshes composed of muddy and/or peaty deposits are distributed between BRs. Also, in some of coastal strand plain, aeolian sand dunes overlies fluvial sandy deposits. Mii (1966) classified roughly Japanese coastal sand barriers into three types according to their geological structure, i. e. Tsugaru type: sand barriers covers marine terrace formed as ancient bar and lagoon

during the Last Interglacial Period (ca. 125ka); Akita type: sand barriers covers ancient barriers formed since the Last Interglacial Period; Kanazawa type: sand barriers are formed during the Holocene and covers no ancient barriers or terraces.

Coastal sand barrier is one of the most important landforms for the Holocene environmental changes, because it is an indicator of the paleo-shorelines in the past (Tamura 2012). Geomorphic developments of coastal sand barrier has been investigated in many alluvial lowlands in Japan (Matsubara 1989; Matsubara 2000). Coastal sand barriers can be classified into two broad types by their developing processes, i. e., the Primary barriers and the Secondary barriers (Matsubara 1989; Matsubara 2000). The Primary barriers had been formed at transgressive stage during the middle Holocene (the Jomon Transgression) due to accumulation of sandy deposits associated with relative sea-level rise. On the other hand, the Secondary barriers developed in regressive stage after the Jomon Transgression, characterized by gradual accretion of barriers to seaward.

Numbers of radiocarbon ages and sedimentary analyses of core sediments showed detailed environmental changes in Kujukuri Strand Plain, Boso Peninsula and Sendai Plain, northeastern Japan (Masuda *et al.*, 2001; Tamura and Masuda, 2004). Masuda *et al.* (2001) reconstructed relative sea-level curve in the Kujukuri Strand Plain and discussed co-seismic uplifts after the middle Holocene. Tamura and Masuda (2004) showed regional difference of evolutionary process of coastal sand barriers affected by tectonic, geological and geomorphological background of each plain. In the Boso Peninsula, emergence of sand barriers associated with co-seismic uplifting generated by historical earthquakes have been clarified by Shishikura *et al.* (2001, 2005) and Fujiwara *et al.* (2006a). In addition, Optically Stimulated Luminescence (OSL) dating method

and analyses of satellite images allow us to discuss decadal to centennial evolution of barriers (Goy *et al.*, 2003).

Discussions on geomorphic development of coastal sand barriers in previous studies were based on “simple model”, which assumes sequential accretion of barriers. The simple model does not take into account for relative sea-level change after the accretion of barriers. In Japan islands, local tectonic activities are able to make high amplitude of relative sea-level curves. In the previous studies, timings of the beginning of formation of sand barriers were determined by radiocarbon datings taken at the bottom of muddy or peaty sediments in inner-ridge marshes and drowned lowlands (e. g. Matsumoto, 1984; Ohira 1995; Ito, 2003; Ito, 2006; Matsubara, 2007). These studies did not consider sedimentary environmental changes. However, sedimentation processes in inner-ridge marshes and drowned lowlands may have affected by local tectonic events. In this case, discussions on geomorphic development of coastal sand barriers by the simple model have chronological mislead.

In order to resolve this problem, it is important to reconstruct for detail sedimentary environmental changes in drowned lowlands, inter-ridge marshes and lakes closed by coastal sand barriers. It is important for accomplishment of reconstructions of environmental transition of them to conduct successive analyses about paleo-environment and construct accurate age models. For successive analyses, paleontological indicators of microfossils are useful due to their abundance and various habitats. Also, to establish accurate age models of sediments using radiocarbon datings and tephra chronologies are the key for reconstructing detailed sedimentary environmental changes.

1-3. Purpose of this study

The purpose of this thesis is to reconstruct geomorphic development of coastal sand barriers in the Lake Hamana and alluvial lowlands around the lake during the middle to late Holocene. Considering relative sea-level change, climate change and tectonic deformation, the author detected a series of sedimentary environmental changes in alluvial lowlands and lake sheltered by sand barriers at centennial time scale.

The study area is the Lake Hamana and alluvial lowlands around it. The Lake Hamana is a brackish lake located in Enshu-nada Coast, Shizuoka Prefecture, central Japan. In the southern part of the Lake Hamana, total of six coastal sand barriers are well-developed and close the mouth of the lake (Matsubara 2001; Matsubara, 2007). Previous studies such as Ikeya *et al.* (1990) discussed paleo-environmental change around the Lake Hamana employing lake bed sediments. However, paleo-environmental studies focusing on lacustrine and sedimentary environmental changes in and around the Lake Hamana are limited. In addition, development process of beach ridges distributed in the southeastern coast of the lake has not been clarified yet.

The author performs investigation and analyses in the following three regions in and around the Lake Hamana. Firstly, diatom fossil assemblages in a lake bed core were analyzed to clarify transition of lacustrine environment during middle to late Holocene. Secondly, coring surveys and diatom analyses were carried out in four alluvial lowlands where in landward from the sand barriers. Thirdly, sedimentary investigation and diatom analyses were performed in inter-ridge marshes between beach ridges in the western Hamamatsu Strand Plain. Finally, the author synthesizes paleo-geographical changes in the study area and discusses geomorphological development processes of coastal sand barriers in the middle to late Holocene.

CHAPTER II

Methodology and Study Area

2-1. Methodology

Reconstruction of sedimentary environment around the Lake Hamana was based on analyses about the depositional facies and diatom fossil assemblages with radiocarbon ages and tephra chronology.

2-1-1. Observation of lowland and lake bed sediments

Sediment samples used in this study were taken from the lake bed and alluvial lowlands around the Lake Hamana (Fig.2-1). Total of six alluvial lowlands around the lake were selected for investigation, Rokkengawa Lowland, Higashi-Kandagawa Lowland, Miyakodagawa Lowland, Shinjo Lowland and two inter-ridge marshes along the Enshu-nada Coast (Fig.2-1).

The lake bed core is bored by Prof. Okamura of Kochi University in September 28th, 2008 at the central part of the lake (Okamura *et al.*, 2009; Matsuoka, personal communication). Observation and description of geology and depositional facies were conducted in the laboratory of Kochi University by the author.

On the other hand, Holocene sediments of alluvial lowlands were taken by array boring with handy corer and handy geoslicer and exposed at outcrops. Observation and description of geology and depositional facies were conducted in fields and the laboratory of Kyushu University. Surface geology of each lowland already have been reported as below, Rokkengawa Lowland by Sato *et al.* (2010a), Sato *et al.* (2011) and Fujiwara *et al.* (2013); Higashi-Kandagawa Lowland by

Sato and Kashima (2012); Shinjo Lowland by Sato *et al.* (2010b) and Sato *et al.* (2011); western Hamamatsu Strand Plain by Fujiwara and Sato (2012) and Sato *et al.* (2013).

2-1-2. ¹⁴C dating

Radiocarbon ages were measured by AMS method in Paleo Lab *Co. Ltd.*, IAA *Co. Ltd.*, Geo-Science Laboratory *Co. Ltd.* and Center for Chronological Research, Nagoya University. Calibration of all radiocarbon ages were estimated by using CALIB6.0 (Stuiver *et al.*, 2004). Datasets for calibration were IntCal09.14c (Reimer *et al.*, 2009) for continental samples and Marine09.14c (Reimer *et al.*, 2009) for marine samples respectively.

On the calibration of marine samples, it is necessary to conduct correction for the local marine reservoir effect. However, the ΔR value for this correction around the Lake Hamana has not been clarified yet. Along the Pacific Coast of the Japanese Island, ΔR values have been reported 82 ± 33 yr and 77 ± 32 yr from the Miura Peninsula (Shishikura *et al.*, 2007), 73 ± 17 yr in the Taiwan Island, 29 ± 18 yr in the Ryukyu Islands and -22 ± 18 yr in the Ogasawara Islands (Yoneda *et al.*, 2007). These ΔR values, obtained in regions belonging to the Kuroshio Current system, are much smaller than those of the Sakhalin Island and eastern Hokkaido Island belonging to the Oyashio Current system, i. e., 392-399 yr (Yoneda *et al.*, 2007). Because the study area belongs to the Kuroshio Current system, the ΔR value around the Lake Hamana is probably near zero. Therefore, the author conducted calibration of marine samples assuming that the ΔR value was zero.

2-1-3. Tephra chronology

Tephra layers, such as volcanic ashes and scoria, are useful for determining

sedimentation ages (Machida and Arai 2003). If tephra layers are not able to be found with visual observation, measuring content ratio of volcanic ashes among core samples were carried out for check of them. In addition, refractive indices of volcanic ashes at the peak of content ratio were measured. Identification of tephra was presumed by refractive indices, volcanic glasses morphology, stratigraphy and radiocarbon ages above/beneath them.

Measurement of content ratios of volcanic ashes was conducted in the following means. Subsamples for analysis were taken from core sediments in 2 cm intervals with approximately 1-2 g weight. After water washing and ultrasonic cleaning of them, sediment grains were sieved into $>1/8$ mm and $1/8 - 1/16$ mm groups with 120 and 250 mesh cloth shirts. The dried subsamples with $1/8$ to $1/16$ mm grain size were mounted on slides with Photocuring Adhesive ($n_d=1.54$, produced by the Nichika *Co. Ltd.*). Total of more than 300 particles of grains were identified and counted under a polarization microscope at $400\times$ magnification with respect of each mineral. In addition, refractive index of mine heavy minerals and volcanic ashes taken from the abundance peak of them were measured by the Measuring Actual Immersion Oil Temperature method (MAIOT; Furusawa 1995) by the FURUSAWA geological survey *Co. Ltd.*

2-1-4. Diatom analysis

Diatom fossil assemblages are used as indicator for paleo-environment in the Lake and lowlands. Diatoms are one of the most common phytoplankton and classified to Eukaryota, Chromalveolata, Heterokontophyta, Bacillariophyceae. Diatom species lives in various environments from marine to fresh water. Diatom fossil assemblages have following two biological and morphological advantages for reconstruction of paleo-environmental changes. Firstly, diatoms

can live various environments in condition that they can get sunlight and water. Diatom assemblages are quite different depending on their habitats such as pH, salinity, current velocity, degree of pollution, water temperature, bottom materials and so on. Variable distribution of diatom assemblage suggests that diatoms can be indicator for estimate sedimentary environment from sea to land. Secondly, Diatoms have a set of silicate valves so that strong against chemical weathering and physical wreck. This obdurability enables to analyze statistically with a small amount (~1 mg) of samples and to conduct high resolution analyses for detail reconstruction of paleo-environment. Diatoms have two valves with innate geometric pattern each species. We can identify them according to their patterns using optical microscope of $\times 1000$ magnification.

Diatom analyses were carried out according to the method shown by Kosugi (1993) and Ishikawa *et al.* (2011). Subsamples of each sediment for analyses were taken from the cores and the outcrop. Subsamples were transferred into centrifuge tubes with around 5% H_2O_2 solution and kept in water at 40-50 degrees Celsius for more than three hours. After the acid treatments, the concentration of the solutions of treated subsamples was adjusted for counting of diatom fossils. And then the solutions were placed them with distilled water on glass slides. After drying, the suspension was mounted using Mount media (Wako Pure Chemical Industries *Ltd.*, Japan). At least 300 individuals or identifiable parts were counted under an optical microscope at $1000\times$ magnification. Diatom identification and nomenclatures were based on Hustedt (1930a, 1930b, 1959, 1961-1966), Krammer and Lange-Bertalot (1986, 1988, 1991a, 1991b), Watanabe (2005) and Kobayashi (2006). The habitats of diatom species were based on Kashima (1986), Kosugi (1988), and Ando (1990).

2-2. Study area

2-2-1. Geological and Geomorphological setting

The geomorphological classification map around the study area according to observation of aerial photos on a scale of 1/10,000 taken by the GSI in 1962 is shown in Fig.2-1.

At the northern to northwestern coast of the Lake Hamana, mountains and hills are distributed. They consist mainly of the Mesozoic chert belonging to the Chichibu belt (Isomi and Inoue, 1972; Sugiyama, 1991). The well-developing middle to late Peistocene terraces are distributed in the eastern and western coastal area around the lake (Isomi and Inoue, 1972; Sugiyama, 1991; Koike and Machida 2000; Nakajima *et al.* 2008). The Tenpakubara terrace is distributed from the western coast of the Lake Hamana to the Atsumi Peninsula and consists of the Atsumi Group. The Atsumi Group shows cyclic depositional facies associated with glacio-eustatic sea-level change (Hiroki and Kimiya, 1990; Nakajima *et al.* 2008). According to Nakajima *et al.* (2008), the Atsumi Group developed during the Marine Isotope Stage (MIS) 9 to 11 inferred from the tephrostratigraphy. On the other hand, in the eastern side of the Lake Hamana, the Kamoe terrace and the Mikatagahara terrace are distributed. The Kamoe terrace is found only in the southern margin of the Mikatagahara terrace and consists of three fining-upward sedimentary cycles and an overlying deltaic fan gravel bed deposited at the regressive stage after MIS 7c (Sugiyama, 1991). The Mikatagahara terrace shows wide distribution with southward gradient. This terrace consists of the overlying deltaic gravel bed on the Kamoe terrace or a mud bed (Yamasaki mud bed; Sugiyama, 1991) and presumed to have been formed as riverine terraces in regressive stage after the MIS 5e (Muto, 1987; Sugiyama 1991). The southern margin of the Mikatagahara

terraces is eroded during the Jomon Transgression to have been formed sea cliffs. In the seaward area of the sea cliffs, some wave cut benches are supposed to be buried by the Holocene sediments (Matsubara, 2004; Fujiwara *et al.*, in press).

The Lake Hamana is a brackish lake distributed at the large incised valley incised the Pleistocene terraces. There are many alluvial lowlands with various shapes and sizes developed in the valleys incised these mountains, hills and terraces around the Lake Hamana and the Enshu-nada Coast. These alluvial lowlands classified into the drowned type lowland (Umitsu, 1994). The morphological differences between alluvial lowlands suggest the distinction of geological and geomorphological backgrounds. In addition, some narrow segments are recognized in the valleys reflecting the difference of hardness around the rivers and/or the river channel morphologies.

In the southern part of the study area (the western Hamamatsu Strand Plain), total of six coastal sand barriers are distributed along the Enshu-nada Coast and shelter the lake inlet. These sand barriers were named beach ridge (BR) I to VI after Matsubara (2001) and Matsubara (2007). While six sand barriers can be recognized easily on the eastern side from the Lake Hamana, these converge with total of three barriers on the western side (Matsubara, 2001). The BR IV, distributed along the present shoreline, is aeolian sand dune affected by human activity after recent historical period. Inter-ridge marshes are well developed between beach ridges.

Along the channels of the Magome River and the Miyakodagawa River, natural levees are distributed sporadically. It is easy to distinguish between natural levees and beach ridges in the western Hamamatsu Strand Plain by considering the orientations of long axis of landforms. However, artificial change around the urban area of Hamamatsu City, western side of the Magome River channel, is too large to identify natural levees. The drowned alluvial lowlands have no

developed natural levee and shows low and flat ground surfaces.

2-2-2. Tectonic setting

The study area is located beside the Nankai Trough, a subduction zone where the northwestward moving Philippine-sea plate beneath the Eurasian plate. Therefore, tectonic activity is considered to be high. Historical documents illustrate serious damages induced by repeated huge earthquakes generated along the Nankai Trough (Yata, 2009). For example, the Meio earthquake in 1498 AD seems to have caused dynamic geomorphological deformation around the Lake Hamana (Shizuoka Pref., 1996; Yata, 2005; Fujiwara *et al*, in press). Before the Meio earthquake, the Hamana River, a small river running from the lake to the Enshu-nada Coast is recognized in historical maps. After the earthquake, the present inlet of the lake opened associated with tectonic movement and/or tsunami.

Although the accurate co-seismic displacements have not been clarified yet, several geodetic data indicate possibility of co-seismic subsidence around the study area. Kato and Tsumura (1979) showed the utility of tidal gauge in tidal stations for monitoring of inter-seismic deformation. According to Kato and Tsumura (1979) and the Coastal Movements Data Center (CMDC, 2013), inter-seismic emergence has occurred around the study area, reflecting accumulation of stress. The annual emergence rate in the Lake Hamana was estimated to be 2.85 mm/yr approximately by CMDC (2013). Furthermore, Sagiya (2007) pointed out innate pattern characterized by uplift from Nagoya city to Kakegawa city and subsidence from Kakegawa city to Numazu city, Shizuoka Pref. during the inter-seismic period by analysis of recent geodetic data. If much of the cumulative stress presumed by the previous studies can be release in the earthquake,

total deformation in the inter-seismic period would be recovered by co-seismic subsidence.

2-3. Paleo-environmental change in the study area

2-3-1. Lake bed sediments

Since the late 1980s', a number of geological, sedimentological, paleontological and geochemical analyses had been performed using lake bed sediments of the Lake Hamana. As the results, the Holocene lacustrine and geomorphological environmental changes associated with sea-level change were reconstructed (Ikeya *et al*, 1987, 1990; Ikeya, 2000, Fig. 2-2). The previous studies showed that the Lake Hamana went through environmental transition associated with glacio-eustatic sea-level change in common with other alluvial lowlands and coastal lagoons. Rapid rising of sea-level after the LGM caused expanding of sea area and development of tidal delta. After the Jomon Transgression, inner bay environment occurred at the regressive stage to become a fresh water pond around 3000 ¹⁴C yr BP (Fig. 2-2). Timing of the environmental change from a brackish water lake to a fresh water pond is remarked by the Amagi-Kawagodaira tephra falling (Kg, 3126-3145 cal BP; Machida and Arai, 2003)..

2-3-1-1. Sedimentological analysis

Sedimentological studies were performed by Ohtsuka and Kimiya (1987) and Saito (1988). Ohtsuka and Kimiya (1987) showed that lake bed core sediments could be divided into five layers by depositional facies, i. e. thin transgressive sandy deposits, massive silty deposits at brackish to marine well circulated surface water, silty deposits with lamina at a partial circulative brackish lake, massive silt deposits at a fresh water pond and silty deposit with lamina in ascending

order. The core facial change from silt deposits with lamina to massive silt of a fresh water pond occurred after the Kg tephra falling. Formation of lamina was presumably associated with anoxic bottom water to inhibit benthic activity. Furthermore, Saito (1988) performed sequence stratigraphical analysis on lake bed sediments consisting of two parts, the upper-fining sequence and the overlying upper-coarsening sequence. The lower sequence was presumed to be transgressive sediment that deposited from river mouth to lagoon. On contrast, the upper sequence indicated progradation process from seaward to landward of tidal delta, located at the southern part of the Lake Hamana, during ca. 6000 to ca. 9000 ^{14}C yr BP. While barrier lagoon system had been active during the high sea-level stand, it has become inactive since ca. 4000 yr BP at the regressive condition.

2-3-1-2. Geochemical analysis

Nakai *et al.* (1987) reconstructed the lacustrine environmental transition and the Holocene relative sea-level curve by geochemical data. They measured $\delta^{13}\text{C}$ content and C/N ratio of bulk sediment samples. According to Nakai *et al.* (1987), relative sea-level in the study area had rose since ca. 10000 ^{14}C yr BP and reached its maximum at ca. 6500 ^{14}C yr BP. It is recognized that temporarily sea-level falling occurred during ca. 3000 to ca. 3500 ^{14}C yr BP. After ca. 1000 ^{14}C yr BP, relative sea-level became same level as the present sea-level.

2-3-1-3. Paleontological analysis

Paleontological studies employing diatoms (Kashima, 1988; Honda and Kashima, 1997; Morita *et al.*, 1998), dinoflagellate cysts (Kojima, 1989) and foraminifera (Matsubara, 1989 and

2001) were performed. Kashima (1988) divided lake bed sediments into five parts based on diatom assemblages. The lowest part suggested that brackish water lake had begun to be formed before ca. 9000 ^{14}C yr BP. During ca. 6000 to ca. 9000 ^{14}C yr BP, marine area expanded and salinity became high. The salinity declined by closure of the inlet during ca. 3000 to 6000 ^{14}C yr BP. After ca. 3000 ^{14}C yr BP, water input from the ocean to the lake decreased drastically. The similar water condition to the present was formed after ca. 1000 ^{14}C yr BP. Morita *et al.* (1998) improved diatom diagram shown in Kashima (1988) for reconstruction of detail environmental change after the Jomon Transgression. Morita *et al.* (1998) suggested that environmental change from fresh water pond to brackish water lake had occurred in ca. 2300 ^{14}C yr BP and brackish environment continued until ca. 1600 ^{14}C yr BP. Honda and Kashima (1997) reconstructed detail environmental transition after the Meio earthquake in 1498 AD and showed drastic environmental change accompanied with the earthquake and fluctuation of salinity of lake water after that.

Dinoflagellate cysts of lake bed sediments indicated transgressive and regressive processes occurred after the LGM (Kojima, 1989). According to Kojima (1989), lake bed sediments could be divided into six parts. The lowest part was presumed to be the inner bay sediment during ca. 7500 to ca. 9700 ^{14}C yr BP. Above this layer, environmental succession from brackish lake to ocean occurred during ca. 6400 to ca. 7500 ^{14}C yr BP. Although much seawater input into the lake was indicated during ca. 5400 to ca. 6400 ^{14}C yr BP, salinity of lake water declined temporarily during ca. 5200 to ca. 5400 ^{14}C yr BP. It is recognized a stable inner bay environment during ca. 3000 to ca. 5200 ^{14}C yr BP. After ca. 3000 ^{14}C yr BP, environmental change from an inner bay to a fresh water pond occurred.

Foraminiferal assemblages were used to estimate seawater inflow into inner bays and

lagoons (Matsubara, 1989). Matsubara (1989 and 2000) suggested that inner bay environment had occurred in ca. 10000 ^{14}C yr BP and seawater inflow from the outer bay increased after ca. 7000 to ca. 8000 ^{14}C yr BP. Since then coastal lagoon environment occurred in ca. 6000 – 7000 ^{14}C yr BP, which indicated embayment related to coastal sand barrier developments.

2-3-2. Coastal sand barriers

Coastal sand barriers distributed along the Enshu-nada Coast are recognized total six series of sand barriers and considered to have developed in regressive stage after the Jomon Transgression. Matsubara (2000 and 2001) suggested that BR I, the most landward barrier, began to de formed around 8000 ^{14}C yr BP and finished during 6000 to 8000 ^{14}C yr BP. The geomorphological development of the BRs located in the seaward area were discussed by Ikeya *et al.* (1990) and Matsubara (2004 and 2007) based on geological survey in inter-ridge marshes and location of archeological sites on the BRs. Matsubara (2004) estimated the emergence age of the BR I to be ca. 6000 ^{14}C yr BP by measuring the radiocarbon ages taken from the bottom sediment of the inner-ridge marsh located between BR I and II. It was also suggested that the BR III had been formed until the Yayoi period (ca. 2000 ^{14}C yr BP) at latest and the BR IV had developed after ca. 2000 ^{14}C yr BP.

2-3-3. Alluvial lowlands

A few studies investigated at the alluvial lowlands around the Lake Hamana. Ikeya *et al.* (1985) conducted coring survey in the Rokkengawa Lowland and clarified the Holocene geology of the lowland. The Holocene sediments of this lowland consist of sand, silt and peat layer in

ascending order. Sand layer was different between the northern part and the southern part of lowland. The former was composed of riverine sandy deposits including sub-angular gravels, the later was composed of well-sorted fine sand indicating marine environment. In the silt layer, Kikai-Akahoya tephra (K-Ah, ca. 7.3ka; Machida and Arai 2003) was recognized at – 5 m T.P. The overlying peat layer yielded two tephra layers, Kg and Osawa-scoria (Os, 2.5-2.8 ka, Machida and Arai, 2003). Ikeya *et al.* (1985) suggested that fresh water marsh or pond had occurred since ca. 5000 ¹⁴C yr BP to form the thick peat layer based on geology and tephra chronology.

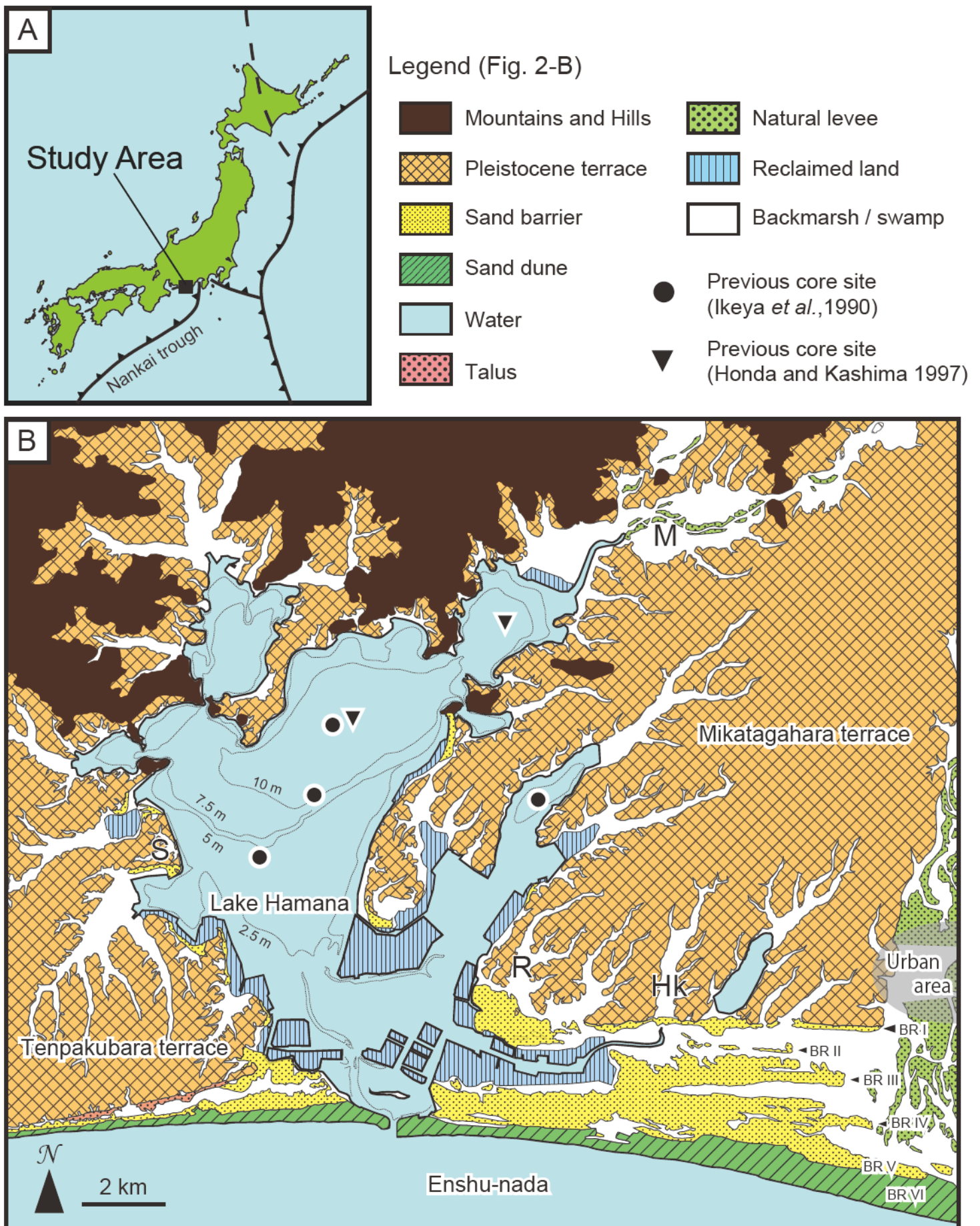


Fig. 2-1. Location and geomorphological classification map of the study area. 2-1A: Location map of the Lake Hamana. 2-1B: geomorphological classification map around the study area based on the observation of aerial photos on a scale of 1/10,000 taken by Geospatial Information Authority of Japan (GSI) in 1962. Bathymetric data is based on the topography map described in 2007 by the GSI. The urban area was changed artificially too much associated with civilization of Hamamatsu city to identify original topography. Locations of the lake bed core analyzed by previous studies (Ikeya *et al.*, 1990; Morita *et al.*, 1998) are described. R, Hk, M and S letters represent investigated alluvial lowlands in the present study, R: Rokkengawa; Hk: Higashi-Kandagawa; M: Miyakodagawa; S: Shinjo Lowlands.

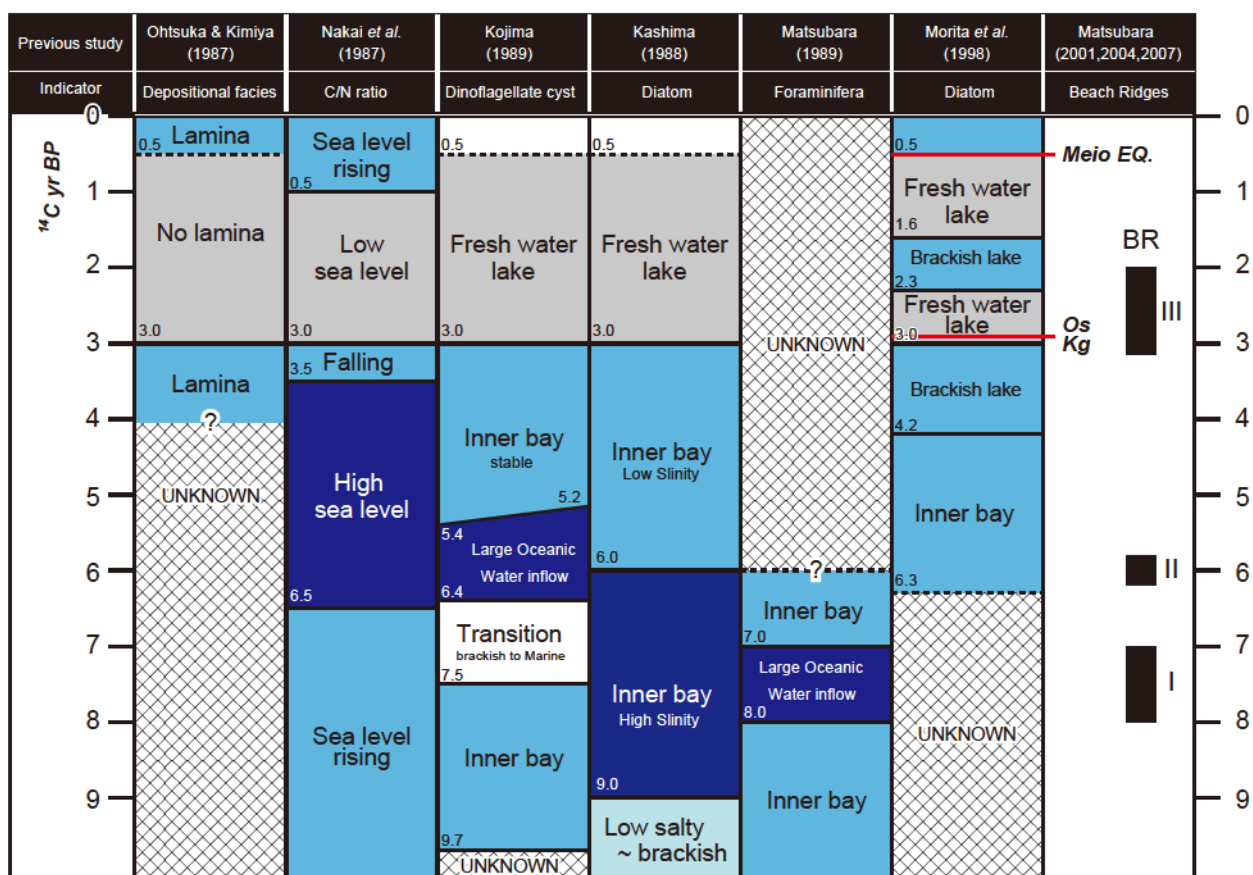


Fig. 2-2. Environmental changes around the Lake Hamana during the Holocene were suggested by previous studies. Depositional facies of the lake bed cores was reported by Ohtsuka and Kimiya (1987). Geochemical analyses (C/N ratio) were performed by Nakai *et al.* (1987). Paleontological analyses were conducted by Kojima (1989), Kashima (1988), Matsubara (1989) and Morita *et al.* (1998). The geomorphic developments of the coastal beach ridges along the Enshu-nada Coast were discussed by Matsubara (2000, 2004 and 2007). Eruption ages of Kg and Os tephra rely on Machida and Arai (2003). According to the historical information, the Meio earthquake (EQ) occurred at 1498 AD.

CHAPTER III

Late Holocene changes in lacustrine environment of the Lake Hamana

3-1. Introduction

As mentioned in the Chapter II (2-2), several geological, sedimentological, paleontological and geochemical analyses had been performed using lakebed core samples in the Lake Hamana (Saito 1988; Kashima 1988; Ikeya *et al.*, 1990; Matsubara 2001). These previous studies provided fruitful knowledge about paleo-environmental changes associated with the Holocene relative sea-level change in this region. They presumed that coastal sand barriers have developed in the regressive condition after the Jomon Transgression period (ca. 7000 cal BP) and environmental change from inner bay to brackish or fresh water lake occurred (Ikeya *et al.*, 1990). Around the coastal area of the Suruga Bay and the Enshu-nada Coast, coastal sand barriers, developed after the Jomon Transgression period, were recognized (Matsubara, 2001).

As radiocarbon dating by using the AMS method, enable to obtain precise radiocarbon age with a few sample, became popular after 1990s', it have been easier to discuss about reconstruction of the Late Holocene plaeo-envionment at high temporal resolution than before (Masuda, 1998; Tamura and Masuda, 2004). Detail reconstruction of paleo-environmental change is important for clarifying relationship between geomorphic development and short-term natural phenomena, such as relative sea-level change, earthquake and climate change. It is also illustrated that historical tectonic movement, occurred repeatedly in short time scale (at the interval of decadal to millennial time scale) caused geomorphic deformation and developments. Understanding on the affection of these short-term environmental changes can provide new insights into not only natural

science but also disaster reduction.

Some short-term environmental change would be recorded in the sediments around the Lake Hamana. Because the Lake Hamana, is located beside the Nankai trough which is the subduction zone where the northwestward moving Philippine Sea plate beneath the Eurasian plate, it is presumed to be high tectonic activity. Therefore, tectonic deformation can affect the geomorphic development in this area as well as the climatic change. Based on historical documents, the Meio earthquake generated in the Nankai trough at AD 1498 caused the collapse of coastal sand barriers in the southern part of the Lake Hamana and changed lacustrine condition from fresh to brackish (Shizuoka Pref., 1996; Yata 2005).

Morita *et al.* (1998), one of the previous studies on paleo-environmental change around this area, showed detail environmental reconstruction after ca. 3000 ^{14}C yr BP by diatom analyses. Morita *et al.* (1998) suggested that salinity of the Lake increased at ca. 2300 ^{14}C yr BP and AD1498 and decreased at ca.1600 ^{14}C yr BP. These environmental changes were induced by short-term climatic change or tectonic movement. However, there is no previous study clarified the detail paleo-environmental changes of the Lake Hamana through the late Holocene. Because the geological and geomorphological settings around the lake imply that short-term environmental changes occurred before 3000 ^{14}C yr BP, it is necessary to reconstruct the detail paleo-environmental changes in decadal to scale.

In this chapter, the author performs geological and paleontological analyses on lakebed sediment taken at the central part of the Lake Hamana for reconstruction of lacustrine environment during the late Holocene. The results of analyses indicate that some short-term environmental changes also occurred in the Lake Hamana.

3-2. Material and methods

3-2-1. Core sample (HMN08-7 core)

The lakebed sediment core (HMN08-7 core) was obtained in September 28th, 2008 by the research group of Prof. Okamura, Kochi University by the piston coring system (Okamura *et al.* 2009). The location of the HMN08-7 core is the central part of the Lake Hamana, at latitude 34° 44' 55.20" north and longitude 137° 34' 02.64" east (Fig.3-1 ; Matsuoka, personal communication). Bathymetric map of the Lake Hamana indicates that the core site is located at approximately 1.6 km north from the sloop and has about 10 m depth beneath the lake water surface (Fig.3-1). According to Ikeya *et al.* (1990), present bottom material around the HMN08-7 core site is muddy deposit probably.

HMN08-7 core was 350 cm in length and composed of grayish muddy sediment mainly (Fig. 3-2). During 295 to 335 cm depth of the core, lamina which showed alternate layer of grayish and brownish-red layers was well developed. At 285 to 287 cm depths, a thin sandy layer was recognized. During 64 to 113 cm depth, many shell fragments were yielded. The top of the core, above ~25 cm depth, was very soft and characterized by smell of hydrogen sulfide gas.

3-2-2. Age model

Age model of the HMN08-7 core was constructed based on radiocarbon ages of bulk sediments and volcanic ashes (Fig. 3-2).

A total of seven AMS radiocarbon dates including three previous dates measured at Geo-Science Laboratory *Co. Ltd.* (Table3-1; Matsuoka, personal communication). Matsuoka (personal communication) showed three radiocarbon ages from sediment samples (Table 3-1), i. e. 930-1085 cal BP (2σ , as the case may be) at 78-81 cm depth; 905-1010 cal BP at 111-114 cm depth; 1610-1825 cal BP at 199-202 cm depth. In addition to them, new four radiocarbon ages of bulk samples of the core sediments were measured (Table 3-1), i.e. 2125-2315 cal BP at 216-220 cm depth; 4955-5075 cal BP at 280 cm depth; 4425-4580 cal BP at 290.5-293 cm depth; 4515-4650 cal BP at 324-326 cm depth.

Two volcanic ashes layers were found in the core sediment by visual observation of the lakebed sediment. From the lower one, subsamples for estimation of refractive indices of volcanic ash and main heavy minerals were taken by means as mentioned in Chapter II (2-1-3). These subsamples were analyzed in the FURUSAWA geological survey *Co. Ltd.* Identification of each tephra was based on refractive indices and core stratigraphy with the help of radiocarbon ages above/beneath them.

Two volcanic ashes were observed at 261-263 cm depth and 265 cm depth respectively. The lower layer yielded pumice type and bobble-wall type volcanic glasses with some heavy minerals. Their refractive indices were estimated to be 1.501-1.503 from volcanic glasses, 1.705-1.708 from Pyroxene and 1.669-1.679 from Hornblend respectively. These reflection indices show coincidence with those of Amagi-Kawagodaira Pumice (Kg) erupted at 3126-3145 cal BP (Machida and Arai, 2003) in Kawagodaira volcano, Izu Peninsula, Central Japan. The result of tephra analysis and stratigraphy of the core indicate that the lower layer is Kg tephra. Based on the tephra catalogue around the study area (Machida and Arai, 2003) and core stratigraphy of

HMN08-7 (just above the Kg tephra), the upper tephra layer was presumed to be Fuji-Osawa scoria (Os) which erupted at 2.5-2.8 ka (Machida and Arai, 2003).

According to the Age model in Fig. 2-1, age reversal of radiocarbon dating was found at 280 cm depth of HMN08-7 core. Based on comparison between the age-depth plots of the HMN08-7 and HMN08-8, obtained from almost the same location as HMN08-7 core (Okamura *et al.*, 2009), the author eliminated the radiocarbon date at 280 cm depth of HMN08-7 from age control point by judging as reworked sediments.

3-2-3. Diatom analyses

A total of 250 subsamples were taken from the core sediment at 0.5 to 1.0 cm intervals for diatom analyses. As mentioned in the Chapter II (2-1-4), these subsamples were treated according to Kosugi (1993) and Ishikawa *et al.* (2010). The most upper part of the core, 0 to 28 cm depth of the core, was eliminated from subsamples because their depositional facies is too humic and soft to analyze.

3-3. Results of diatom fossil analysis

The diatom diagram of the HMN08-7 core based on diatom analysis is shown in Fig. 3-3. Based on the change in diatom assemblages, the author divided into six diatom zones in HMN08-7 core as zone I to VI from bottom to top, and of which the zone V and zone VI were subdivided into three sub-zones from a to c respectively.

3-3-1. Zone I (Depth: 337-348 cm)

The Zone I was corresponding to the lowest part of the core which show massive muddy facies. Based on the Age model of the core, this diatom zone deposited during ca. 4600-4700 cal BP (Fig. 3-2).

The Zone I was characterized by abundant brackish and marine water species, particularly outer bay indicator such as *Thalassiosira* sp. with around 10-20% abundance of the total counts. On the other hand, inner bay indicator such as *Cyclotella striata* was few in this zone. Other marine to brackish water species, e. g. *Diploneis pseudovalis*, *Diploneis smithii*, *Rhaphoneis surirella* and *Openphora martyi*, were much more than the other upper diatom zones.

3-3-2. Zone II (Depth: 297-336 cm)

The Zone II was corresponding to the lamina well-developing layer. The Age model showed that this zone deposited at ca. 4500-4600 cal BP (Fig. 3-2).

The Zone II was characterized by abrupt increasing and dominance of *C. striata*, which is one of the most significant indicators of brackish lake environment (Kashima, 1988; Kashima, 2001). Relative abundances of *Cyclotella striata* in this zone reached to approximately 40%. *Thalassiosira* sp. and *Thalassiosinema nitzschioides* yielded as much as those of the Zone I, i. e. ~10-15% and ~10% respectively. On the other hand, *Cocconeis scutellum*, benthic marine to brackish water species, increased by about 10-15% than those in the zone I.

In the middle part of this diatom zone, temporarily dominance of *Plagiogramma* sp. was found at 320-322 cm depth of the core. This part was coincident with the sediments with no lamina. The just upper sediments of this part show increasing slightly *Pralia sulcata* and *T. nitzschioides* to

occupy ~5-10% than the lower sediments.

3-3-3. Zone III (Depth: 261-296 cm)

The zone III was massive muddy sediments at 261 to 296 cm depth. The upper limit of this zone was bounded by the Os layer. The age model shows that this zone deposited at ca.2650-4500 cal BP (Fig. 3-2).

Relative abundances of *Cyclotella striata* in zone III showed around 20%, which was lower than those of zone II. While total of planktonic brackish to marine species, such as *C. striata*, were dominant, *Staurosira construens*, fresh to brackish water species, and *C. scutellum*, benthic brackish to marine water species increased slightly from the Zone II. Temporarily increasing of fresh and fresh to brackish water species, e.g. *S. construens*, *Fragilaria* spp. and *Aulacoseira ambigua*, was found at 284 to 287 cm depth, which approximately corresponding to the sandy layer.

The Upper part of this zone, above 275 cm depth (after ca. 3500 cal BP) was remarked by some obvious peaks of relative abundance of *Thalassiosira* sp. with gradual decreasing upward. These peaks were recognized at 272-275 cm, 267-269 cm and 261-263 cm depth from bottom to top.

3-3-4. Zone IV (Depth: 222-260 cm)

The zone IV was massive humic mud at 222 to 260 cm depth overlying the Os layer. The Age model shows that this zone deposited at ca.2250-2650 cal BP (Fig. 3-2).

This diatom zone was remarked by great reduction of brackish to marine water species

from the Zone III and abundance of fresh to brackish and fresh water species. *Thalassiosira* sp., *P. sulcata* and *T. nitzschioides*, marine planktonic species, decreased about 5-10% from the Zone III to be almost 0% abundance. In addition, *Cyclotella striata* and *Cocconeis scutellum* declined gradually from the bottom to top of the zone and the percentage of them changed from ~25% to ~5% and from ~25% to ~0% respectively. On the other hand, *Staurosira construens*, fresh to brackish tycho planktonic species, and *Fragilaria* spp., fresh water species, increased gently upward to replace *C. striata* and *C. scutellum*. In particular, *Staurosira construens* become dominant in the upper part of this zone with ~35%.

During the 234-247 cm depth of the core, temporarily abundance of fresh water planktonic species is recognized. While the lower and upper part of this layer yielded many *Aulacoseira granulata* to account for 10-15% abundance, the middle part yielded *Aulacoseira ambigua* to occupy ~10%.

3-3-5. Zone V (Depth: 111-221 cm)

The Zone V was corresponding to massive muddy layer at 111 to 221 cm depth. The Age model shows that this zone deposited before ca. 2250 cal BP (Fig. 3-2). The sedimentation age of the upper limit of this zone was presumed to be after ca. 1000 cal BP.

This diatom zone was characterized by dominance of fresh water species, such as *Fragilaria* spp., *A. granulata* and *A. ambigua*. Marine water species are depleted except for petty existence of *C. striata*.

This diatom zone was able to be subdivided into three parts from Zone V-a, V-b and V-c according to amount of *S. construens*. The Zone V-a, 146-221 cm depth, was characterized by high

percentage of *Fragilaria* spp. and *A. ambigua*. The lower part of this subzone showed more abundance of *Fragilaria* spp. than that in the upper part. *Aulacoseira granulata* increased gradually upward in the subzone. The Zone V-b, 127-145 cm depth, showed dominance of *S. construens* and drastic decreasing of *A. ambigua* from the Zone IV. *Cyclotella striata* also rose slightly from the Zone IV and relative abundance of this reached ~2%. The Zone V-c, 111-126 cm depth, was shared by *A. granulata* and *A. ambigua*.

3-3-6. Zone VI (Depth: 28-110 cm)

The Zone VI was roughly corresponding to grayish muddy layer with many shell fragments at 28 to 110 cm depth. Although sedimentation age of this diatom zone was difficult to detect from the Age model of the HMN08-7 core, it seems to be at least after ca. 1000 cal BP.

This diatom zone was characterized by re-dominance of brackish to marine water species and absence of fresh water species. In particular, *Cyclotella striata*, *C. scutellum*, *D. pseudovalis* and *P. sulcata* showed abrupt increasing from the Zone V. Only in the lowest part of this zone, *A. granulata* and *S. construens* accounted for approximately 10-20% and 20% respectively.

This diatom zone was able to be subdivided into three subzones from Zone VI-a to Zone VI-c. The Zone VI-a (79-110 cm depth) showed high percentage of *C. striata*, ranged from 14.5 to 54.9%, and abundant amounts of *C. scutellum* and *D. pseudovalis* with around 10-20% and 5-10% respectively. The Zone VI-b (52-78 cm depth) was distinguished according to abundance of *T. nitzschioides* and *Thalassiosira* sp. from the other subzones. The Zone VI-c (28-51 cm depth) was characterized by dominance of *C. striata* with abundant *C. scutellum*, *Thalassiosira* sp. and *D. pseudovalis* as those of the Zone VI-a.

3-4. Transition of lacustrine environment inferred from diatom assemblages

The Late Holocene changes in lacustrine environment in the Lake Hamana were reconstructed based on diatom zones defined in Chapter III (3-4).

3-4-1. Stage I (ca. 4600-4700 cal BP)

The low percentage of indicators of inner bay environment, e. g. *C. striata* (Kosugi, 1988) in this diatom zone indicates that coastal sand barriers had not developed enough to form inner bay. Because *Thalassiosira* sp., which is an indicator of an outer bay environment, yielded more abundantly than *C. striata*, seawater inflow to the core site from the opened ocean is suggested to have been obviously active.

3-4-2. Stage II (ca. 4500-4600 cal BP)

Dominance of *Cyclotella striata* and development of lamina suggests a closed inner bay environment formed after ca. 4600 cal BP. Abrupt and extremely increasing of *C. striata*, one diatom species of indicators of inner bay environment (Kosugi, 1988), at the bottom of the Zone II shows a rapid formation of an inner bay environment in ca. 4600 cal BP. Considering that coastal sand barriers are distributed between the Lake Hamana and Enshu-nada Coast to obstruct the lake inlet, the author suggests that environmental change from outer bay to inner bay was probably induced by development of coastal sand barriers resulting in reduction of seawater inflow before. Because the percentage of *Thalassiosira* sp. was almost similar as the zone I, the seawater inflow still existed in this period. The seawater supplying and sheltering by sand barriers were likely to

make strong density stratification of lacustrine water and resulted in formation of lamina.

In this study, timing of an inner bay formation is estimated ca. 4500 cal BP, which supports previous study by Morita *et al.* (1988). Morita *et al.* (1988) pointed out that lacustrine salinity decreased after ca. 4200 ¹⁴C yr BP based on the diatom analysis. The main diatom components of the inner bay sediments are almost same between the Zone I (the present study) and Morita *et al.* (1988). Morita *et al.* (1988) used the Age model of the core based on not calibrated radiocarbon ages and tephra dates. Modifying this Age model by roughly calibration of radiocarbon and tephra ages inferred from the IntCal09.14c curve (Reimer *et al.*, 2009), timing of this environmental change is estimated to be ca. 4240 cal BP. Because of similarity temporal proximity of environmental change found in both lakebed cores, the author suggests that both of environmental changes are presumably same phenomenon.

The abundant spike of *Plagiogramma* sp., brackish to marine water species, implies that seawater inflow increased temporarily. It is difficult to estimate precise age of this episodic peak as period of the Stage II is too short. Above this spike, *Thalassiosira* sp. and *T. nitzschioides* increased slightly than beneath, and which indicates that seawater more easily inflow to the inner bay than beneath the spike. The diminishment of lamina of the core facies is coincident with the temporal peak. Because the inner bay environment had been maintained during and above the spike inferred from abundance of *C. striata*, coastal sand barriers which closed the Lake Hamana continued to exist and close the lake.

3-4-3. Stage III (ca.2650-4500 cal BP)

Decreasing of *Cyclotella striata* and massive muddy facies indicate a circulative

lacustrine environment. Most of the decreasing percentage of *C. striata* is replaced by some benthic species such as *S. construens* and *C. scutellum*. It is implied from high taxonomical diversity that active mixture of riverine fresh water and oceanic high salinity water in a brackish lake between ca. 2600 cal BP and ca. 4500 cal BP.

After ca. 3500 cal BP, the amount of seawater inflow became larger than before. *Thalassiosira* sp. is an indicator of outer bay environment (Kosugi, 1988). In the same horizon, *Cyclotella striata* and *C. scutellum* showed as high percentage as those in the lower part. Therefore, oceanic species *Thalassiosira* sp. must have been transported by seawater inflow from the Pacific.

In addition, a short-term event occurred in ca. 3500 cal BP (284 to 287 cm depth). Temporal abundant diatom species indicating fresh and fresh to blackish water were caused by two processes. One is transportation of inland sediments, and the other is temporarily salinity reduction of the lake. This horizon was corresponding to the sandy thin layer. This sandy deposit presumably indicates a kind of “event sediment”, for example flood, storm or tsunami sediments. Therefore, the later process is more likely.

3-4-4. Stage IV (ca.2250-2650 cal BP)

After the eruption of the Os tephra, salinity reduced continuously until ca. 2250 cal BP. Absence of diatom indicator of outer bay environment indicates that seawater inflow ceased. At the early period of this stage, salinity was still high enough to be *C. striata* as a dominant species. Upward decreasing of *C. striata* and *C. scutellum* were obvious in the zone IV. In contrast, increase in *S. construens* is presumed that gradual salinity decline from 2250 cal BP to 2650 cal BP. Accompanying fresh water diatom species implies that the surface water changed to fresh water

partially.

Stepwise environmental changes after the Kg and the Os tephra fallings were found in the Lake Hamana. Previously, lacustrine water of the Lake Hamana changed to fresh water around 3000 ¹⁴C yr BP, after the Kg and the Os tephra (Kashima, 1988; Kojima, 1989; Ikeya *et al.*, 1990). However, in the present study, the brackish lake had lasted for a while after the Os tephra, which indicates that reducing of seawater inflow occurred just after the Os tephra. The gradually transition of diatom assemblages presumably reflects dilution process of the lake water.

A Number of episodic environmental changes are recognized in this stage. In the middle period of this stage, abundance of fresh water species such as *A. granulata*, *A. ambigua* and *Achnanthes minutissima*, suggests that short-term salinity reduction occurred. In addition, *C. striata* shows a small peak of abundance in the top of the zone IV. Morita *et al.* (1998) pointed out that environmental change from fresh water lake to brackish water lake occurred in ca. 2300 cal BP inferred from abundance of *A. granulata* and *C. striata*. Although magnitude of environmental change found by this study is much smaller, this environmental change is possibly corresponding to temporal formation of brackish lake shown by Morita *et al.* (1998).

3-4-5. Stage V (1498 AD – ca. 2250 cal BP)

Environmental change from brackish water lake to fresh water lake occurred around 2250 cal BP. Almost all diatom was freshwater species and only a few brackish to marine species were found. Upward increase of *A. granulata*, an indicator of fresh water lake (Ando, 1990), and decrease of *Fragilaria* spp., fresh to brackish tycho planktonic species, imply that water depth of the lake became deeper gradually.

The environmental change from brackish water lake to fresh water lake is recognized by previous studies at almost same time. Pioneering studies about paleo-environmental change around the Lake Hamana clarified that fresh water lake occurred in ca. 3000 ^{14}C yr BP (Kashima, 1988; Kojima, 1989; Ikeya *et al.* 1990). The present study confirmed that this environmental change occurred after the Kg and the Os tephra eruption based on the core stratigraphy. Stratigraphical relationship between tephra layers and forming of fresh water lake have previously mentioned by Morita *et al.* (1998). The result of diatom analysis and geological columnar reported by Morita *et al.* (1998) show clearly that the environmental change occurred after the Kg and Os tephra event.

According to previous studies, the fresh water lake environment had lasted until the Meio earthquake in 1498 AD and has not been formed again since then. According to Honda and Kashima (1997) and Morita *et al.* (1998), two environmental changes from fresh water lake to brackish water lake in the Late Holocene occurred around 1498 AD and around 2300 ^{14}C yr BP. The boundary of environmental change associated with the Meio earthquake clarified by Honda and Kashima (1997) and Morita *et al.* (1998) were ranging from 140 to 190 cm depths below the lake bottom. On the other hand, horizon of the 2300 ^{14}C yr BP event was at 405 cm depth below the lake bottom. In the present study, boundary between brackish water lake and fresh water lake was at 111 cm depth below the lake bottom, which more likely corresponding to the Meio earthquake event than ca. 2300 ^{14}C yr BP event. Based on the Age model of the HMN08-7 core (Fig. 3-2), sedimentation age at 111 cm depth is estimated to be around 1000 cal BP, which is about 500 yr older than those of the previous studies. This time gap between the present study and the previous studies is presumed to be caused by dead carbon reworking, bioturbation or hiatus of core sediments.

Because dominance of *Staurosira construes*, fresh water species, are found in the zone V-b, it is suggested that temporal salinity increase in the middle period of this stage. Age model of the HMN08-7 core indicates that this environmental change occurred during ca. 1300 cal BP to ca. 1150 cal BP. However, this estimated age is possible to become much newer because of time gap between historical documents and the core Age model as mentioned above.

3-4-6. Stage VI (after 1498 AD)

As discussed in previous section (3-4-5), this stage probably appeared after the Meio earthquake in 1498 AD. Because of dominance of *Cyclotella striata* in the whole of the zone VI, an inner bay environment have developed after the Meio earthquake and lasted until present.

After the Meio earthquake, seawater inflow is fluctuated inferred from the increasing and decreasing of *Thalassiosira* sp. which is an indicator of outer bay environment (Kosugi, 1988). The middle subzone (zone VI-b) is characterized by high percentage of these diatom species and decreasing of *C. striata*. This taxonomical change probably indicates that seawater inflow became larger and salinity increased. If the sedimentation ratio during the Meio earthquake to the present is constant (as about 0.45 mm/yr), period of the zone VI-b is estimated to be from approximately 350 yrs before to 200 yrs before, i. e. 1600 AD to 1750 AD. A similar environmental change around this period, which is characterized by abundance of *Thalassiosira* sp. and *T. nitzschioides*, is already reported and estimated to have occurred during ca. 1700 to 1850 AD by Honda and Kashima (1997). The similarity of age and diatom assemblage indicates coincidence of both environmental changes. Also, Honda and Kashima (1997) pointed out that another salinity increasing occurred just after the Meio earthquake, but it could not be recognized obviously in the result of the present

study.

Table 3-1. AMS radiocarbon ages from the HMN08-7 core were calibrated with CALIB 6.0 (Stuiver *et al.*, 2004) using dataset of IntCal09.14c (Reimer *et al.*, 2009) and Marine09.13c (Reimer *et al.*, 2009). Location map of the core site and geological columnar are shown Fig. 3-1 and Fig. 3-2 respectively.

Site	Depth (cm)	Sample material	$\delta^{13}\text{C}$ (permil)	^{14}C age (yr BP, 1σ)	Calibrated age (cal BP, 2σ)	Lab. No. (Beta-)	Reference
HMN08-7	78 - 81	organic sediments	-18.8	1100 \pm 40	930 - 1085	251570	Matsuoka (personal communication)
	111 - 114	organic sediments	-22.8	1030 \pm 40	905 - 1010	251571	Matsuoka (personal communication)
	199 - 202	organic sediments	-23.9	1800 \pm 40	1610 - 1825	251572	Matsuoka (personal communication)
	216 - 220	organic sediments	-25.7	2190 \pm 30	2125 - 2315	333478	
	280	organic sediments	-23.5	4440 \pm 30	4955 - 5075	334352	
	290.5 - 293	organic sediments	-22.3	4040 \pm 30	4425 - 4850	333480	
	324 - 326	organic sediments	-23.2	4090 \pm 30	4515 - 4650	333481	

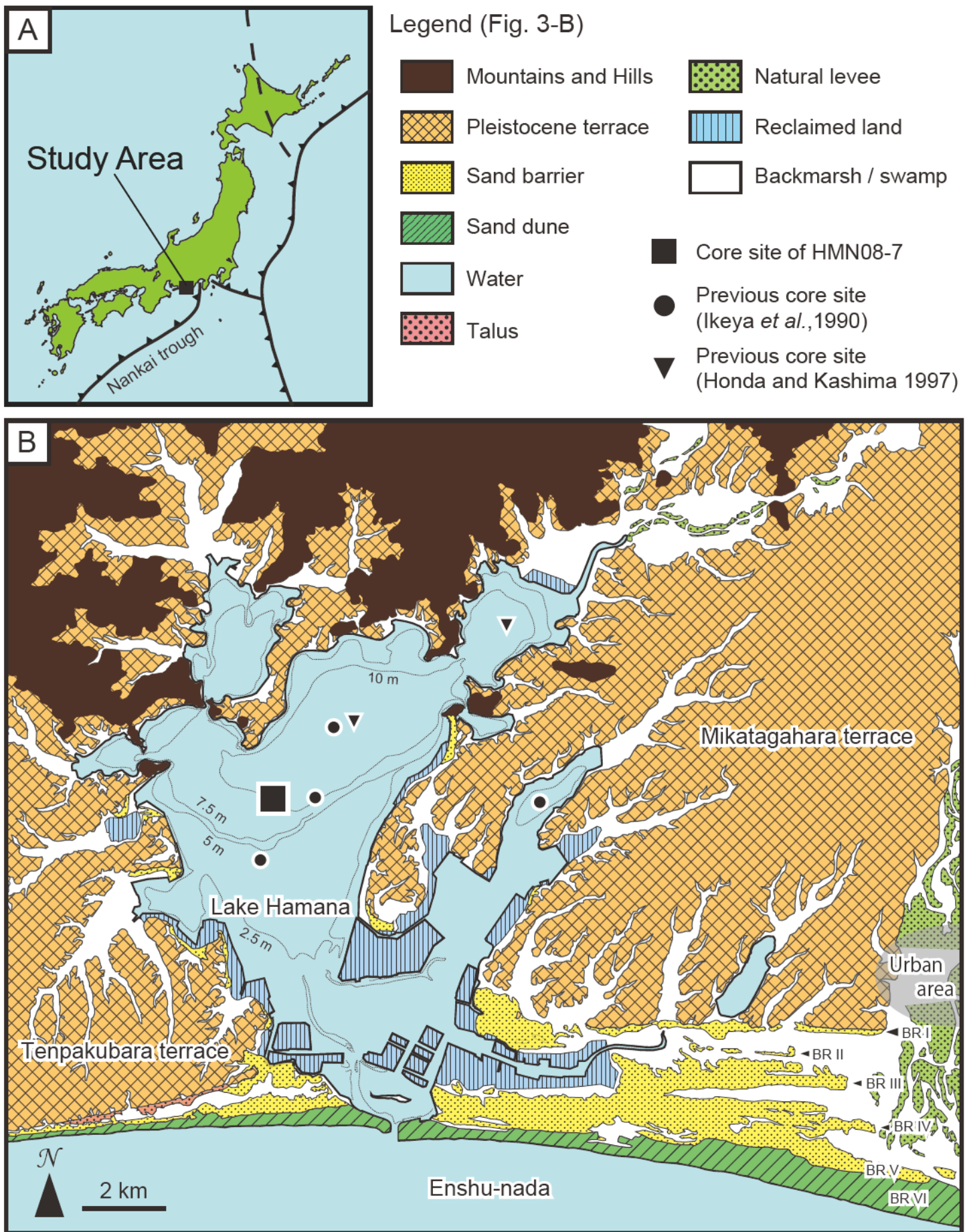


Fig. 3-1. Location map of the HMN08-7 core, a lake bed core drilled in 2008 by Project Pref. Okamura of Kochi Univ. 3-1A: Location map of the Lake Hamana. 3-1B: Location map of the HMN08-7 core. Bathymetric map of the Lake Hamana indicates that the core site is located at approximately 1.6km north from the sloop and has about 10 m depth beneath the lake water surface.

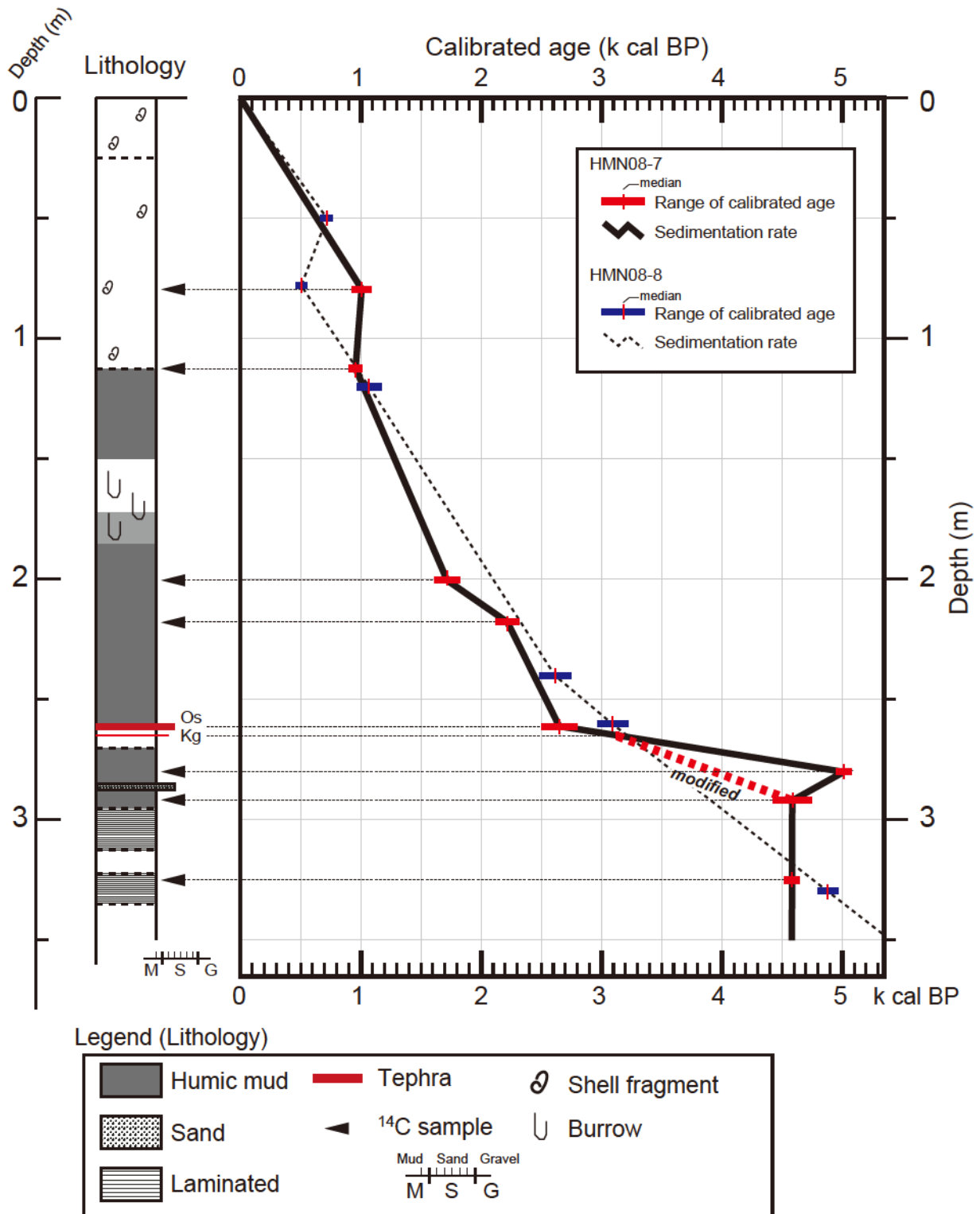


Fig. 3-2. Geological columnar and sedimentation curve of the HMN08-7 core. The sedimentation curve estimated from radiocarbon ages and tephra layers assumed that sedimentation rates are constant between each age controlling points. The detail information of AMS radiocarbon ages are shown in Table 3-1. Eruption ages of Kg and Os tephra rely on Machida and Arai (2003).

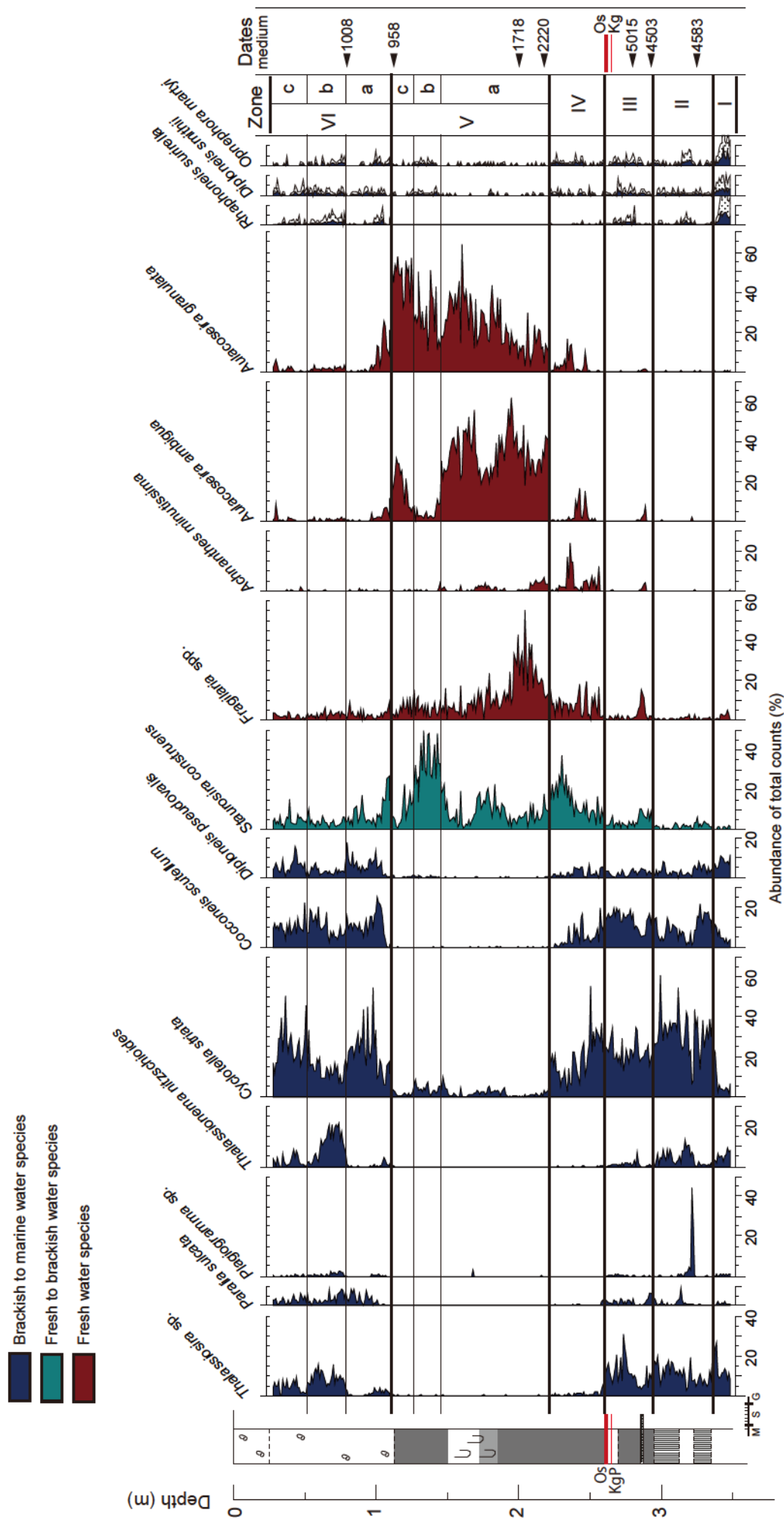


Fig. 3-3. The diatom assemblage diagram of the HMN08-7 core. The legend of geology is same as that of Fig. 3-2. Diagram of diatom assemblage with exaggeration factor of 3x for lesser taxa.

CHAPTER IV

Middle to late Holocene sedimentary environmental changes of alluvial lowlands around the Lake Hamana

4-1. Introduction

Around the Lake Hamana, numbers of alluvial lowlands with various landforms and scales are located in the valleys incised hills and the Pleistocene terraces. They seem to have developed associated with the glacio-eustatic sea-level change (Ikeya *et al.*, 1990). In addition, as mentioned in the chapter II (2-2), geomorphic developments of them presumably have been affected by short-term phenomena, such as climate change, earthquake and so on. Alluvial lowlands around the Lake Hamana are generally classified into the drowned lowland type of the categories of geomorphic development shown in Umitsu (1994). Because this lowland type likely is composed of finer deposits, geological investigation for reconstruction of detail environmental changes is more easily to be conducted than the other lowland types.

However, geomorphic developments of these alluvial lowlands have not been clarified yet except for Ikeya *et al.* (1985). Many of previous studies about the Holocene environmental changes were focused on only lacustrine environment of the lake, and which indicated stepwise environmental changes occurred. Although Ikeya *et al.* (1985) carried out core survey in the Rokkengawa Lowland, located at the southeastern coast of the lake, and suggested only brief developing process affected by the Holocene relative sea-level change, they had not yet mentioned detail sedimentary environmental change as well as those of the central part of the lake.

The goal of this chapter is to reconstruct for paleo-environment in the alluvial lowlands

are. Geological surveys and paleontological analysis were carried out at lowlands and clarify environmental change during the Late Holocene by coring survey and collecting existing core data and samples. Chronologies of these core sediments are established by radiocarbon ages and tephra layers. Through the comparison with results in lowlands, characters of the geomorphic development are discussed.

4-2. Geological and Geomorphological backgrounds of the investigated alluvial lowlands

In this study, geological and paleontological investigations were carried out in the following four alluvial lowlands. Reconstruction of detail environmental changes these are available to conduct reconstruction due to their geomorphological features, i. e. drowned lowland distributed in incised valleys. For comparison among alluvial lowlands located around the Lake Hamana widely, total of four lowlands were selected for geological survey from eastern, northern and western coast of the lake (eastern coast: Rokkengawa Lowland and Higashi-Kandagawa Lowland; northern: Miyakodagawa Lowland; western: Shinjo Lowland, Fig. 4-1). Geomorphological and geological backgrounds of these lowlands are mentioned in detail below.

4-2-1. Rokkengawa Lowland

The Rokkengawa Lowland is located at the southeastern coast of the Lake Hamana, and has approximately 3 km length and 0.7 km width (Fig. 4-1 and Fig. 4-2). This lowland is distributed in a valley incising the Mikatagahara terrace. A small river, named Rokkengawa River, runs to southward into the Lake Hamana. This lowland is characterized by low and flat surface

without riverine landform such as natural levees. In the southern part of this lowland, sandy beach ridge is distributed with ~1.5 km width in north-south and about 0.5-1 m height above sea-level. This beach ridge is probably corresponding to the BR I and/or BR II inferred from the geomorphological succession of the BRs (Matsubara 2001).

According to Ikeya *et al.* (1985), the thickness of Holocene sediments exceeds 18 m. These consist of mud, sand and peat layer in ascending order. In the peat layer, Amagi Kawagodaira tephra (Kg, 3126-3145 cal BP; Machida and Arai, 2003) and Osawa scoria tephra (Os, ca. 2.5-2.8 ka; Machida and Arai, 2003) were found.

4-2-2. Higashi-Kandagawa Lowland

Higashi-Kandagawa Lowland is located approximately 5 km east from the Lake Hamana (Fig. 4-1, Fig.4-3). This is drowned lowland in an incised valley between the Mikatagahara terraces, and which width is up to approximately 500 m and length is ~3 km in north-south. At the southern margin of the lowland, sand beach ridge is distributed with ~2.5 m height above sea and corresponding to the BR I. Much area of the Higashi-Kandagawa lowland has no riverine landform and has low and flat ground surface.

4-2-3. Miyakodagawa Lowland

Miyakodagawa Lowland is located at the northeastern coast of the lake and distributed at the lower part of the Miyakodagawa River which is the largest river running to the lake (Fig. 4-1, Fig. 4-4). This lowland is the largest one among the alluvial lowlands around the lake to be ~11.5 km length and ~3 km width. This lowland is surrounded by mountains and the Pleistocene terraces.

Some well-developing natural levees are distributed along the channels and abandoned channels of the Miyakodagawa River. Some archeological sites, e. g. Idori remains and Houda remains, were found on these natural levees. Riverine delta is developed at the lowest part of lowland with ~0.5-1 m height above sea-level.

4-2-4. Shinjo Lowland

Shinjo Lowland is located at the western coast of the lake (Fig. 4-1). This lowland is quite small one developing in an incised valley between the Tenpakubara terraces (Fig. 4-5). The width in north-south is ~150 m and the length is ~750 m. A series of sand barrier is recognized along the coastal line and presumed to be BR I. This lowland includes no riverine landform.

4-3. Methods

To detect the lowland deposit of the study areas, coring surveys were carried out by using hand corer and handy geoslicer. In addition to these, geological columnars and samples of drilling cores collected by local government of Hamamatsu City and private companies, the Meisei Industrial *Co. Ltd.*, the Stanley Electric *Co. Ltd.* and the Nippon-Keical *Co. Ltd.*, were also used as geological data of lowlands. Coring survey was performed at total of 30 sites along a ~4 km-long section in north-south in the Rokkengawa Lowland (Fig.4-2), total of 7 coring sites along a ~km section in north-south in the Higashi-Kandagawa Lowland (Fig.4-3). In the Miyakodagawa Lowland, three geological sections, C-C', D-D' and E-E' section, were made based on total of 13 coring data and 22 drilling cores (M-1 to 22, Fig.4-4). At the Shinjo Lowland, total of 8 cores are bored along a

longitudinal section with ~650 m length (Fig.4-5). Measurement of altitude of coring site and ground surface carried out using the automatic leveling. Total of 24 radiocarbon dating samples, taken from the core sediments, were measured using AMS method and calibrated by CALIB6.0 (Stuiver *et al.*, 2004) as shown in Table4-1. These samples include organic materials (woods and seeds), shell fragments, peaty sediments, soils and charcoals.

Diatom assemblages were analyzed about total of 7 cores (Rokkengawa Lowland: 0511-1 and 0511-1 core, Higashi-Kandagawa Lowland: 0307-1 and 0308-1 core, Miyakodagawa Lowland: 0429-3 core, Shinjo Lowland: 0512-1 core). Subsamples for analysis were taken from the cores in 1 to 5 cm interval. The means of treatment of them is according to Kosugi (1993) and Ishikawa *et al.* (2011) as mentioned in detail in Chapter II (2-1-4).

It is noted that identification of molluscan shell species from core samples is conducted by Dr. Fujiwara of the Active Fault and Earthquake Research Center, Advanced Industrial Science and Technology based on Habe (1977) and Okutani (2000).

4-4. Lowland deposits

4-4-1. Rokkengawa Lowland

The lowland deposits of the Rokkengawa Lowland consist of total five layers, mud layer, sandy mud layer, fine sand layer, sand layer and peat layer from bottom to top inferred from the A-A' section (Fig.4-6). The top sediments of the peat layer 0.5 to 1.0 m beneath the ground surface are disturbed by human cultivation.

The mud layer included many molluscan shells, which habitat on muddy bottom

sediments between tidal range in inner bays, such as *Cerithidea djadjariensis* and *Reticunassa festiva*. Shell fragments of *Macoma tokyoensis* at -2.2 m T.P. of 0410-3 core provided a datum of 6175-6280 cal BP based on radiocarbon dating.

The sandy mud layer was found at the southern part of the lowland and composed of alternative layers of fine sand and silt with trace fossils. This depositional facies is similar to “tidal sediments” shown in Sakakura (2004), which is made by tidal sandy transportation landward and seaward tidal currents and deposition of suspended particulates during them. Some inner bay molluscan fossils yielded in this layer, such as *M. tokyoensis* and *Umbonium costatum*, and suggested inner bay or tidal flat environment. It was recognized that this layer become thin landward transitionally and changes to the mud layer at the central part of the lowland.

The sand layer was distributed at the northern part of lowland and composed of poor-sorted fine to medium sand with sandy gravels. This layer overlay the mud layer. The thickness of this layer became thinner seaward and indicates that sediments had been supplied from landward.

The peat layer was distributed widely in the lowland. This layer was divided into two parts, the upper and the lower, by a wedged mud layer and sandy mud layer. The lower part of the peat layer was recognized at approximately -1 to -1.5 m T.P. (Tokyo Peil) between the mud layers. A radiocarbon age from the bottom of this part was measured to be 4150-4300 cal BP (wood, -1.55 m T.P. of 0511-1 core). In addition, the top of this part showed two calibrated ages, 3705-3845 cal BP (plant fragment, - 1.0 m T.P. of 0423-4 core), 3845-3935 cal BP (charcoal, -0.9 m T.P. of 0423-5 core) and 4145-4295 cal BP (plant fragment, -1.3 m T.P. of 0511-1 core). These radiocarbon ages indicates that the lower part occurred during ca. 3800 cal BP to ca. 4200. On the other hand, the

upper part is distributed between -0.5 to -1.0 m T.P. Radiocarbon ages from the bottom of this part were estimated to be 3385-3465 cal BP (plant fragment, -0.5 m T.P. of 0423-2) and 3250-3365 cal BP (seed, -0.7 m T.P. of 0423-6). Of the 0410-3 core at the southern part of the lowland, the Kg tephra layer was found ~15 cm above the bottom of the peat layer (Fujiwara *et al.* 2013). Based on these ages, it is presumed that formation of the upper part began around 3400 cal BP. In addition to them, young ¹⁴C ages were obtained in the top of the upper part of peat layer showing 520-555 cal BP (wood, -0.2 m T.P. of 0410-3 core) and 320-395 cal BP (seed, 0.0 m T.P. of 1010-1 core).

The fine sand layer beneath the upper part of the peat layer was recognized at the southern part of the lowland. This layer was characterized by well-sorted upward fining fine sand with cross bedding and becoming finer and thinner landward. Fujiwara *et al.* (2013) suggested that this layer were supplied from seaward associated with tsunami or storm surge events because of their depositional facies and distribution.

4-4-2. Higashi-Kandagawa Lowland

The geological columnar sections of the Higashi-Kandagawa Lowland were described in Fig. 4-7. The lowland deposit generally consists of sand layer, grayish mud layer and dark brownish red peat layer in ascending order.

The grayish mud layer was found beneath ~-1.0 m T.P. and composed of massive clay mostly. It was recognized that this layer covers the sand layer at the southern part of the lowland. The boundary between the grayish mud layer and the sand layer was ~ 2.2 m at the 0201-3 core and became deeper landward from the 0201-3 core. The sand layer was probably a part of sediment composing of sand barrier. In the grayish mud layer, at least two thin peaty sub-layers with

approximately 10-30 cm thickness were recognized. The altitude of lower sub-layer was ~-3 to -4 m T.P., and that of upper one was ~-2.5 m T.P. Radiocarbon ages from the bottom sediment of each sub-layer were estimated to be 5655-5750 cal BP (peat, -4.0 m T.P. of 0307-1 core) of the lower one and 4875-4985 cal BP (soil, -2.7 m T.P. of 0307-1 core) of the upper one. The mud layer overlying the upper peaty sub-layer yielded a calibrated age (4245-4420 cal BP, wood, -2.3 m T.P. of 0307-1 core). These ages suggest that sedimentation of each sub-layer occurred after ca. 5700 cal BP and during ca. 4400 cal BP to ca. 4900 cal BP. There were also a few centimeters thick sand layers wedging between the mud layers. These sand layers were inclined to be coarser and thicker at the northern part of the lowland.

On the other hand, the overlying dark brownish red layer developed above ~-2 m T.P. The top sediments of this layer, ~0.5 to 1.5 m beneath the ground surface, were eroded and disturbed by recent human activity such as cultivation. A radiocarbon age from the bottom of the peat layer was measured to be 2845-3005 cal BP (wood, -1.8 m T.P. of 0307-1 core). The content ratio of volcanic glasses on core sediment of the 0307-1 core shows an obvious peak with abundant pumice type volcanic glass at -1.91 to -1.93 m T.P., ~10 cm above the bottom of the peat layer (Fig. 4-8). The refractive indices of volcanic glasses, orthopyroxene and amphibole taken from this peak horizon were estimated to be 1.4998-1.5028 (n=28) to 1.5115-1.5140 (n=2), 1.7065-1.7082 (n=1, particle attached to glass) and 1.6700-1.6776 respectively. These results were similar to those of Kg tephra, 1.493-1.503, 1.704-1.709 and 1.669-1.685 (Machida and Arai 2003). According to the mineralogical feature and core stratigraphy, the tephra layer found in the lowland was identified as the Kg tephra. Therefore, the peat layer presumably developed since ca. 3200 cal BP.

4-4-3. Miyakodagawa Lowland

The three geological sections are shown in Fig.4-9: longitudinal sections; C-C' and E-E', transverse section; D-D'. The lowland deposit was divided into total of seven layers, sandy gravel layer, lower sandy mud layer, middle mud layer, upper sand layer, peat layer, top sand and top mud layer in ascending order.

The sandy gravel layer was distributed at ~ -10 to 30m T.P. overlying the basement rocks which composed of the Chichibu Belt and the Pleistocene sediments (Isomi and Inoue, 1972). Thickness of this layer showed difference between coring sites, which seems to reflect undulation of the basement rocks.

The lower sandy mud layer was found around -10 to -20 m T.P. showing approximately 5 m thickness. This layer was composed of silt to sandy silt deposits with gravels. Some molluscan shell fragments were observed in this layer. An intertidal molluscan, *Batillaria cumingii*, yielded from core samples during -6.3 m to -9.5 in site M-3 (C-C' and D-D' section, Fig. 4-9). A radiocarbon age of the shell fragments was estimated to be 7960-8125 cal BP.

The middle mud layer, composed of clay and silt, showed 5 to 15 m thickness. This layer included many molluscan shell fossils living in an inner bay such as *Batillaria zonalis* and *Dosinella* sp. The landward margins of this layer were distributed around site M-3, which indicates approximately the most expanding inner bay area during the Jomon Transgression. Of the lower part of this layer, two radiocarbon ages were measured to be 7400-7530 cal BP (shell fragment, -6.1 to -5.8 m T.P. of the site M-20, D-D' section) and 5770-5945 cal BP (shell fragment, -5.0 to -4.7 m T.P. of the site M-11, C-C' section). In addition to them, the top part provided a radiocarbon age, 5890-5930 cal BP (shell fragment, -1.6 m T.P. of 0228-2 core, E-E' section).

The upper sand layer was composed of poor-sorted fine to coarse sand with 2-5 m thickness. The bottom of this layer was found at 0 to -6 m T.P. Depositional facies and distribution trend of this layer imply riverine sediment supply. An intertidal molluscan shell yielded at -0.9 to -1.2 m T.P. in the site M-4 (C-C' section) and was identified to be *Batillaria cumingii*. This shell fragment indicated a radiocarbon age, 6710-6900 cal BP. In addition to this, four radiocarbon ages of charcoal samples taken from this layer were measured to be 6315-6440 cal BP (-0.2 to -0.5 m T.P. of the site M-20, D-D' section), 4075-4155 cal BP (-4.7 to -5.0 m T.P. of the site M-11, C-C' section) and 3580-3690 cal BP (-4.4 to -4.9 m T.P. of the site M-14, C-C' section) respectively from landward to seaward.

The peat layer is recognized at backswamps behind the main channels of the Miyakodagawa River and around the delta. This layer has developed in the northern area along the channel, and thickness reaches up to ~2 m. A radiocarbon age from the bottom of this layer was estimated to be 3465-3570 cal BP (plant fragment, -0.4 m T.P. of the 0302-1 core, E-E' section) and indicates peat deposited after ca. 3500 cal BP.

The top sand layer and the top mud layer contained poor-sorted medium to coarse sand or viscous clay respectively. These layers covered the upper sand layer and the peat layer widely. Thickness of the top sand layer and the top mud layer are up to ~5 m. On the southern area from the Miyakodagawa River channel, sandy deposits were often observed.

4-4-4. Shinjo Lowland

The lowland deposit of the Shinjo Lowland consists of mud layer, peat layer and sand layer from bottom to top (Fig. 4-10). The top sediment overlying the peat layer above ~1.0 m T.P.

was composed of muddy deposit with sub-rounded gravels. Thickness of this sediment decreased from landward to seaward, which implies riverine sediment and/or distributed artificial soil.

The mud layer was distributed beneath ~0.5 m T.P. mainly. Some shell fragments yielded in the lower part of this layer. Above ~ 2.0 m T.P., depositional facies changed to be humic and include many plant fragments.

The peat layer was divided into three parts, the upper, the middle and the lower, by intercalated muddy sediments and their lateral succession. The lower and the middle peat layer were distributed at the central part of the lowland, between 0212-6 core and 0213-1 core. The lower peat layer was recognized between approximately -2.0 m and -1.5 m T.P. Radiocarbon age from the bottom sediment of this layer was estimated to be 6435-6635 cal BP (plant fragment, -2.1 m T.P. of 0512-1 core). The middle peat layer was found around ~-1.0 m T.P. Of this layer, a radiocarbon age was measured to be 5645-5770 cal BP (plant fragment, -1.2 m T.P. of 1125-2 core). On contrary, the upper peat layer was found commonly in the lowland and distributed above ~-0.5 m T.P. A radiocarbon age taken from the bottom sediment was measured to be 5035-5300 cal BP (plant fragment, -0.6 m T.P. of 0512-1 core). Stratigraphy and radiocarbon ages suggest that each peat layer had developed after ca. 6500 cal BP, around 5750 cal BP and after ca. 5150 cal BP in ascending order.

The sand layer was recognized only at the eastern part of lowland. This layer contacted the mud layer and the lower and middle peat layers between 0218-7 core and 0212-6 core and was covered by the upper peat layers. The altitude transition of this layer was not concrete. Based on the geomorphological distribution in this lowland, the sand layer seemed to compose a part of sand barrier (BR I) sediments.

4-5. Results of diatom analysis

4-5-1. Rokkengawa Lowland

4-5-1-1. 0511-1 core

The 0511-1 core is a 550 cm long core taken at the central part of the Rokkengawa Lowland (Fig. 4-2, Fig. 4-11). According to diatom assemblages, core sediment was able to be divided into six diatom zones, R1-1 to R1-6 (Fig. 4-11). The diatom Zone R1-1 to R1-3 and R1-5 were corresponding to the mud layer, and the R1-4 and R1-6 were comparable to the lower peat and the upper peat layer respectively. In addition, the Zone R1-3 and R1-6 were subdivided into two subzones respectively.

Zone R1-1 (-4.35 to -4.50 m T.P.)

Zone R1-1 was characterized by dominance of *Cyclotella striata*. The percentage of *Cyclotella striata* reached up to ~30%. *Diploneis suborbicularis* and *Cocconeis scutellum*, brackish to marine water species, and *Staurosira construens*, a fresh to brackish water species, coexists with *C. striata* to showed approximately 10% abundance.

Abundance of brackish to marine water species suggests that sea area had been expanded around the core site. According to the habitat of *C. striata*, this diatom assemblage indicates that inner bay environment already occurred in sedimentation period of this zone.

Zone R1-2 (-4.00 to -4.30 m T.P.)

Zone R1-2 showed that *S. construens*, fresh to brackish species, appeared exclusively to make up more than half of total counts. On contrast, *Cyclotella striata* diminished significantly.

Fresh water species such as *Fragilaria* spp. and *Aulacoseira* spp. was found with ~5% abundance.

Abrupt increase of *S. construens* and accompanying some fresh water species, *Fragilaria* spp. and *Aulacoseira* spp. from the Zone R1-1 indicates that salinity decreased temporarily.

Zone R1-3 (-1.60 to -3.95 m T.P.)

Zone R1-3 was shared by brackish to marine water species mainly. In particular, *Cocconeis scutellum*, a brackish to marine water benthic species, showed dominant appearance at the whole part. This zone was subdivided into two parts by difference of main coexisting species. The lower subzone, R1-3a, is -2.20 to -3.95 m T. P., and the upper subzone, R1-3b, is -1.60 to -2.15 m T.P. In the R1-3a, *Tryblionella granulata* and *Thalassiosira* sp. made up ~10% respectively. These species decreased in the Zone R1-3b and are replaced by fresh to brackish water species such as *S. construens* and *Rhopalodia gibberula*. Besides, *Diploneis suborbicularis* made up about 10%.

Dominance of brackish to marine water species indicates that salinity increased. Dominantly appearance of *Cocconeis scutellum*, aquatic plant vegetation in saline water, suggests that the core site was located nearby these vegetations. Because the accompanying *Tryblionella granulata* and *Diploneis suborbicularis* were indicators of a mud flat in saline water, it is suggested that a tidal flat developed around the core site.

Zone R1-4 (-1.35 to -1.55 m T.P.)

Zone R1-4 was characterized by high percentage of fresh water species such as *Fragilaria* spp., *Eunotia* spp., *Aulacoseira* spp., *Gomphonema* spp. The percentage of them reached up to ~10%, ~20%, ~10% and ~5% respectively. On the contrary, brackish to marine

water species decreased drastically from the Zone R1-3 and made up a few percentages.

Dominance of fresh water species indicates that fresh water environment occurred in this period. Much of the abundant species were characteristic species prefer a stable water condition. Hence, it is suggested that a fresh water pond or marsh with shallow water depth developed.

Zone R1-5 (-0.80 to -1.30 m T.P.)

Zone R1-5 was characterized by abundance of brackish to marine water species. *Cocconeis scutellum* and *Diploneis suborbicularis* showed high amounts of total counts and made up around 20-30% respectively. In the upper part of this zone, *T. granulata* increased until ~20% to be dominant species. *Rhopalodia gibberula* and *Staurosira construens*, fresh to brackish water species, indicated to be higher amounts than the Zone R1-4. On the other hand, fresh water species was not recognized in this zone.

The diatom assemblages of this zone were similar to that of the Zone R1-3. This resemblance between the Zone R1-5 and R1-3 indicates that the Zone R1-5 had deposited under a tidal flat condition as well as the Zone R1-3.

Zone R1-6 (above -1.70 m T.P.)

In Zone R1-6, diatom fossils were very few except for the bottom horizon (- 1.7 m T.P.). *Aulacoseira* spp., a fresh water planktonic species, appeared exclusively with approximately 93% of total counts in the bottom horizon.

The bottom horizon of this zone is presumed to have deposited at the fresh water environment inferred from the abundant fresh water species. Absence of diatom fossils and the peaty depositional facies indicates that ground surface became drier and backmarsh developed

around the core site.

4-5-1-2. 0511-2 core

The 0511-2 core is a 350 cm long core and located at ~200 m northward from the 0511-1 core (Fig. 4-2, Fig. 4-12). According to diatom assemblages, core sediment was divided into five diatom zones, R2-1 to R2-5 (Fig. 4-12). The diatom Zone R2-1 to R2-2 and R2-4 were corresponding to the mud layer, and the R2-3 and R2-5 was comparable to the lower peat and the upper peat layer respectively. The Zone R2-2 showed sandy depositional facies with many plant fragments.

Zone R2-1 (-1.45 to -2.20 m T.P.)

Zone R2-1 was characterized by high amounts of brackish to marine water species such as *C. scutellum*, *D. suborbicularis*, *T. granulata* and *C. striata*. In particular, *Cocconeis scutellum* showed high percentage making up around 15-20% of total counts to be dominant in this zone.

Dominance of brackish to marine water species indicates that sediments of this zone accumulated under seawater affection. Because accompanying *Diploneis suborbicularis* and *Tryblionella granulata* are indicators of a mud flat in saline water (Kosugi, 1988), it is suggested that the Zone R2-1 had deposited in a tidal flat.

Zone R2-2 (-1.25 to -1.40 m T.P.)

In Zone R2-2, *Staurosira construens* yielded exclusively with about 60-70%. On contrary, *Cocconeis scutellum* decreased drastically from the Zone R2-1 to be few except for that at – 1.35 m T.P. Accompanying *Eunotia* spp. is found with ~10-15% abundance.

High percentage of *Staurosira construens*, fresh to brackish water species, and appearance of *Eunotia* spp. indicate that salinity decreased.

Zone R2-3 (-1.05 to -1.20 m T.P.)

Zone R2-3 was characterized by abundance of fresh water species. *Aulacoseira granulata*, a fresh water planktonic species, made up ~20-50%. Fresh water benthic species such as *Cymbella* spp. and *Pinnularia* spp. showed high percentages reaching to about 20-35%. On the other hand, brackish to marine water species and fresh to brackish water species were few in this zone.

Dominance of fresh water species indicates that environmental change from tidal flat to fresh water condition occurred. High percentage of *Aulacoseira granulata*, an indicator of a fresh water lake (Ando, 1990), and other benthic fresh water species suggest that a fresh water lake was formed and coastal sediments including some inland diatom species were supplied to the lake.

Zone R2-4 (-0.75 to -1.00 m T.P.)

Zone R2-4 was shared by brackish to marine species, e. g. *C. scutellum*, *D. suborbicularis* and *R. gibberula*. The fresh water species which were found in the Zone R2-3 diminished from the Zone R2-3 to become very few.

Dominance of brackish to marine water species suggests that affection of marine water reached again to the core site. The same abundant species as the Zone R2-1, i. e. *C. scutellum* and *D. suborbicularis*, are recognized and indicates that tidal flat environment developed again in this period.

Zone R2-5 (above -0.70 m T.P.)

Zone R2-5 was characterized by dominance of fresh water species such as *A. granulata*, *Cymbella* spp. and *Pinnularia* spp. In this zone, *Cymbella* spp., *Pinnularia* spp. and *Eunotia* spp. were dominant widely. *Aulacoseira granulata* made up ~75% of total counts at -0.6 m T.P., but it decreased upward. At the boundary between the Zone R2-4 and R2-5, *Tabellaria fenestrata* yielded high amounts to make up about 30% at the maximum. The middle part of this zone included no diatom fossil.

High amounts of fresh water species indicate appearance of a fresh water environment. The fresh water environment had been formed as shallow water marsh inferred from abundance of an indicator species of a marsh such as *T. fenestrata* (Ando, 1990) at the early period. Since then, the resemble assemblages found in the upper horizons of this zone suggest that fresh water lake developed around the core site. Increased benthic fresh water species and absence of diatom fossil imply that inland environment occurred associated with sedimentation of riverine deposits.

4-5-1-3. 0511-3 core

The 0511-3 core is a 400 cm long core. The core site is located at ~300 m northward from the 0511-1 core (Fig. 4-2). In this core site, the peat layer showed successive deposition and no muddy sediment wedging between them was recognized. According to diatom assemblages, core sediment was divided into three diatom zones, Zone R3-1, R3-2 and R3-3 (Fig. 4-13). While the diatom Zone R3-1 and R3-2 were corresponding to the mud layer, the R3-3 was comparable to the peat layer. The Zone R3-3 was subdivided into four subzones, R3-3a to R3-3d.

Zone R3-1 (-1.50 to -2.55 m T.P.)

Zone R3-1 was characterized by high percentage of brackish to marine water species. *Cocconeis scutellum* was dominant species and occupies ~20-30% of total counts. *Cyclotella striata* also was found in whole of this zone with around 5-10%. *Diploneis suborbicularis*, brackish to marine species, increased upward from ~0% to ~15% to transit the Zone R3-2.

Dominance of brackish to marine water species indicates that sediments of this zone accumulated under marine water affection. Accompanying *Cyclotella striata*, indicator of inner bay environment (Kosugi, 1988), suggests that an inner bay had occurred in this period. *Cyclotella scutellum* is one of indicators of aquatic plant vegetation in saline water (Kosugi 1988), which indicates that this zone deposited around the tidal flat where aquatic vegetations were distributed around.

Zone R3-2 (-1.30 to -1.45 m T.P.)

Zone R3-2 was characterized by abrupt increasing of *S. construens* to occupy nearly 40%. And *Diploneis suborbicularis*, brackish to marine benthic species, made up around 10-15%.

In this zone, salinity of the inner bay is implied from increased *S. construens*. Besides, accompanying *Diploneis suborbicularis*, one of indicators of a mud flat in saline water (Kosugi, 1988), suggests that salinity above the sea bottom is still high as well as the Zone R3-1. Therefore, this diatom assemblage transition is presumed to have been induced by fresh water inflow into the inner bay from coastal river.

Zone R3-3 (-0.05 to -1.25 m T. P.)

Zone R3-3 was characterized by dominance of fresh water species, such as *A. granulata*, *Pinnularia* spp. *Eunotia* spp. Brackish to marine water species and fresh to brackish water species declined drastically. The Zone R-3-3a, the lowest one at -1.25 to -1.30 m T.P., showed

higher amount of *T. fenestrata* and *Gomphonema* spp. than the other subzones. In the Zone R3-3b (-0.80 to -1.20 m T.P.), *A. granulata* and *Pinnularia* spp. replaced them to be dominant species. While *Aulacoseira granulata* decreased upward, *Pinnularia* spp. increased from the Zone R3-3a. The Zone R3-3c (-0.35 to -0.80 m T.P.) included few diatom fossils. And the diatom assemblage of the Zone R3-3d (-0.05 to -0.30 m T.P.) was similar to that of the Zone R3-3b and characterized by abundance of *A. granulata* and *Pinnularia* spp.

Abundance of fresh water species indicates that environmental change from tidal flat to fresh water condition. According to the diatom subzones, it is interpreted development of the fresh water area as following. At the early stage, this fresh water condition was a fresh water marsh with shallow depth inferred from abundance of *T. fenestrata*, an indicator species of a marsh (Kosugi, 1988) and *Gomphonema* spp. Above this subzone, high percentage of *A. granulata*, an indicator of a fresh water lake (Ando, 1990), and other benthic fresh water species suggest that a fresh water lake developed under riverine supplying of coastal sediments. No diatom fossil horizon found between the lacustrine deposits indicates that an inland environmental occurred temporarily.

4-5-2. Higashi-Kandagawa Lowland

4-5-2-1.0307-1 core

The 0307-1 core is a 550 cm long core taken at the central part of the Higashi-Kandagawa Lowland (Fig.4-3, Fig.4-14). According to its diatom assemblages, core sediment was divided into five diatom zones, i. e. Hk1-1 to Hk1-5 (Fig. 4-14). Furthermore, the Hk1-1 was divided into five subzones, the Zone Hk1-1a to Hk1-1e. Considering lateral succession

of geology shown in Fig.4-7, the Zone Hk1-1 to Hk1-3 were corresponding to the grayish mud layer. Of these diatom zones, the Zone Hk1-1d and Hk1-2 were comparable to the thin peat sub-layers respectively. The Zone Hk1-4 and Hk1-5 were corresponding to the brownish red peat layer.

Zone Hk1-1 (-2.78 to -4.65 m T.P.)

Zone Hk1-1 was characterized by dominance of brackish to marine water species. *Cyclotella striata* was abundant to make up around 20-30% of total counts. *Diploneis pseudovalis* and *Cocconeis scutellum*, which both are benthic species, also yielded at ~10% abundance.

According to the percentage of *Staurosira construens*, this zone was subdivided into five subzones; Hk1-1a: -4.59 to -4.65 m T.P., Hk1-1b: -4.47 to -4.58 m T.P., Hk1-1c: -4.04 to -4.46 m T.P., Hk1-1d: -3.96 to -4.03 m T.P., Hk1-1e: -2.78 to -3.95 m T.P. The Hk1-1b and Hk1-1d showed high amount of *S. construens*. While the percentage of *Staurosira construens* was around 20% in the Zone Hk1-1a and Hk1-1b, those in the Zone Hk1-1b and Hk1-1d reached up to ~40%. In the Zone Hk1-1b and Hk1-1d, *Aulacoseira* spp. was more abundant than the other subzones. In particular, the percentage in the Zone Hk1-1d was very high to occupy around 25%. The Zone Hk1-1e was characterized by increasing of *Cyclotella meneghiniana*, fresh to brackish planktonic species. *Staurosira construens* yielded at 20% abundance and increased upward at the top of this subzone.

Dominance of *Cyclotella striata*, an indicator of inner bay environment (Kosugi, 1988), suggests that the Zone Hk1-1 accumulated at an inner bay. Benthic species such as *D. pseudovalis* and *C. scutellum* indicates that tidal flat was distributed nearby the core site. High

percentage of *Staurosira construens* and some fresh water species in the Zone Hk1-1b and Hk1-1d indicates that salinity had decreased at least twice. Besides, increasing of *Cyclotella meneghiniana* and successive abundance of brackish to marine water species in the Zone Hk1-1e implies that the lake surface water was attenuated by riverine fresh water.

Zone Hk1-2 (-2.30 to -2.75 m T.P.)

Zone Hk1-2 was characterized by exclusive appearance of *S. construens* at around 60-80% abundance. In addition, *Aulacoseira granulata* increased from the Zone Hk1-1 to occupy around 10-20%. On the other hand, brackish to marine water species were almost imperceptible.

Remarkable increasing of *Staurosira construens* and *A. granulata* indicates that salinity of the inner bay decreased from the Zone Hk1-1. Considering the humic depositional facies, it is implied that this zone accumulated at a fresh to slightly brackish marsh or pond.

Zone Hk1-3 (-2.05 to -2.29 m T.P.)

Zone Hk1-3 also showed high percentage of *S. construens* as well as in the Zone Hk1-2. However, some brackish to marine water species such as *C. striata*, *D. suborbicularis*, *C. scutellum* and *Achnanthes submarina* yielded at around 5-20% abundance respectively.

Obvious increasing of brackish to marine water species indicates that salinity increased in this period. Because *Diploneis suborbicularis*, an indicator of a mud flat in saline water, showed the highest percentage among these species, it is high possibility that muddy tidal flat was distributed around the core site.

Zone Hk1-4 (-1.80 to -2.04 m T.P.)

Zone Hk1-4 was characterized by dominance of fresh water planktonic species *A.*

granulata which made up ~40%. Besides, *Staurosira construens* also was commonly found at ~30-40% abundance. On the other hand, brackish to marine water species were few.

Because *Aulacoseira granulata* is an indicator of a fresh water lake (Ando, 1990), it is suggested that a fresh water lake occurred in this period.

Zone Hk1-5 (-0.20 to -1.75 m T.P.)

Zone Hk1-5 was shared by fresh water species such as *A. granulata*, *Pinnularia* spp. *Eunotia* spp. and *Fragilaria* spp. Benthic species increased upward and reached up to around 40%. On contrast, the percentage of *Staurosira construens* decreased from the Zone Hk1-4.

Upward increasing of benthic fresh water species indicates that the fresh water marsh or pond had become shallower associated with accumulation of peaty deposits.

4-5-2-2. 0308-1 core

The 0308-1 core is a 435 cm long core (Fig.4-15). The core site is located at ~1.3 km southward from the 0307-1 core. According to diatom assemblages, core sediment was divided into five diatom zones, Hk2-1 to Hk2-5 (Fig. 4-15). Considering lateral succession of geology shown in Fig.4-7, the author suggests that the Zone Hk2-1 to Hk2-4 were corresponding to the grayish mud layer. Of these diatom zones, the Zone Hk2-3 was comparable to the upper one of thin peat sub-layers. The Zone Hk2-5 was corresponding to the brownish red peat layer.

Zone Hk2-1 (-3.20 to -3.70 m T.P.)

Zone Hk2-1 was characterized by dominance of brackish to marine water species such as *C. striata*, *D. pseudovalis*, *D. suborbicularis* and *C. scutellum*. *Cyclotella striata* yielded dominantly at around 15-40% abundance of total counts.

Dominance of *Cyclotella striata*, an indicator of inner bay environment (Kosugi, 1988), suggests that this zone accumulated at an inner bay area.

Zone Hk2-2 (2.75 to -3.15 m T.P.)

Zone Hk2-2 was shared by brackish to marine water species and fresh to brackish water species. Benthic brackish to marine water species, *D. pseudovalis*, *D. suborbicularis* and *C. scutellum*, showed large percentage as those in the Zone Hk2-1. However, *Cyclotella striata* declined upward from ~30% to less than ~5%. On contrast, *Cyclotella meneghiniana*, a fresh to brackish species, showed much higher percentage than that in the Zone Hk2-1. In the top part of this zone, *S. construens* increased largely from the Zone Hk2-1 and reached up to ~40%.

Increasing of *Cyclotella meneghiniana* and abundance of benthic brackish to marine water species indicate that the lake surface water was attenuated by riverine fresh water.

Zone Hk2-3 (-2.40 to -2.70 m T.P.)

Zone Hk2-3 was characterized by huge percentage of *S. construens*. The percentage of it reached to ~70%. In the upper part of this zone, fresh water species were found. In particular, *Aulacoseira* spp. yielded abundantly to make up approximately 10%. Much of brackish to marine water species diminished drastically.

Dominance of *Staurosira construens* and accompanying of some fresh water species indicates that salinity of the inner bay decreased. Considering the humic depositional facies, it is implied that this zone accumulated at a fresh to slightly brackish marsh or pond.

Zone Hk2-4 (-1.90 to -2.35 m T.P.)

Zone Hk2-4 was characterized by huge percentage of *S. construens* and appearance of

brackish to marine water species. *Cyclotella striata*, *Diploneis suborbicularis* and *Cocconeis scutellum* occupied around 3-5% respectively.

Appearance of brackish to marine water species indicates that salinity became slightly higher than that in the Hk2-3 in this period.

Zone Hk2-5 (-1.45 to -1.85 m T.P.)

Zone Hk2-5 was shared by *Staurosira construens* and *Aulacoseira* spp. Benthic fresh water species, i. e. *T. fenestrata*, *Gomphonema* spp., *Eunotia* spp. and so on, were found. *Aulacoseira* spp. increased upward and reached almost half percentage of total counts.

The abundance of *Aulacoseira* spp., a fresh water planktonic species, suggests that a fresh water pond developed in this period.

4-5-3. Miyakodagawa Lowland

4-5-3-1. 0429-1 core

The 0429-1 core is a 275 cm long core taken at the backmarsh distributed at the northern side of the Miyakodagawa River (Fig. 4-4). According to diatom assemblages, core sediment was divided into five diatom zones, M1-1 to M1-5 (Fig. 4-16). The Zone M1-1 to M1-3 was corresponding to the middle mud layer. The Zone M1-4 was the lowest part of the peat layer, and the much of the peat layer above this and the top mud layer was classified to the Zone M1-5.

Zone M1-1 (-2.25 to -2.75 m T.P.)

Zone M1-1 was characterized by dominance of brackish to marine water species. *Cyclotella striata* was abundant making up about 20% of total counts.

High amount of *Cyclotella striata* indicates inner bay environment due to their habitats.

The molluscan shells of the middle mud layer support this interpretation.

Zone M1-2 (-1.55 to -2.25 m T.P.)

Although Zone M1-2 also showed high amounts of brackish to marine species, *C. striata* decreased to around 20-30% and was replaced by *C. scutellum*, a indicator of aquatic plant vegetation in saline water (Kosugi 1988).

High amount of brackish to marine water species indicates that inner bay environment have occurred in this zone continuously from the Zone M1-1. However, dominance of a benthic species *Cocconeis scutellum* suggests that water depth in the core site became shallower than the Zone M1-1 to induce salinity decreasing.

Zone M1-3 (-0.90 to -1.55 m T.P.)

Zone M1-3 was shared by *Staurosira construens* and *C. striata*. *Staurosira construens* increased drastically from the Zone M1-2 and occupied around 20%. The percentage of *Cyclotella striata* was ~10-20% abundance and became outstanding at the top of this zone (-0.90 m T.P.).

Diatom assemblage of this zone indicates that salinity of an inner bay became even lower than the Zone M1-2. However, at the last stage of this zone, temporarily abundant peak of *C. striata*, brackish to marine water planktonic species, implies that salinity rose and water depth increased.

Zone M1-4 (-0.75 to -0.90 m T.P.)

Zone M1-4 was characterized by dominance of fresh water species such as *Eunotia* spp., *Frustulia rhomboids*, *T. fenestrata* and *Encyonema gracile*. The percentage of *Eunotia* spp. reached ~20% of total counts.

Dominance of fresh water species indicates that fresh water environment occurred. Peaty material composing this zone suggest that fresh water pond or marsh formed and plant fragment accumulated on the bottom at the stable condition without riverine power.

Zone M1-5 (2.05 to -0.75 m T.P.)

In this zone, no diatom fossils are recognized. Considering the depositional facies, the author suggests that backmarsh environment with lower water level than one of the M1-4 was formed.

4-5-4. Shinjo Lowland

4-5-4-1. 0512-1 core

The 0512-1 core is a 425 cm long core taken at the central part of the Shinjo Lowland (Fig. 4-5, Fig.4-9, and Fig. 4-16). According to diatom assemblages, core sediment was divided into six diatom zones, S1-1 to S1-6 (Fig. 4-17). In addition, the Zone S1-2 was subdivided into three subzones, i. e. Zone S1-2a, S1-2b and S1-2c. The boundaries between the diatom zones were comparable to geological boundaries. While the Zone S1-1, S1-3 and S1-4 are corresponding to the mud layer, the Zone S1-2, S1-4 and S1-5 to 6 were comparable to the lower, middle and upper peat layer respectively.

Zone S1-1 (-2.15 to -2.45 m T.P.)

Zone S1-1 was characterized by dominance of brackish to marine water species. In particular, *Cocconeis scutellum* and *Cyclotella striata* showed high percentage. While *Cocconeis scutellum* declined upward from ~20% to ~5%, *C. striata* increased up to around 50%.

Dominance of brackish to marine water species indicates the accumulation under affection of marine high salinity water. Due to the habitats of dominant species, it is suggested that inner bay or tidal flat was distributed around the core site in this period.

Zone S1-2 (-1.50 to -2.10 m T.P.)

Zone S1-2 was characterized by abundance of fresh water and fresh to brackish water species such as *S. construens*, *Aulacoseira* spp., and *Tabellaria* spp. Depending on the amounts of these diatom species, this zone was subdivided into three subzones: S1-2a, S1-2b and S1-2c. The Zone S1-2a laying at -1.95 to -2.10 m T. P. showed high percentage of *S. construens*. The Zone S1-2b (-1.75 to -1.90 m T.P.) was shared mainly by fresh water species. The percentages of *Aulacoseira* spp. and *Tabellaria* spp. were around 20% respectively. In the Zone S1-2c laying at -1.25 to -1.70 m T.P., *S. construens* yielded dominantly and *C. striata* accompanies to it. The abundance spikes of *Cyclotella striata* were recognized in this subzone.

Increasing of fresh to brackish and fresh water species indicates salinity reduction. Succession of diatom assemblage from the Zone S1-2a to S1-2b suggests that fresh water marsh had been developed. Appearance of *Cyclotella striata* in the Zone S1-2c implied that submergence occurred to have formed an inner bay.

Zone S1-3 (-1.25 to -1.45 m T.P.)

Zone S1-3 was characterized by dominance of brackish to marine water species. The main diatom components of this zone were *C. striata* and *Nitzschia frustulum*. While *Nitzschia frustulum* was dominant in the lower part, *C. striata* replaced it in the upper part.

Abundance of brackish to marine water species indicates submergence beneath marine water surface. High percentage of *Cyclotella striata*, an indicator of inner bay environment

(Kosugi, 1988), suggests that an inner bay environment had developed in this period. Successive environmental change occurred inferred from the vertical transition of diatom assemblage.

Zone S1-4 (-1.00 to -1.20 m T.P.)

Zone S1-4 showed similar diatom assemblage as those in the Zone S1-2b. *Staurosira construens* yielded dominantly at 60-80% abundance. *Aulacoseira* spp. and *Tabellaria* spp. yielded accompanying to *Aulacoseira* spp.

The diatom assemblage of this zone suggests that a fresh water marsh developed again in this period.

Zone S1-5 (-0.70 to -0.95 m T.P.)

Zone S1-5 showed similar diatom assemblage as those in the Zone S1-3. The main diatom components of this zone were *C. striata*, *A. submarina* and *N. frustulum*. In whole of this zone, *Cyclotella striata* yielded abundantly and occupies around 20%. While *Nitzschia frustulum* was dominant in the lower part, *A. submarina* replaced it in the upper part.

Abundance of brackish to marine water species suggests that a submergence beneath marine water surface occurred. High percentage of *Cyclotella striata* and *Achnanthes submarina* indicates that an inner bay had developed in this period. The vertical transition of diatom assemblage implies a successive environmental change.

Zone S1-6 (0.80 to -0.65 m T.P.)

Zone S1-6 was characterized by dominance of fresh to brackish and fresh water species. This zone included few brackish to marine water species. The lower part of this zone showed extremely high amount of *S. construens*, ~40-60% and accompanying of *Tabellaria* spp. at

around 10% abundance. Besides, *Aulacoseira* spp., fresh water planktonic species, increased upward up to approximately 60%. In the middle part, diatom fossils were few not enough for analysis. The main components of the upper part of this zone were *Pinnularia* spp. and *Aulacoseira* spp. occupying around 20% respectively.

High percentage of fresh water and fresh to brackish water species indicates that salinity decreased drastically. Appearance of *Tabellaria* spp., an indicator species of a fresh water marsh, suggest that sedimentary environment had been a fresh to slightly brackish water marsh with shallow water depth at the early stage of this zone. According to the upward increasing of *Aulacoseira* spp., fresh water planktonic species, the marsh are presumed to have changed to a fresh water pond after then. The no diatom fossil horizon and a large amount of fresh water benthic species indicate that the fresh water pond changed to an inland environment.

4-6. The Middle to Late Holocene sedimentary environmental changes

4-6-1. Paleo-environmental changes of alluvial lowlands

4-6-1-1. Rokkengawa Lowland

Based on the stratigraphy and chronology of the lowland deposits and diatom fossil analysis in core sediments, paleo-environmental changes were reconstructed as following (Fig.4-18).

In the Rokkengawa Lowland, an inner bay environment had occurred associated with the Jomon Transgression at latest after ca. 6200 cal BP. The muddy deposits including many inner bay

molluscan fossils and abundant of *C. striata* indicate that an inner bay expanded in the central to inland area of the lowland. In contrast, a sandy tidal flat formed in the southern part of the lowland inferred from distribution of the sandy mud layer. In addition, the diatom assemblage of the Zone R1-2 suggests that temporal salinity decline had occurred before ca. 4200 cal BP. Accurate timing of the low salinity event was not determined due to lack of radiocarbon age around the Zone R1-2.

After ca. 4200 cal BP, a muddy tidal flat and a sandy tidal flat had developed widely in the lowland. The muddy tidal flat was distributed at the northern part, which sediments are characterized by benthic brackish to marine water species and large number of molluscan shells. On the other hand, the sandy tidal flat is distributed at the southern part. Based on the results of diatom analysis shown as the Zone R1-3b, R2-2 and T3-2, the upper part of the tidal flat sediment is presumed to have deposited under the less salty water condition than the lower part.

During ca. 4200 cal BP to 3800 cal BP, environmental change from tidal flat to fresh water pond/marsh occurred. The lower peat layer showed humic depositional facies and abundance of fresh water diatom species (the Zone R1-4, R2-3 and R3-3).

After ca. 3800 cal BP, affection of marine water flowed into the central part of the lowland again. The mud layer and the sandy mud layer accumulated over the lower peat layer. The change of the depositional facies and diatom assemblages presumed that a muddy tidal flat and a sandy tidal flat appeared again. The inland margin of tidal flat environment is supposed to be located around the 0511-2 core site by distribution area of the mud layer. Both of these tidal flat environments had continued until ca. 3400 cal BP inferred from radiocarbon ages. In contrast, the fresh water pond/marsh environment, which lasted from 4200 to 3800 cal BP in the northern part of the Rokkengawa Lowland.

After ca. 3400 cal BP, a fresh water pond/marsh had formed widely in the Rokkengawa Lowland. The upper peat layer is recognized almost all area of the lowland. Diatom assemblages of this layer shown in the Zone R1-6, R2-5 and R3-3 indicate that fresh water pond or marsh had been formed and changed to inland environment gradually. The thick peat layer without wedging layers implies a stable environment. Fujiwara *et al.* (2013) pointed to the possibility that environmental change from inner bay or tidal flat to fresh water pond/marsh in ca. 3400 cal BP occurred associated with sedimentation of a kind of event sediment, such as tsunami and storm event, which identified as the fine sand layer in this lowland.

4-6-1-2. Higashi-Kandagawa Lowland

Based on the stratigraphy and chronology of the lowland deposit and diatom fossil analysis, paleo-environmental change is reconstructed as following (Fig.4-18).

After the Jomon Transgression, an inner bay environment had been distributed widely in the lowland. Diatom assemblages indicated that the lower part of the grayish mud layers was an inner bay sediments (the diatom Zone Hk1-1 to Hk1-3; Hk2-1 to Hk2-2). The inner bay environment had already been formed before ca. 5700 cal BP and lasted until ca. 5000 cal BP from radiocarbon ages.

This inner bay environment has at least two times of repetitive salinity changes before ca. 5000 cal BP. The first low salinity stage, corresponding to the lower thin peat layer of the 0307-1 core, occurred just after ca. 5700 cal BP. After then, the Zone Hk1-1b suggests that other low salinity environment had occurred before ca. 5700 cal BP. The salinity reduction occurred at the 0308-1 core probably corresponding to either the Zone Hk1-1b or the Zone Hk1-1d by horizontal

geological succession.

The surface water had become less salty based on the abundance of fresh to brackish water diatom species in the diatom Zone Hk1-1e and Hk2-2. As a result of salinity reduction, a fresh to slightly brackish water pond had been formed in ca. 5000 cal BP, characterized by accumulation of the upper thin peat layer including large amounts of *Staurosira construens* and *Aulacoseira* spp. (the Zone Hk1-2 and Hk2-3).

During ca. 4300 to ca. 3200 cal BP, marine water affected to the water area in the lowland again. Because brackish to marine water diatom species were observed in the Zone Hk1-3 and Hk2-4, inner bay or tidal flat environment had been occurred around both of the core sites.

After ca. 3200 cal BP, a fresh water pond appeared, after then it changed to inland wetland gradually. This environmental change is suggested by following two points: one is depositional facial change from the grayish mud layer to the brownish red peat layer; another is dominance of fresh water diatom species in the Zone Hk1-4 to Hk1-5 and Zone Hk2-5. Timing of this environmental change is estimated to be ca. 3200 cal BP by radiocarbon ages and Kg tephra.

4-6-1-3. Miyakodagawa Lowland

In the Miyakodagawa Lowland, intertidal molluscan shells of the lower sandy mud layer indicate that affection of marine water had reached to the lowland after sedimentation of this layer. Radiocarbon ages suggest that this environment occurred after ca. 8000 cal BP.

The middle mud layer is interpreted by the diatom assemblage (the Zone M1-1) and molluscan fossils as the inner bay sediment of the expanding sea area occurred associated with the Jomon Transgression. The distribution of the middle mud layer and radiocarbon ages indicates that

inner bay had expanded most widely around 6800 cal BP. The shoreline is presumed to have been distributed at ~4.5 km landward from the present coastal line. The upper sand layer covers the inner bay sediments (the middle mud layer) and radiocarbon ages become younger from landward to seaward (Fig.4-5), this layer is interpreted to be deltaic front sediments filling up the inner bay after the Jomon Transgression.

The upper part of the middle mud layer includes a smaller amount of brackish to marine planktonic species than those of the lower part, which implies that fresh water from rivers affect lacustrine algae more strongly by becoming shallow water. However, the percentage of brackish to marine water species is still high to reach more than 20% (the Zone M1-1), implying inflow of seawater. Radiocarbon ages of the middle mud layer suggest that inner bay environment had existed continuously up to at least ca. 5500 cal BP. However, it is remarked that planktonic brackish to marine water species *Cyclotella striata* showed temporal increase at the top of the middle mud layer, indicating relative rising of inner bay water level occurred around 3500 cal BP.

The peat layers, because shared by fresh water diatom species, are presumed to have developed at a fresh water marsh or pond. Radiocarbon ages from the bottom of this layer indicated that environmental change from inner bay to fresh water condition formed around 3500 cal BP. Few diatom fossil above the lowest part of the peat layer seems to be caused by relative falling of water level associated with developing backmarsh. Since then, the top mud layer has been developed in backmarsh environment. After the middle stage of the Yayoi period, some archeological sites formed on natural levees along the Miyakodagawa River.

4-6-1-4. Shinjo Lowland

Based on the stratigraphy and chronology of the lowland deposit and diatom fossil analysis, paleo-environmental change is reconstructed as following (Fig.4-18).

Associated with the Jomon Transgression, an inner bay formed in the Shinjo Lowland. The mud layer with abundant *C. striata* (the diatom Zone S1-1) is presumed to have accumulated in this inner bay.

After around 6500 cal BP, the diatom Zone S1-2 indicates that fresh to brackish environment occurred and the lower peat layer deposited. Considering the geomorphological feature of this lowland, is the author suggests that environmental change from inner bay to fresh to brackish pond/marsh was induced by developing of BR I in seaward margin of the lowland.

Since then, alternative layers composed of the mud layers and the peat layers indicates repeatedly subsidence and emergence. The fresh water species rich assemblage in the diatom Zone S1-2, S-4 and S1-6 imply that salinity had decreased at least three times after ca. 6500 cal BP. Timings of environmental changes from inner bay to fresh water pond/marsh in the diatom Zone S1-2, S-4, and S1-6 were estimated by radiocarbon ages to be after ca. 6500 cal BP, in ca. 5750 cal BP and after ca. 5150 cal BP respectively.

After ca. 5150 cal BP, a fresh water pond/marsh had been formed continuously. The diatom assemblage succession in the Zone S1-6 indicates that this pond/marsh had been buried to become inland area.

4-6-2. Synthesis of environmental changes of alluvial lowlands

Geological survey and diatom analysis revealed the Late Holocene paleo-environmental change of alluvial lowlands around the Lake Hamana (Fig. 4-18). Comparison of these results

provides following four common features about the environmental changes in the region.

Temporal developments of fresh to brackish water pond or marshes after ca. 6500 cal BP were recognized. In the Shinjo Lowland, fresh water pond or marsh had formed at least three times during ca. 6500 cal BP to ca. 5150 cal BP. In the Higashi-Kandagawa Lowland, at least two salinity reductions were found before ca. 5700 cal BP. Environmental change from inner bay to fresh to brackish water pond in the Rokkengawa Lowland occurred before 4200 cal BP. Because these three lowlands are closed by the most inland coastal sand barriers (BR I), such similar salinity-decline events in the three lowlands can be explained by development of BR I. Around the Japanese Islands, highest relative sea-level was observed in ca. 7000 cal BP and gradual lowering since then. Therefore, it is suggested that the stabilization or falling of relative sea-level induced development of coastal sand barriers to shelter the paleo-inner bays at alluvial lowlands after in ca. 6500 cal BP. In addition, re-generation of inner bay environment recognized between these fresh water pond/marsh sediments suggests that coastal sand barriers had not been completely closed paleo-inner bays and fresh water environment is not stable in this period

It is recognized that timing of pronounced developments of fresh water pond/marsh concentrates around 5000 cal BP. In the Shinjo Lowland, environmental change from inner bay to fresh water pond/marsh occurred at ca. 5150 cal BP. Such environmental change was found in the Higashi-Kandagawa Lowland in ca. 5000 cal BP. Because both of two lowlands are closed by BR I, environmental changes from inner bay or tidal flat to fresh water pond/marsh were caused by emergence of the BR I in ca. 5000 to 5150 cal BP.

Between ca.4500 cal BP and ca. 3200 cal BP, signals of seawater inflow was widely observed in lowlands around the Lake Hamana. Environmental change from fresh water

pond/marsh to tidal flat or inner bay occurred in the both Rokkengawa and the Higashi-Kandagawa Lowlands. Timing of the events were estimated to be ca. 3800 cal BP and 4200 cal BP in the Rokkengawa and Higashi-Kandagawa Lowlands, respectively. In addition, the water depth became deeper just before ca. 3500 cal BP in the Miyakodagawa Lowland. Considering the geomorphological setting around the Lake Hamana, the author suggests that collapses of coastal sand barriers distributed at the front of lowlands.

In ca.3500 cal BP to 3200 cal BP, fresh water pond/marshes developed. Environmental change from tidal flat or inner bay to fresh water pond/marsh occurred in this period were recognized in the Rokkengawa Lowland, the Higashi-Kandagawa Lowland and the Miyakodagawa Lowland. These Timings were estimated to be ca.3400, 3200, and 3500 cal BP in the Rokkengawa Lowland, the Higashi-Kandagawa Lowland and the Miyakodagawa Lowland, respectively. Because the peaty deposits are seemed to accumulate continuously to the present inferred from no wedging muddy deposit, fresh water pond or marsh environments are presumed to have been quite stable after this period

Table 4-1. AMS radiocarbon ages from study area are calibrated with CALIB 6.0 (Stuiver et al., 2004) using dataset of IntCal09.14c (Reimer et al., 2009) and Marine09.13c (Reimer et al., 2009). Location map of the core sites are shown Fig. 4-1 to Fig. 4-4.

Alluvial lowland	Core no.	Elevation (m)	Sample material	$\delta^{13}\text{C}$ (permil)	^{14}C age (yr BP $\pm 1\sigma$)	calibrated age (cal BP, 2σ)	Labo No.
Rokkengawa	0410-3	-2.2	shell fragment (<i>Macoma tokyoensis</i>)	-1.12 \pm 0.16	5805 \pm 20	6175 - 6280	PLD-13142
	0410-3	-0.2	wood	-29.57 \pm 0.14	535 \pm 15	520 - 555	PLD-13145
	0423-4	-1.0	plant material	-27.96 \pm 0.14	3510 \pm 20	3705 - 3845	PLD-13144
	0423-5	-0.9	chacoal	-26.92 \pm 0.11	3600 \pm 20	3845 - 3935	PLD-14713
	0423-5	-0.5	plant material	-28.33 \pm 0.14	3215 \pm 20	3385 - 3465	PLD-14712
	0423-6	-0.7	seed	-24.94 \pm 0.12	3080 \pm 20	3250 - 3365	PLD-13143
	1010-1	0.0	seed	-25.82 \pm 0.12	350 \pm 15	320 - 395	PLD-14766
	0511-1	-1.3	plant material	-27.10 \pm 0.13	3820 \pm 25	4145 - 4295	PLD-17933
	0511-1	-1.55	wood	-28.44 \pm 0.20	3840 \pm 25	4150 - 4300	PLD-17935
	0307-1	-1.9	wood	-29.67 \pm 0.63	2,820 \pm 30	2845 - 3005	IAAA-110739
	0307-1	-2.3	wood	-29.60 \pm 0.52	3,900 \pm 30	4245 - 4420	IAAA-110740
Miyakodagawa	0307-1	-2.7	soil	-26.16 \pm 0.45	4,400 \pm 20	4875 - 4985	IAAA-110741
	0307-1	-4.0	peat	-27.46 \pm 0.33	4,990 \pm 20	5655 - 5750	IAAA-110742
	0228-2	-1.6	shell fragment (<i>Batillaria cumingii</i>)	-1.72 \pm 0.13	5135 \pm 20	5890 - 5930	PLD-13155
	0302-1	-0.4	plant material	-30.14 \pm 0.10	3295 \pm 20	3465 - 3570	PLD-14711
	M-3	-9.5 ~ -6.3	shell fragment (<i>Batillaria cumingii</i>)	-0.05 \pm 0.13	7580 \pm 25	7960 - 8125	PLD-14099
	M-4	-1.2 ~ -0.9	shell fragment (<i>Batillaria cumingii</i>)	-1.99 \pm 0.12	6340 \pm 30	6710 - 6900	PLD-14276
	M-11	-8.0 ~ -7.7	shell fragment (<i>Dosinella</i> sp.)	-2.42 \pm 0.11	5495 \pm 25	5770 - 5945	PLD-14710
	M-11	-5.0 ~ -4.7	chacoal	-28.84 \pm 0.14	3715 \pm 20	4075 - 4155	PLD-14709
	M-14	-4.9 ~ -4.4	chacoal	-27.28 \pm 0.11	3390 \pm 20	3580 - 3690	PLD-14098
	M-19	-0.5 ~ -0.2	chacoal	-27.41 \pm 0.14	5610 \pm 25	6315 - 6440	PLD-14275
	M-20	-6.1 ~ -5.8	shell fragment (<i>Batillaria zonalis</i>)	2.14 \pm 0.13	6950 \pm 30	7400 - 7530	PLD-14277
Shinjo	0512-1	-0.55	plant material	-22.9	4490 \pm 40	5035 - 5300	Beta- 282561
	0512-1	-2.1	plant material	N/A	5730 \pm 40	6435 - 6635	Beta- 282560
	1125-2	-1.2	plant material	-26 \pm 1	5000 \pm 35	5645 - 5770	NUTA2-15140

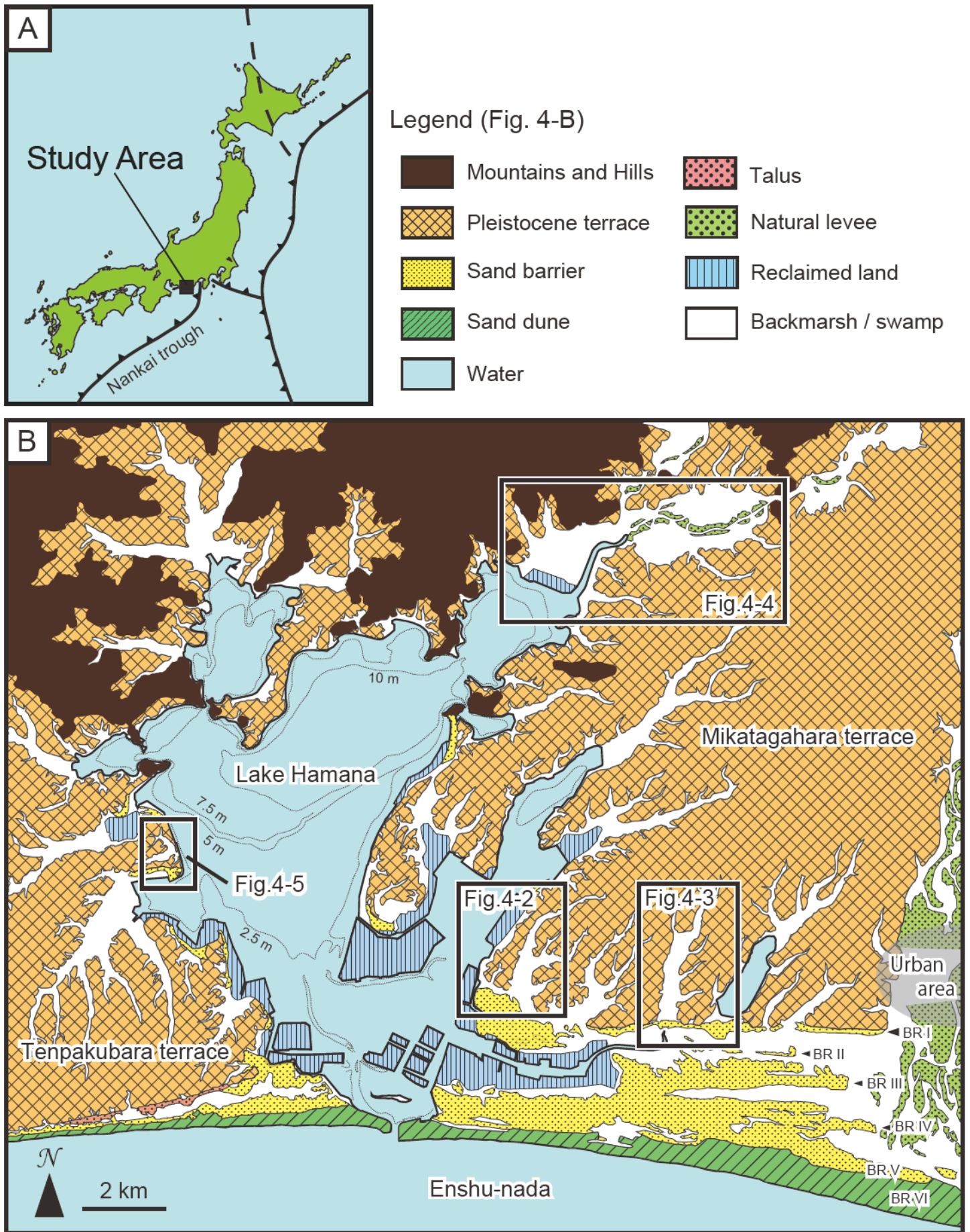


Fig. 4-1. Location map of the investigated lowlands around the Lake Hamana. 4-1A: location map of the Lake Hamana. 4-1B: Geomorphological classification map and location map of alluvial lowlands.

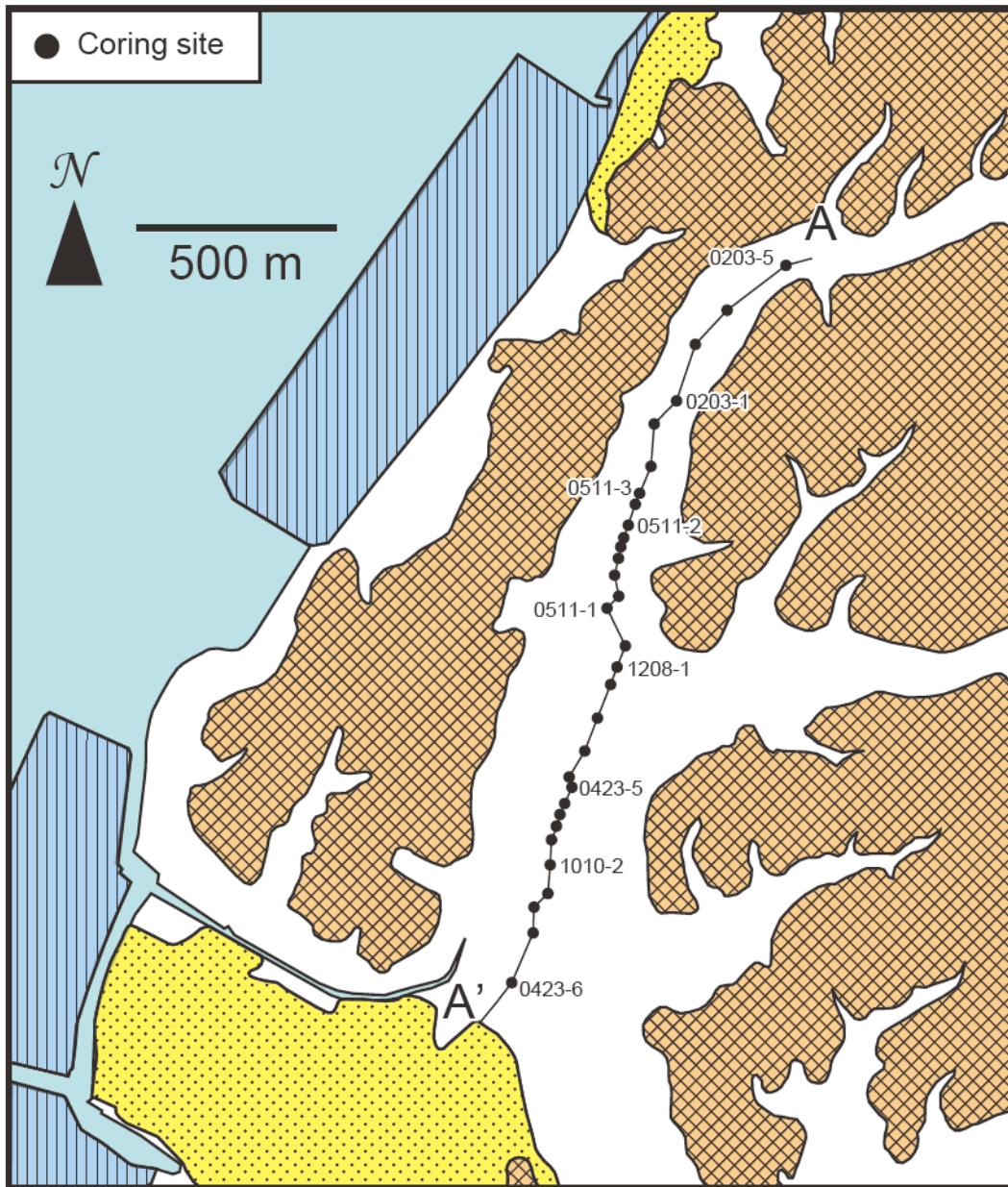


Fig. 4-2. Location map of coring sites and geological section (A-A' section) in the Rokkengawa Lowland. Black circles represent location of coring sites.

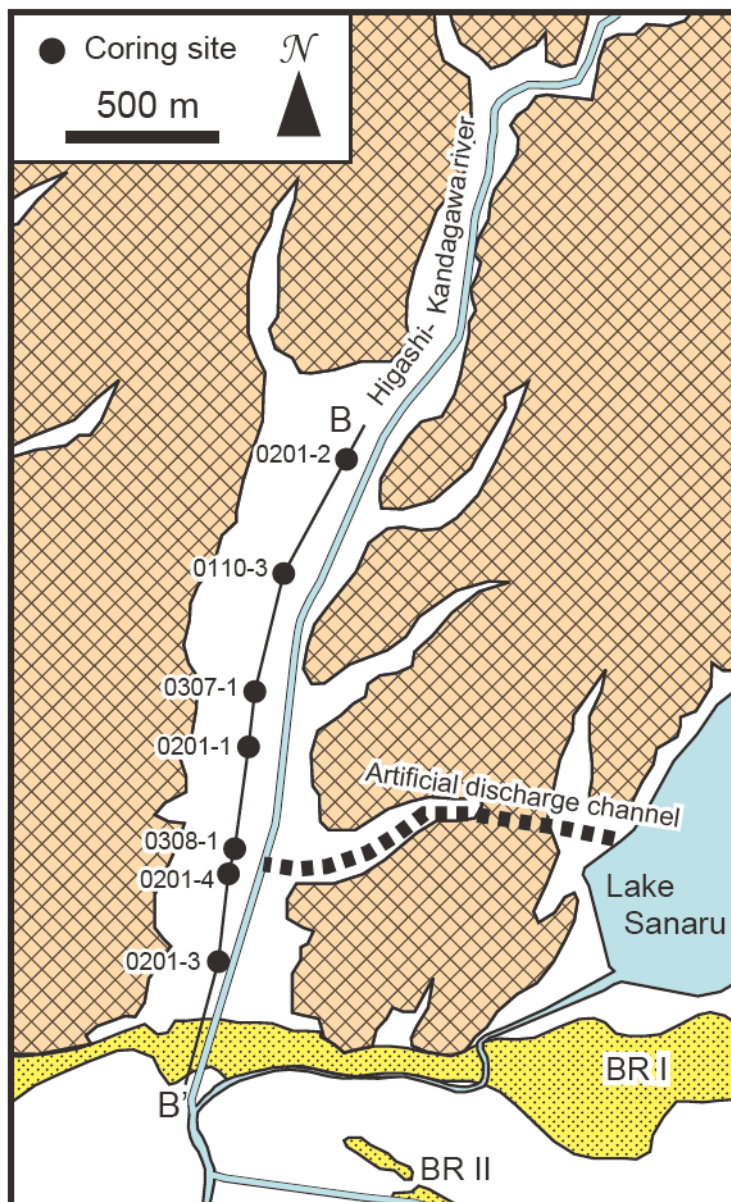


Fig. 4-3. Location map of coring sites and geological section (B-B' section) in the Higashi-Kandagawa Lowland. Black circles represent location of coring sites.

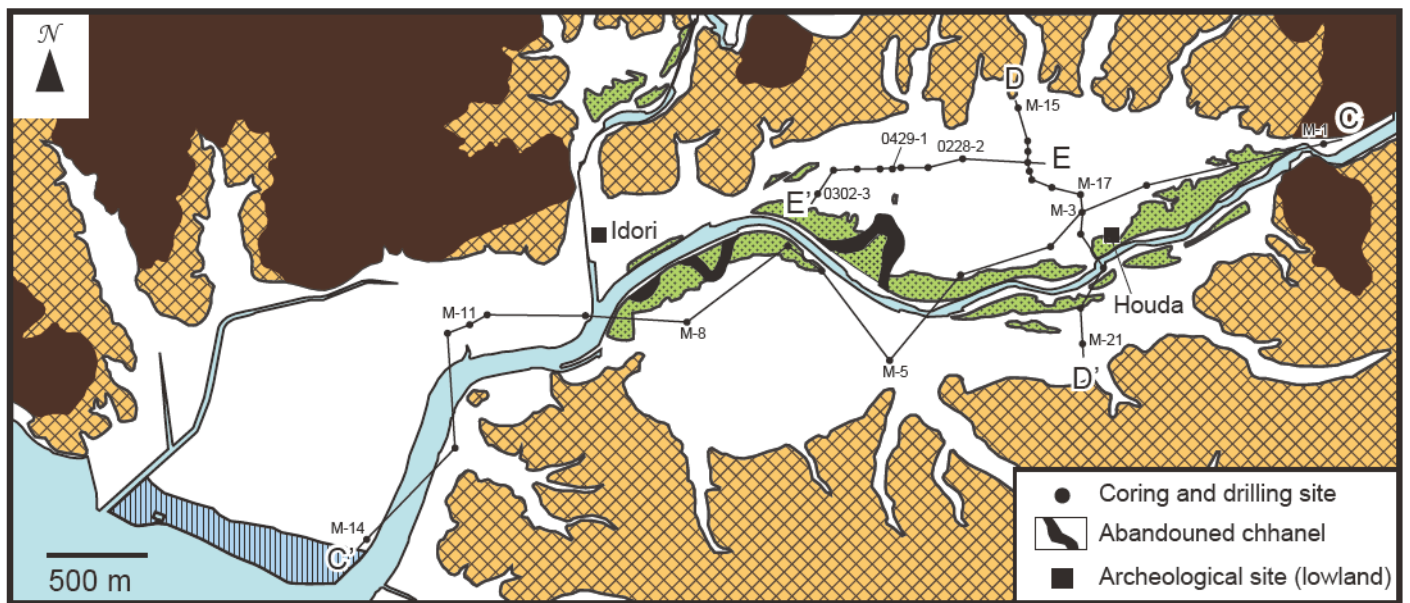


Fig. 4-4. Location map of coring sites and geological sections (C-C' , D-D' and E-E' section) in the Miyakodagawa Lowland. Abandoned channel of Miyakodagawa River are distributed around the middle part of the lowland. Black colored squares show location of archeological remains on natural levees, and black circles represent location of coring site and drilling site.

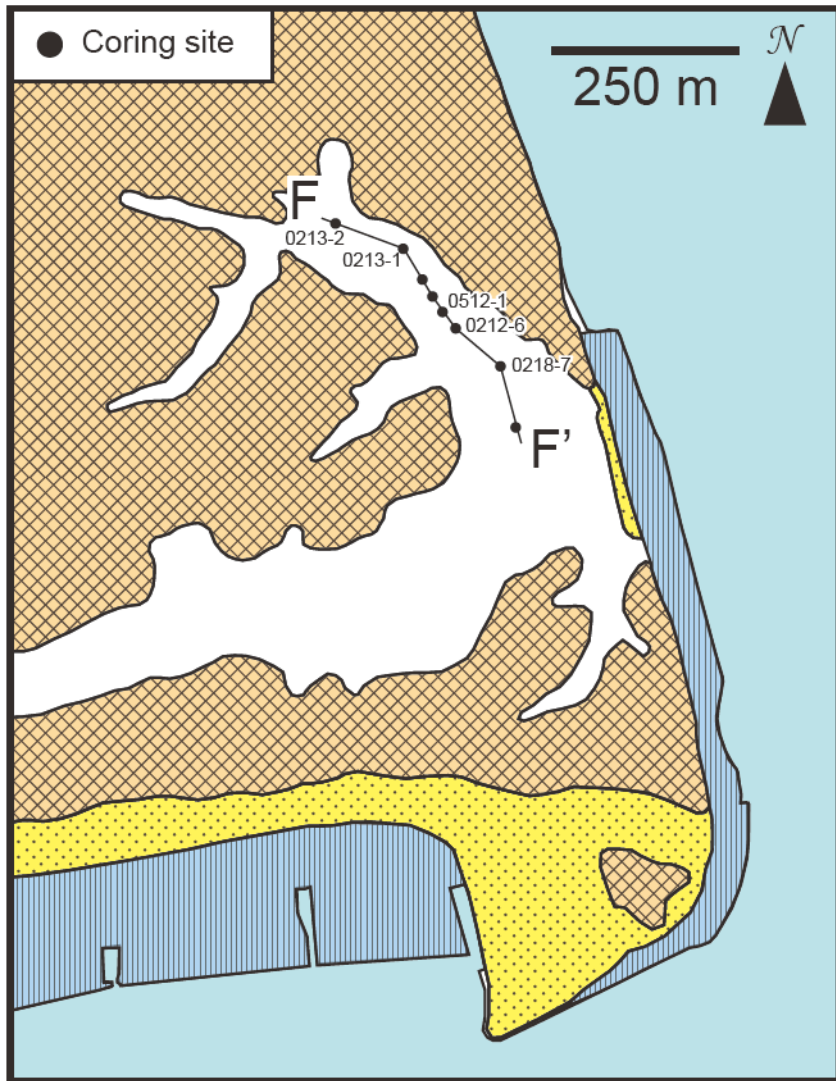


Fig. 4-5. Location map of coring sites and geological section (E-E' section) in the Shinjo Lowland. Black colored circles show location of core sites.

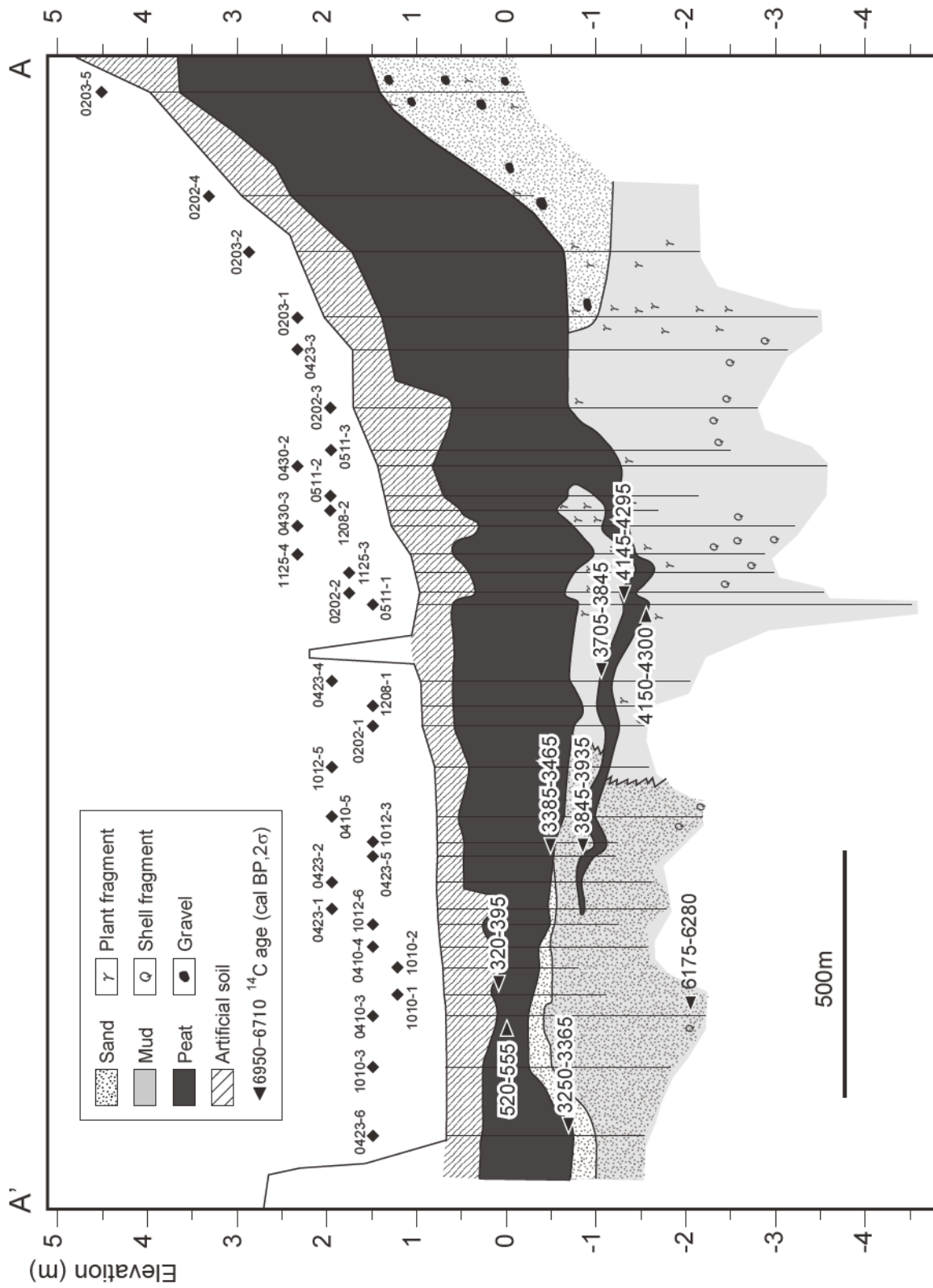


Fig. 4-6. Geological section (A-A') section) in the longitudinal direction in the Rokkengawa Lowland. Location of section and coring sites are shown in Fig. 4-2. Information of radiocarbon ages in this figure are shown in Table 4-1.

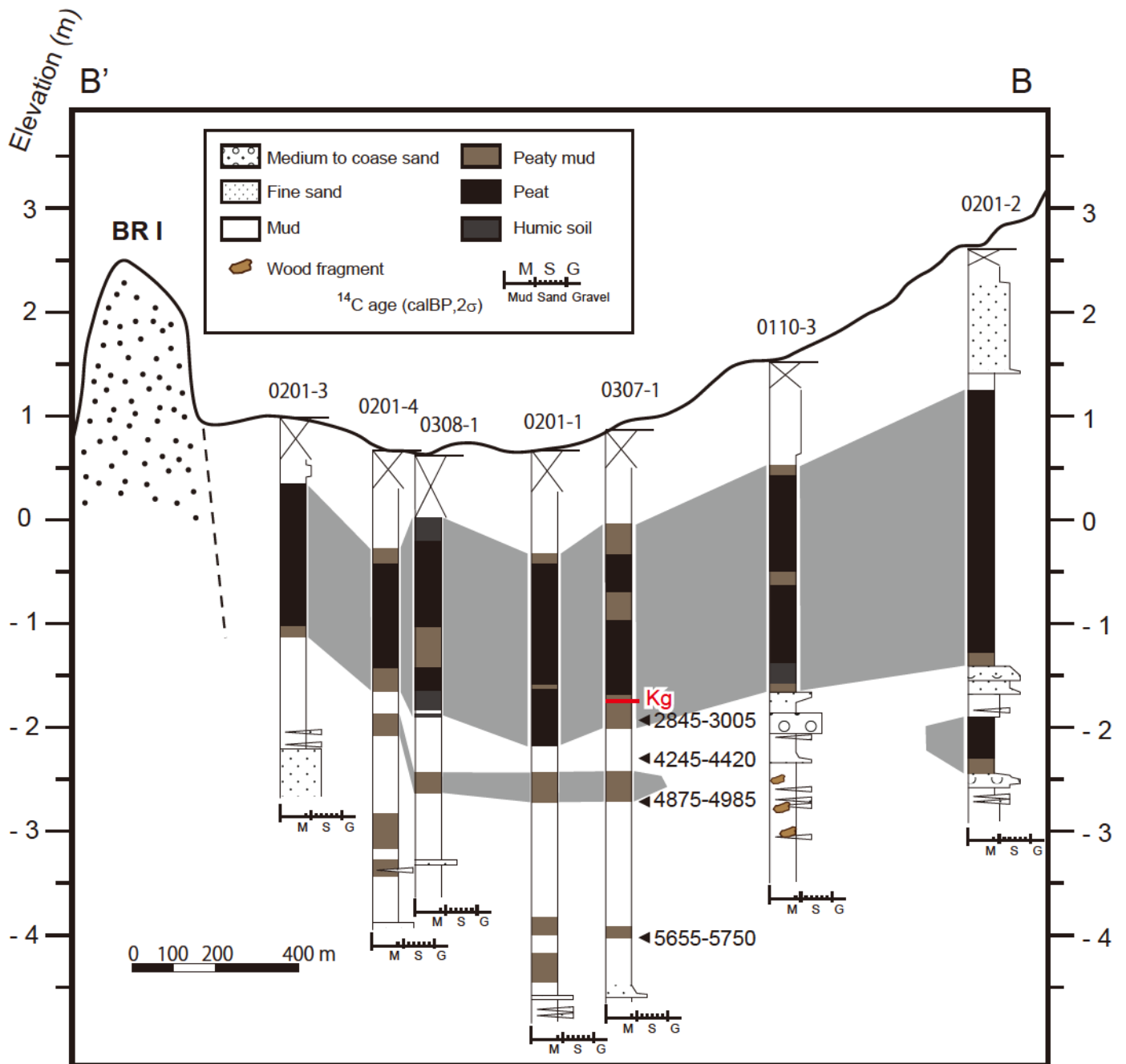


Fig. 4-7. Geological columnar section (B-B' section) in the longitudinal direction in the Higashi-Kandagawa Lowland. Location of section and coring sites are shown in Fig. 4-3. Information of radiocarbon ages in this figure are shown in Table 4-1.

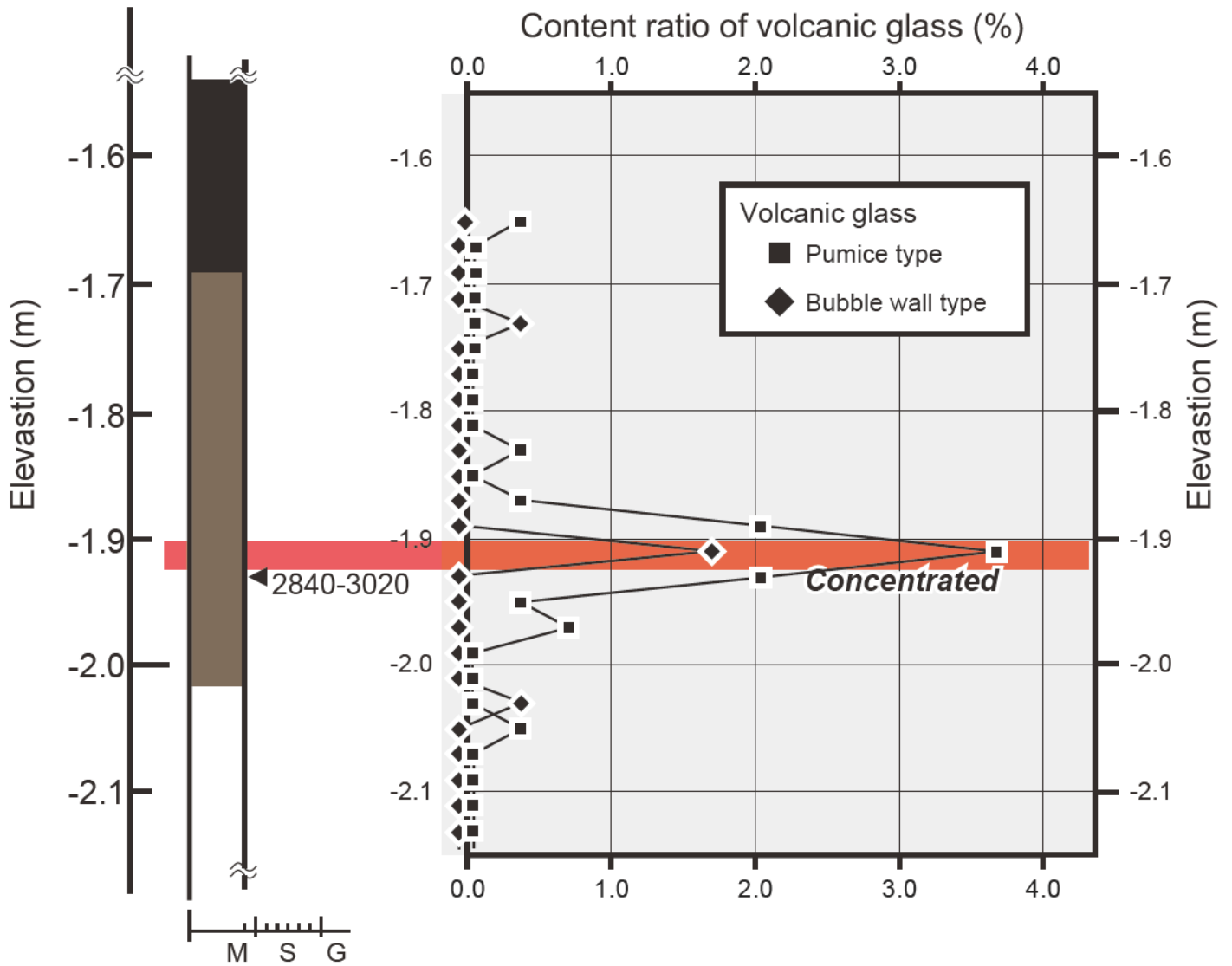


Fig. 4-8. Content ratio of volcanic glass about the 0307-1 core in the Higashi-Kandagawa Lowland. A Concentrated layer of glass was recognized between -1.91 to -1.93 m T. P. Refractive index and a radiocarbon age taken at the same horizon of the core indicates Kg tephra.

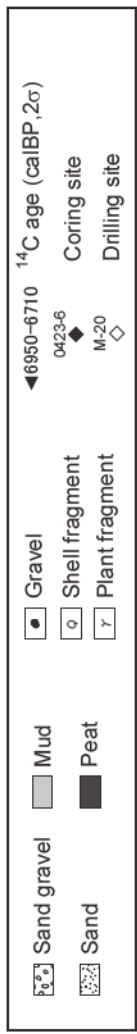
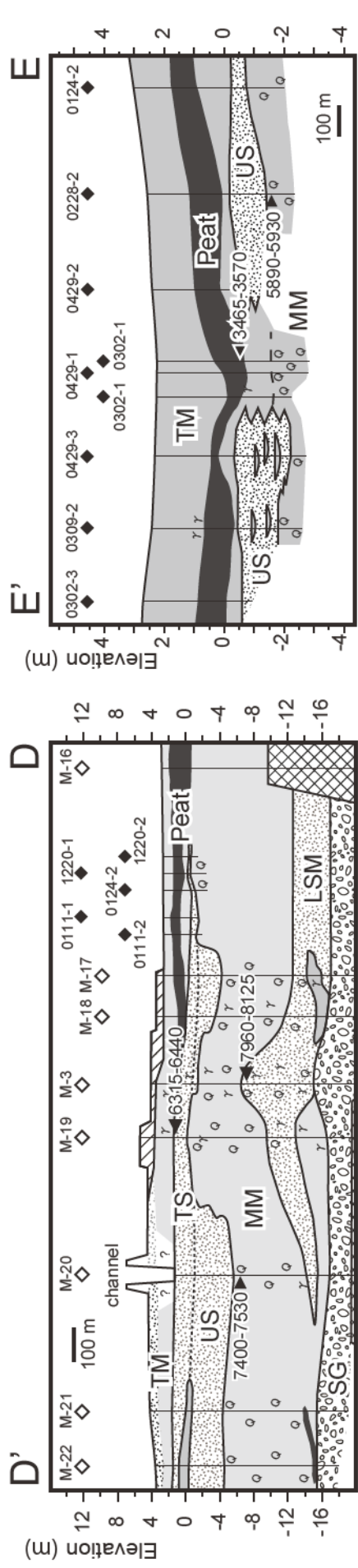
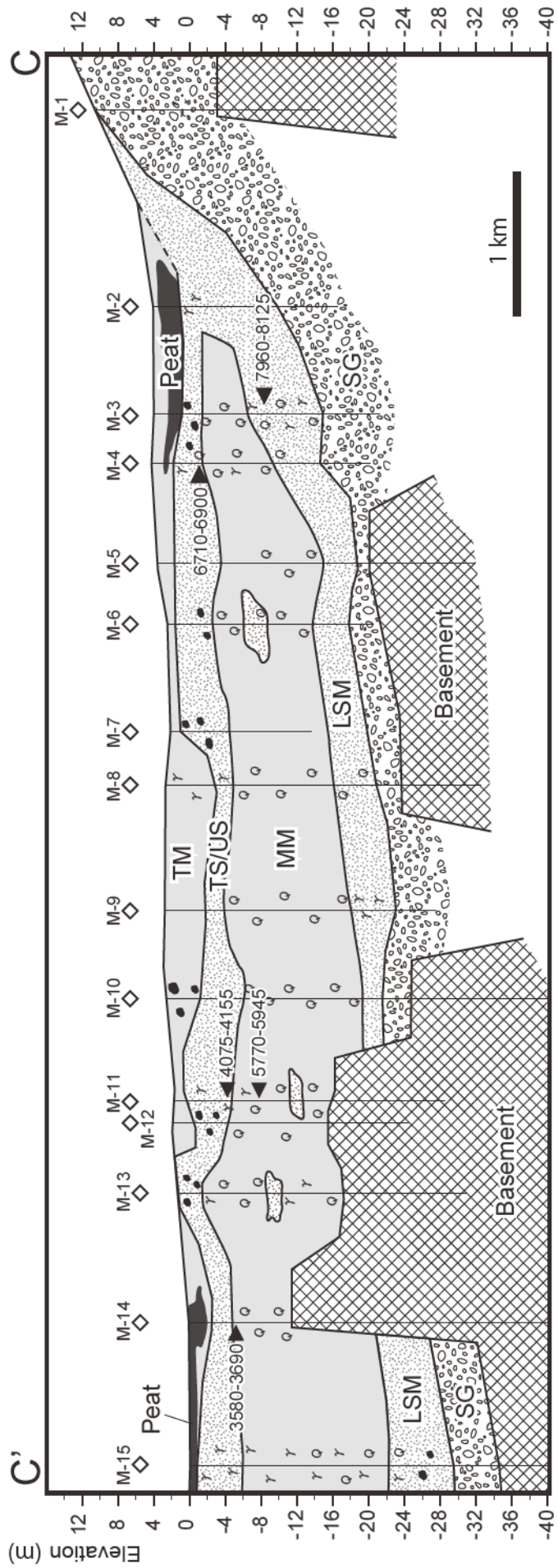


Fig. 4-9. Geological sections (C-C', D-D' and E-E') section) at the Miyakodagawa Lowland. Location of section and coring sites are shown in Fig. 4-4. Information of radiocarbon ages shown in this figure are described in Table 4-1. Classification of the lowland deposit was represented as follow letters, SG: Sand Gravel layer, LSM: Lower sandy mud layer, MM: Middle mud layer, US: Upper sand layer, TS: Top sand layer, TM: Top mud layer, Peat: Peat layer.

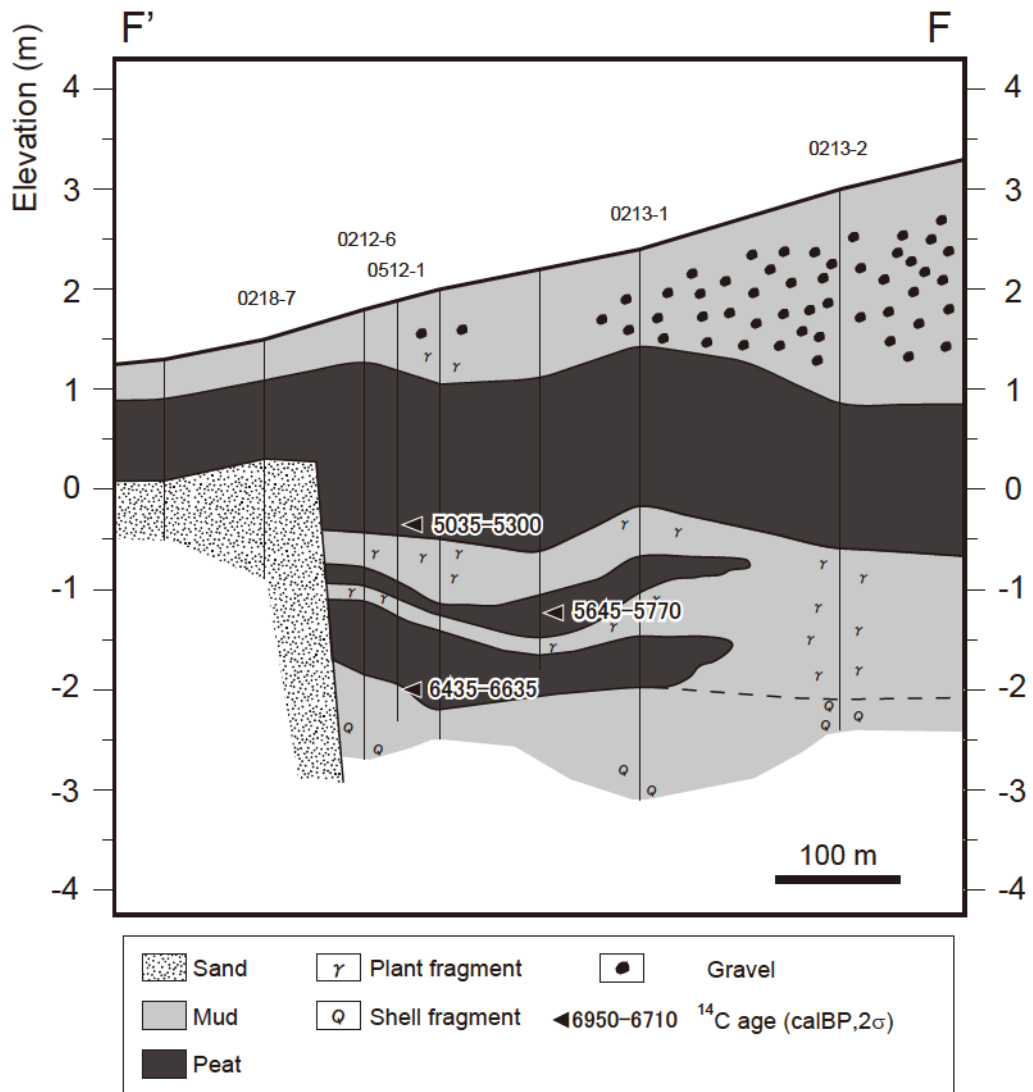


Fig. 4-10. Geological section (F-F' section) in the longitudinal direction in the Shinjo Lowland. Location of section and coring sites are shown in Fig. 4-4. Information of radiocarbon ages shown in this figure are described in Table 4-1.

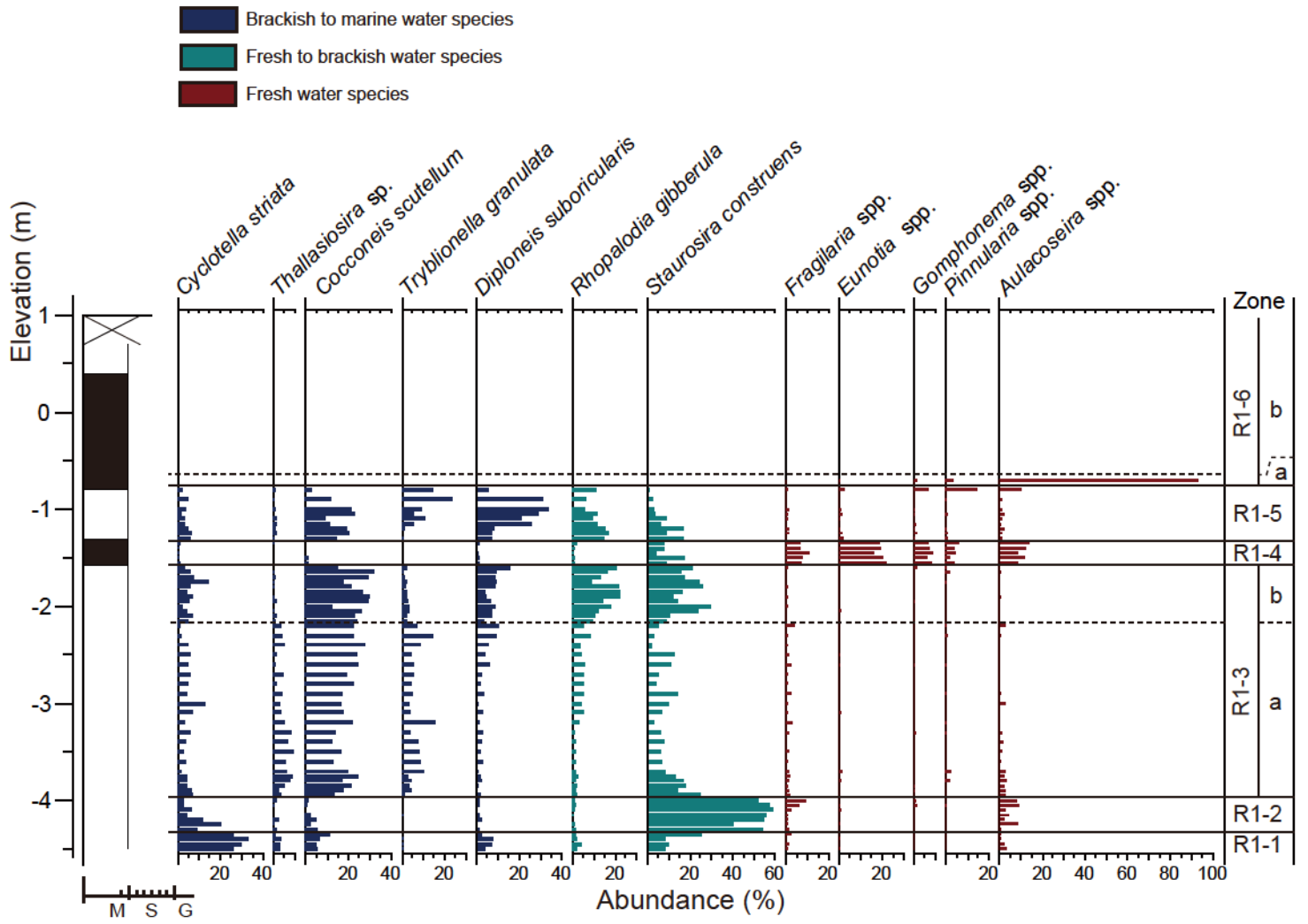


Fig. 4-11. Diatom assemblage diagram of 0511-1 core taken from the central part of the Rokkengawa Lowland. Location of the core is shown in Fig. 4-2.

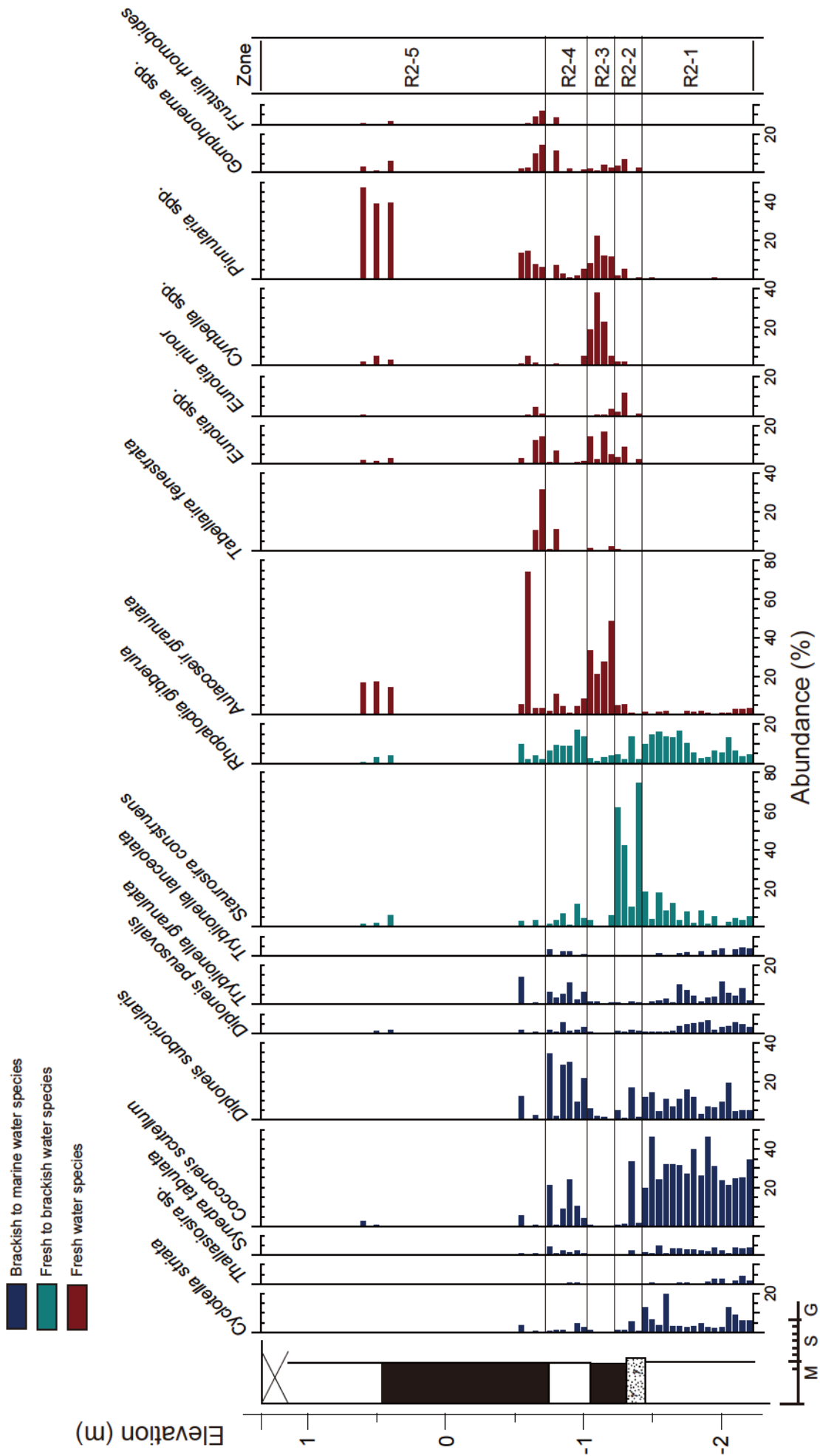


Fig. 4-12. Diatom assemblage diagram of 0511-2 core taken from the central part of the Rokkengawa Lowland. Location of the core is shown in Fig. 4-2.

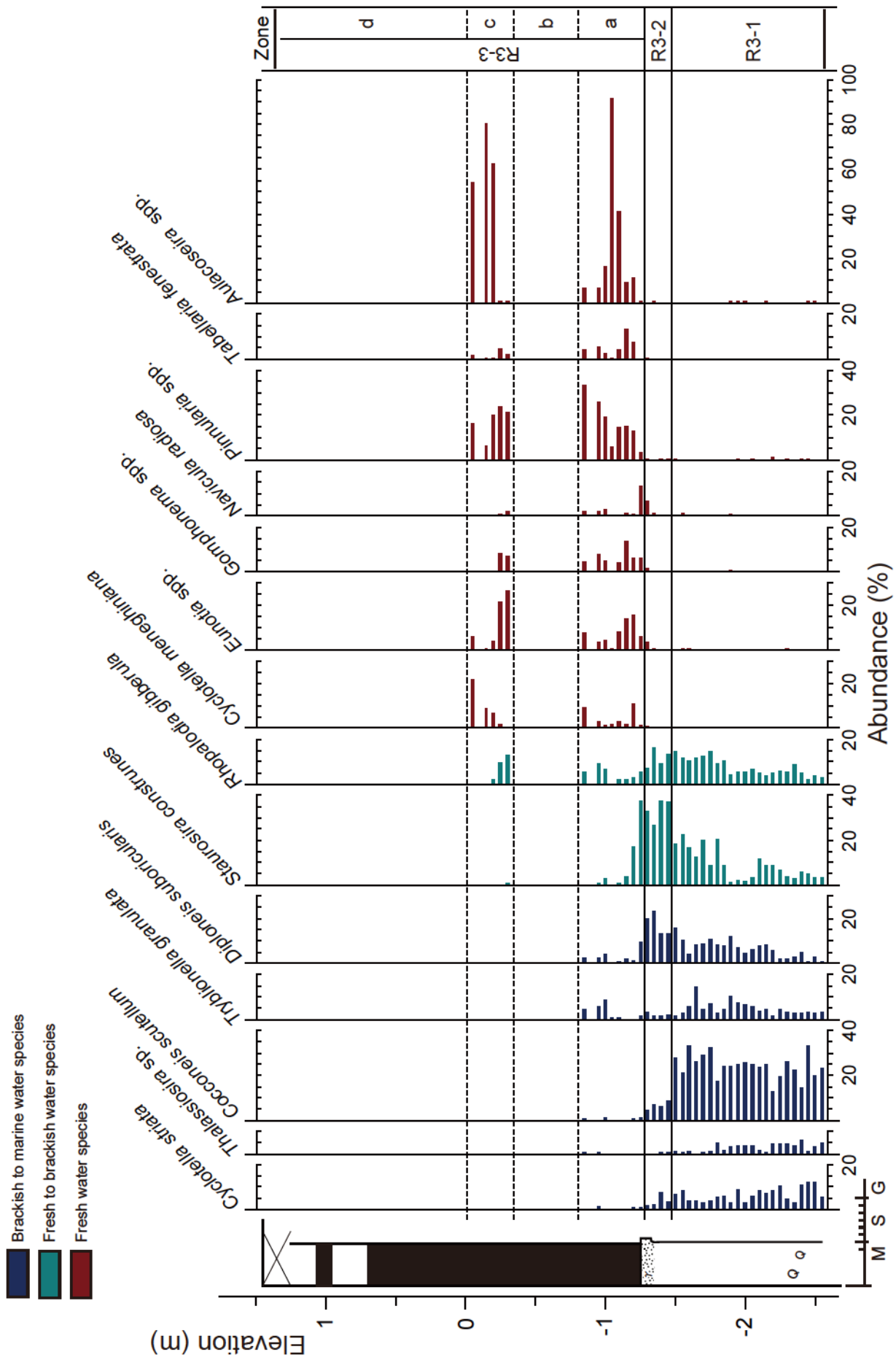


Fig. 4-13. Diatom assemblage diagram of 0511-3 core taken from the central part of the Rokkengawa Lowland. Location of the core is shown in Fig. 4-2.

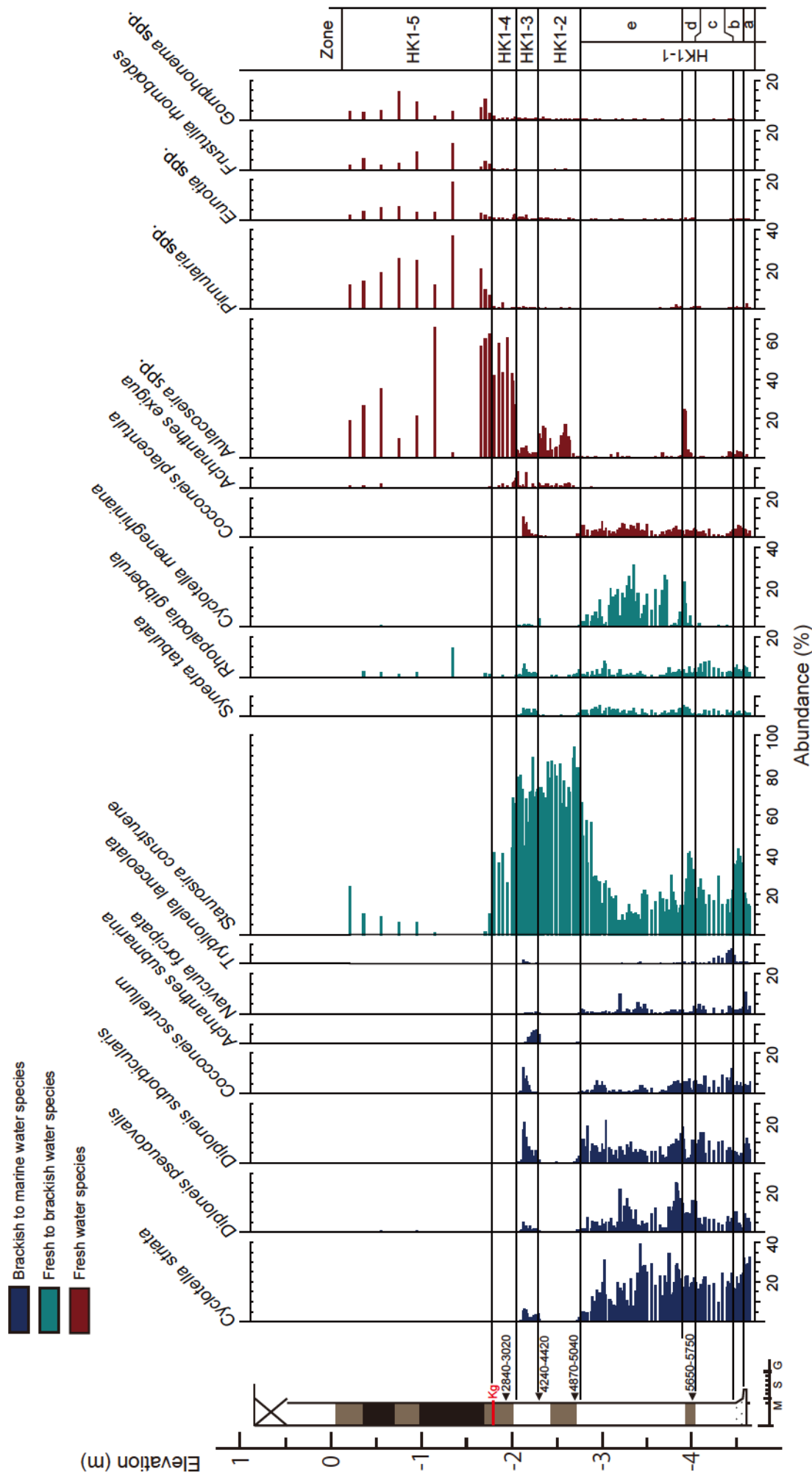


Fig. 4-14. Diatom assemblage diagram of 0307-1 core taken from the central part of the Higashi-Kandagawa Lowland. Location of the core is shown in Fig. 4-3.

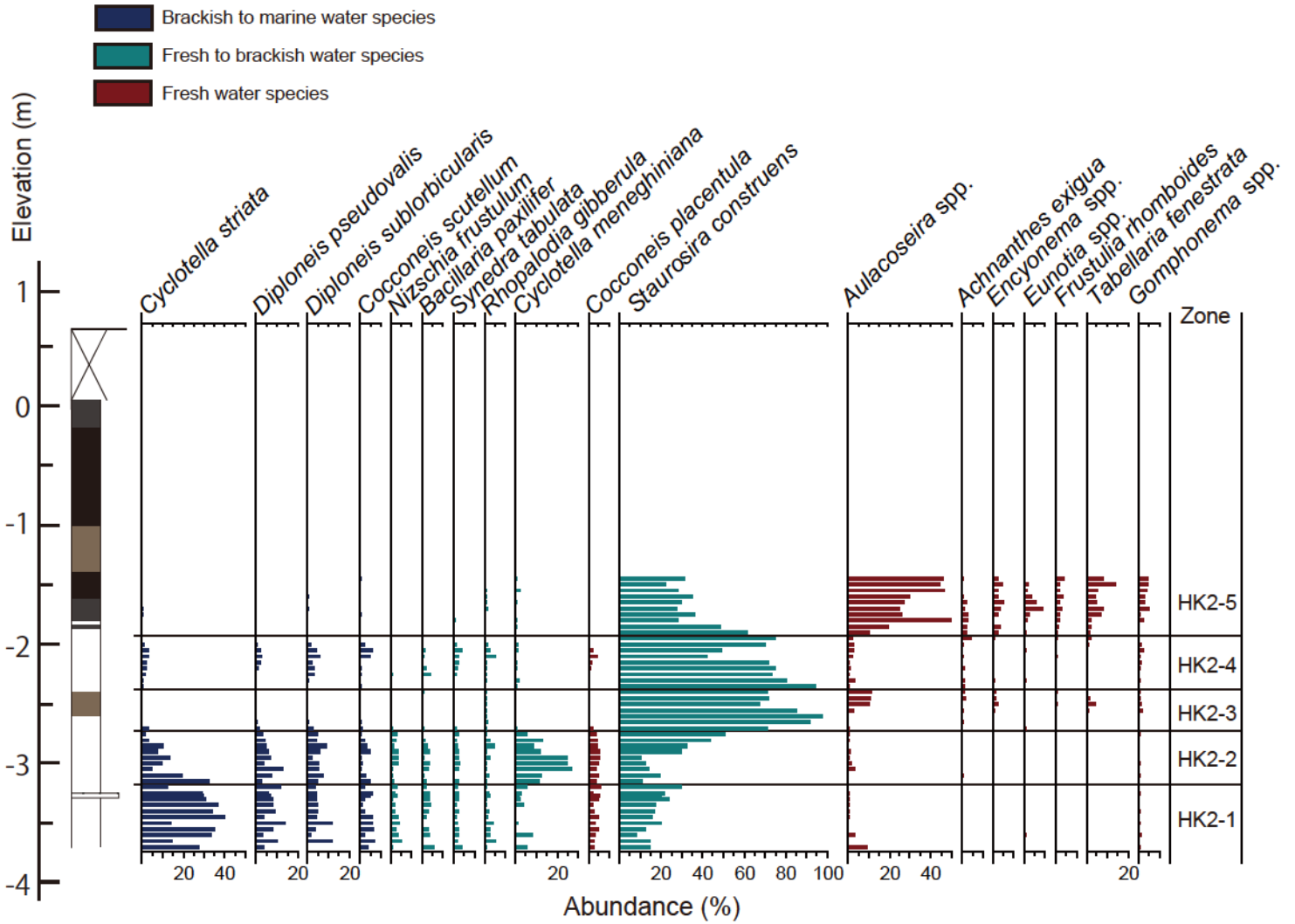


Fig. 4-15. Diatom assemblage diagram of 0308-1 core taken from the central part of the Higashi-Kandagawa Lowland. Location of the core is shown in Fig. 4-3.

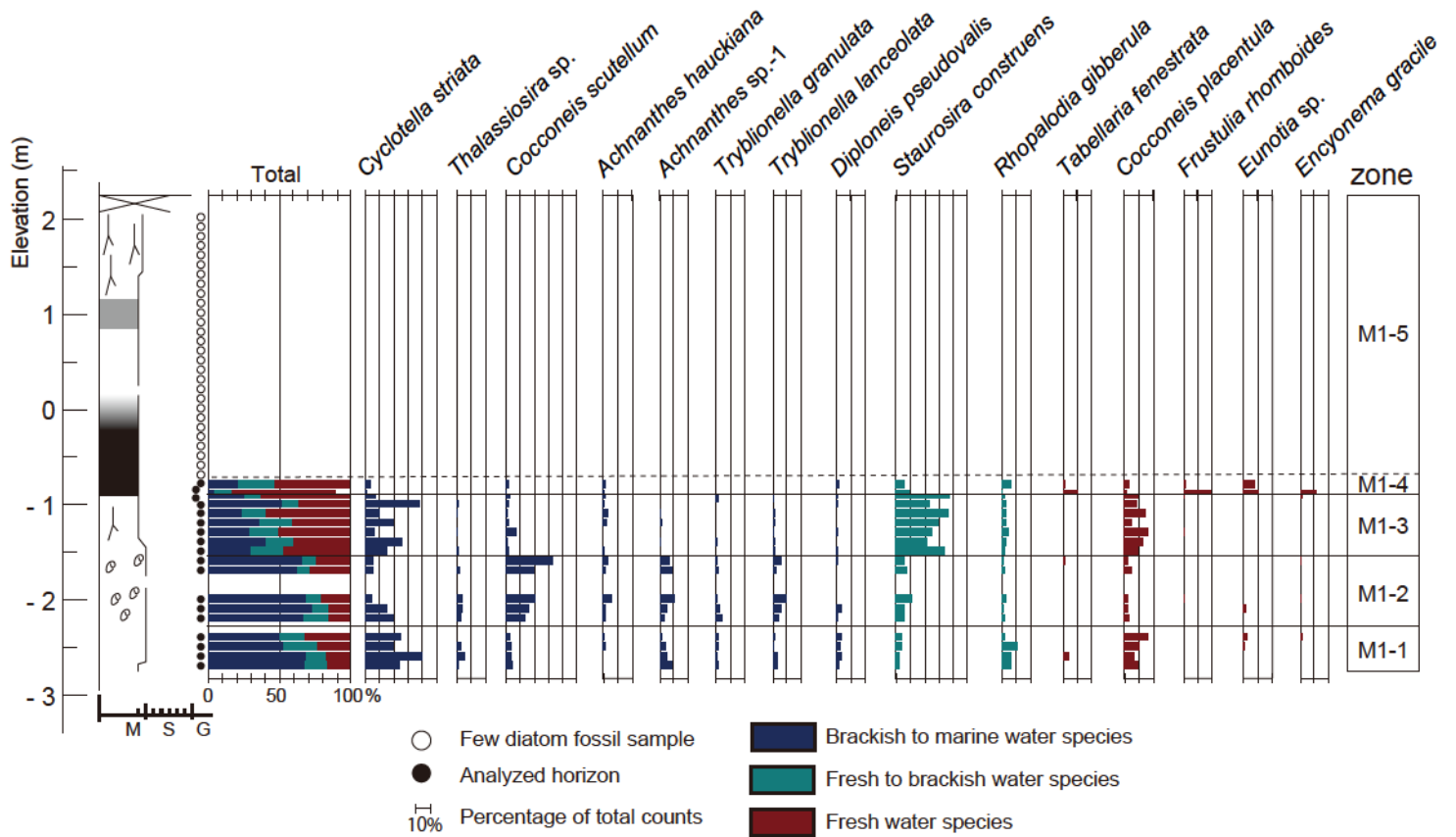


Fig. 4-16. Diatom assemblage diagram of 0429-3 core taken from the Miyakodagawa Lowland. Location of the core is shown in Fig. 4-4.

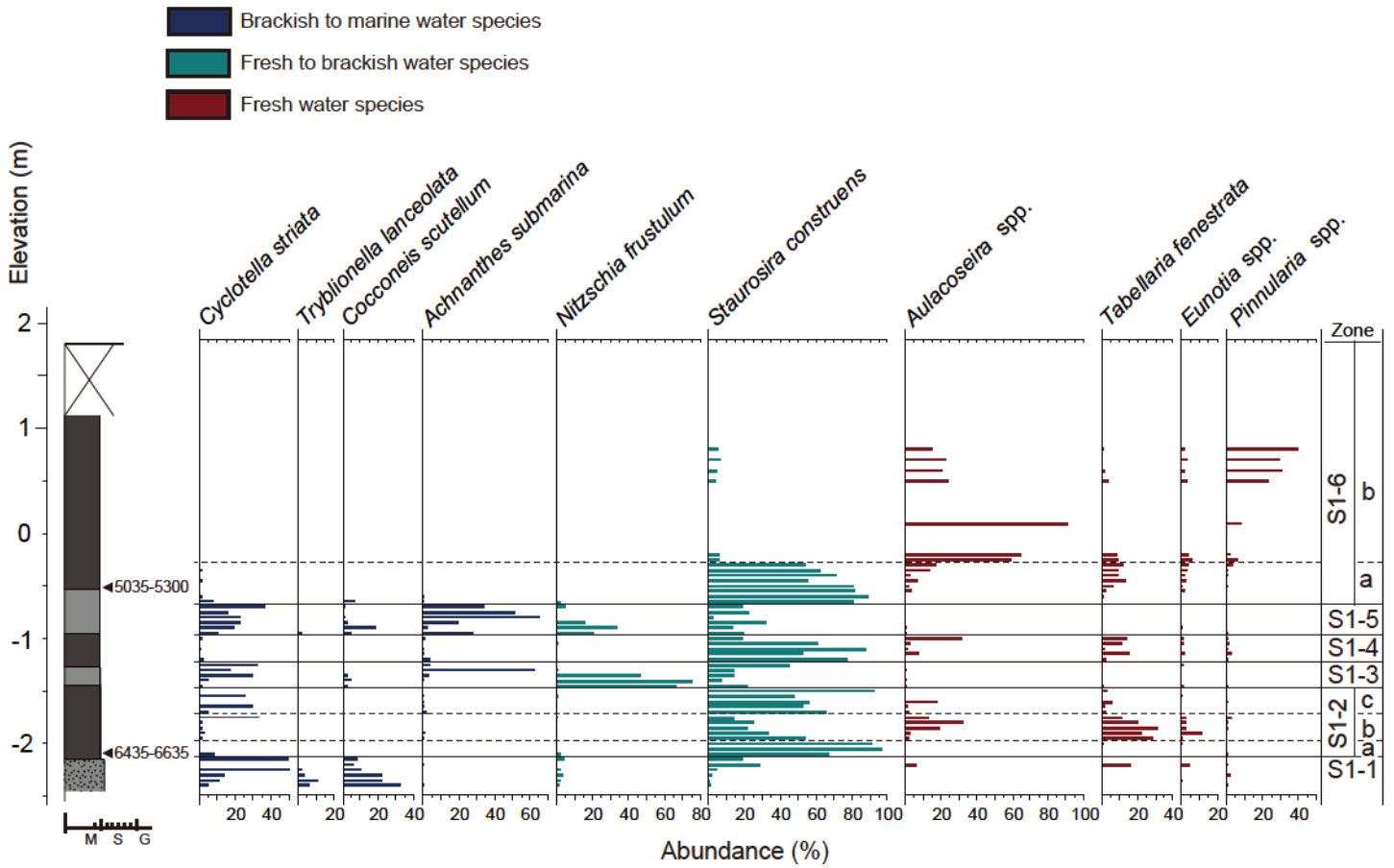


Fig. 4-17. Diatom assemblage diagram of 0512-1 core taken from the central part of the Shinjo Lowland. Location of the core is shown in Fig. 4-5.

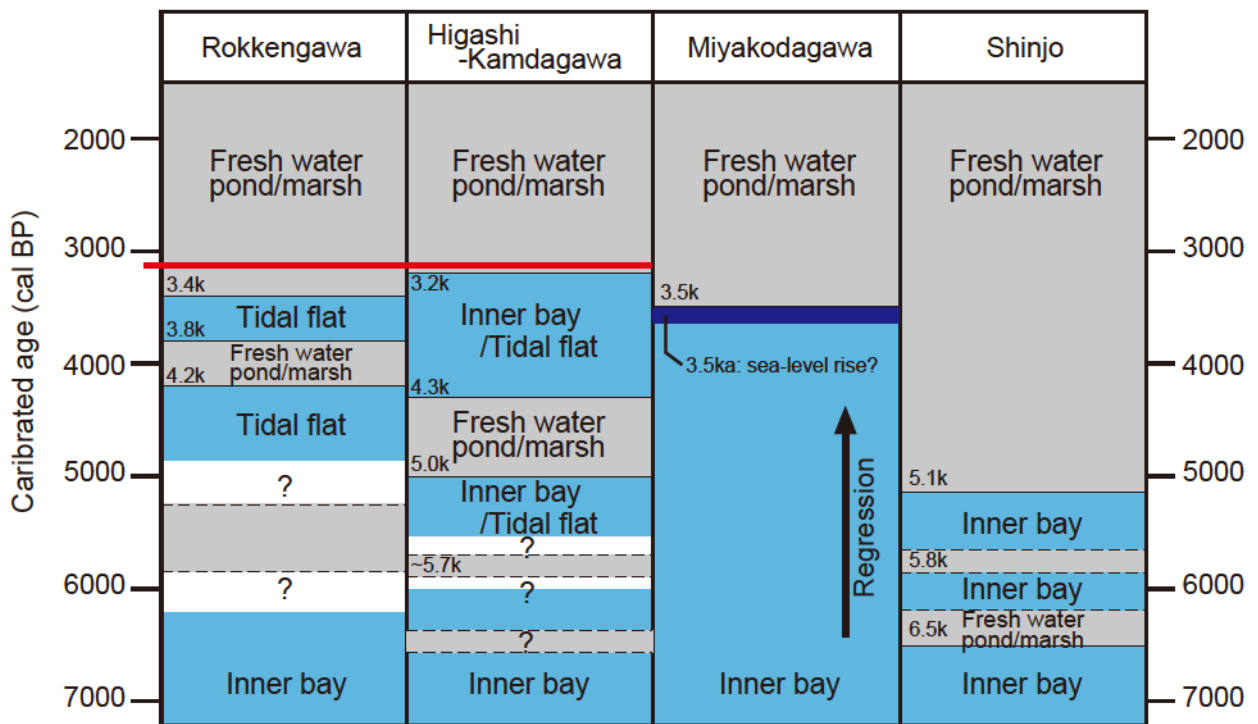


Fig. 4-18. The middle to late Holocene environmental transition of alluvial lowlands around the Lake Hamana based on the results of diatom analyses.

CHAPTER V

Late Holocene changes in sedimentary-environment of the inter-ridge marshes in western Hamamatsu strand plain

5-1. Introduction

The coastal beach ridges (BRs) are well developed in the western Hamamatsu Strand Plain as described in Chapter II (Fig. 5-1). They are divided into six bars, which are named the BR I to VI from landward to seaward by Matsubara (2004). The most inland barriers (BR I) in front of the Pleistocene terraces (Mikatagahara and Tenpakubara terraces), are corresponding to the Primary barrier, which developed at the transgressive stage during the Jomon Transgression (Matsubara, 1989 and Matsubara, 2001). On the other hand, the BR II to VI are located in parallel along the coastal line. In the western part of the plain, some of them combined each other to become three series of BR. The BR II to VI are corresponding to the Secondary barriers, which were formed adding to the Primary barrier at the Regressive stage after maximum of the Jomon Transgression (Matsubara, 1989 and Matsubara, 2001).

Detail geomorphic development of these BRs has been discussed previously by using paleontological and archeological data. Matsubara (2001, 2004 and 2007) suggested that the BR I emerged at ca. 4000 ¹⁴C yr BP and BR II to BR VI were formed after then. Recently, Ishibashi *et al.* (2009) carried out Optically Stimulated Luminescence (OSL) datings of sandy sediment samples obtained from BR III to VI. Measured OSL datings indicated that the BRs have developed and emerged individually and serially from landward to seaward during the middle to late Holocene.

On the other hand, paleo-environmental change in the inter-ridge marshes, which were

closed by the beach ridges, has not been revealed yet. Although some drowned lowlands distributed at incised valleys and inter-ridges marshes have been investigated previously, detail environmental change has not been discussed. As mentioned in the chapter II, it is necessary and important to consider the possibility that short-term environmental change had occurred around the study area. The previous studies had not taken discussions about it.

In this chapter, the late Holocene detail environmental changes in inter-ridges marshes are reconstructed by means of diatom analysis with help of geological information, radiocarbon ages and tephra samples.

5-2. Methods

In this chapter, the author took investigated sites at the two inter-ridge marshes. The first research site is located at the inter-ridge marsh between the BRs I and II (IRM I/II, Fig. 5-1), and the other site is at the inter-ridge marsh between BRs III and IV (IRM III/IV, Fig. 5-1).

To reconstruct paleo-environment of these inter-ridges marshes, diatom analysis of surface sediments of both marshes, which geological survey were performed by Fujiwara and Sato (2012) and Sato *et al.* (2013), were carried out. They observed a Holocene outcrop located at the IRM I/II (Site A, Fig. 5-1) and core sediments of the IRM III/IV by array coring of two sections, A-A' and B-B' section (Fig. 5-1) using core sampler and geoslicer.

Subsamples for analysis were taken from Holocene outcrop (Site A, Fig. 5-2) and coring samples (Site B, Fig. 5-4; Site C, Fig. 5-5) at 1 to 20 cm intervals by using plastic cube (~8 cm³). While the Site B is located at the most inland site of the A-A' section, and the Site C is located at

middle part of the B-B' section. The means of treatment of them is according to Kosugi (1993) and Ishikawa *et al.* (2011) as mentioned in detail in Chapter II (2-1-4). Chronology of sediments and cores are presumed by the tephrochronology and radiocarbon ages by Fujiwara and Sato (2012) and Sato *et al.* (2013). Depositional facies and surface geology of these lowlands were shown in Fujiwara and Sato (2012) and Sato *et al.* (2013).

5-3. Geomorphological and Geological background of lowlands

The description of lowland deposit and chronology of the study sites were already reported by Fujiwara and Sato (2012) and Sato *et al.* (2013). They carried out sediment observations of outcrops and cores. Tephra samples found in the sediments are measured about their main components contents of volcanic ashes using the EDX method in Furusawa geological *Co. Ltd.* (Sato *et al.*, 2013).

5-3-1. Inter-ridges marsh between BRs I and II (Site A)

The inter-ridge marsh between the BRs I and II (the IRM I/II,) is distributed at ~3.5 km inland from the present coastal line (Fig.5-1). This lowland fronts an estuary of the Shinkawa River which runs into the Lake Hamana in the western margin of the IRM I/II, and the Magome River in the eastern margin respectively. The width in east-west direction is about 7 km, and one in north-south direction is about 0.5 to 0.8 km. The BR II is distributed discontinuously; the southern margin of the IRM I/II, is not obvious.

The investigated site (Site A) is located at the northern margin of the IRM I/II between the BRs I and II (Fig. 5-1). Site A is located at ~1.5 km westward from the Magome River. In Site

A, Holocene outcrops composed by the surface sediments of the inter-ridges marsh were able to be observed at the altitude between 1.0 m to -1.9 m T.P. A geological columnar of the Late Holocene deposit in Site A described by Sato et al. (2013) is shown in Fig.5-2. Based on observation in Site A, lowland deposits of the IRM I/II consists of sand layer, humic mud layer, lower grayish mud layer, peat layer, upper grayish mud layer and top humic mud layer in ascending order (Fig. 5-2). The sand layer was found beneath ~ -1.79 m T.P. and covered by thick muddy sediments. The humic mud layer was found at -1.0 to -1.7 m T.P. and includes a number of thin sand layers wedging among it. According to Fujiwara and Sato (2012) and Sato *et al.* (2013), total of three radiocarbon ages from the humic mud layer, 3970-4090 cal BP, 3070-3220 cal BP and 3060-3215 cal BP from bottom to top are measured (Fig. 5-2). The lower grayish mud layer was recognized at ~-0.4 to -1.0 m T.P. and showed radiocarbon ages estimated to be 2950-3080 cal BP and 2770-2860 cal BP (Fig. 5-2) and indicated accumulation after ca. 3000 cal BP (Fujiwara and Sato, 2012; Sato *et al.* 2013). The peat layer wedges between the upper and lower grayish mud layer during -0.1 to -0.4 m T.P. Among the upper part of the peat layer, a radiocarbon age, 2630-2710 cal BP or 2455-2620 cal BP (Fig. 5-2), was reported by Fujiwara and Sato (2012) and Sato *et al.* (2013). This peat layer is covered by the upper grayish mud layer and the top humic mud layer.

At -1.0 m T.P., the bottom of the lower grayish mud layer, a tephra layer was recognized. This tephra layer provides much volcanic ashes. According to Sato *et al.* (2013), the result of main component analysis of the volcanic glass from this tephra sample indicates accordance with the Amagi-Kawagodaira Pumice (Kg) erupted at 3126-3145 cal BP (Machida and Arai, 2003). Radiocarbon ages nearby the tephra layer support this (Fig. 5-2).

5-3-2. Inter-ridges marsh between BRs III and IV

The inter-ridge marsh between the BRs III and IV (IRM III/IV) is distributed at ~2 km inland (Fig.5-1). The width of the IRM III/IV is about 4 km in east-west direction, and about 0.4 km in north-south direction respectively. This lowland also fronts the Magome River in the eastern margin of the IRM III/IV. In the western margin of the IRM III/IV, BRs III and IV are coupled. According to some historical maps drawn in the Edo Period, which named “Aoyama Ryobun Ezu (Aoyama family’s domanical map)” and old topographic maps in 1880s’, there was a huge water area distributed among the lowland (Fujiwara and Sato, 2012). However, it had been buried by human activity to have changed to paddy fields or housing lands.

Two geological columnar sections (A-A’ and B-B’) in north-south direction described by Fujiwara and Sato (2012) are shown in Fig. 5-3. The A-A’ section is located at the western part of the lowland, ~500 m eastward from the western margin. On the other hand, the B-B’ section is located at ~300 m eastward from the A-A’ section. Both of these sections showed similar geologic layers composed by sand layer, massive clay layer and peat layer. Top of the sediments was lost by artificial erosion or buried sediments. The sand layer was deposited below around -0.5 to -1.5 m T.P. The massive mud layer was found at the transition zone between the sand layer and the peat layer. The peat layer was recognized above around -0.5 to -1.5 m T.P. The bottom of the peat layer shows undulate distribution and reflects the difference of the elevation of the pond or marsh bottom. Both of the massive mud layer and peat layer included a number of thin sandy wedging layers ranging from a few millimeters to 25 cm thickness. In the B-B’ section, a thin sand layer having 10-15 cm thickness is observed around -0.4 to -0.7 m T.P. successively. Radiocarbon ages above and beneath of this thin layer indicated that the thin sand layer deposited from 3300 to 3700 cal BP (Fig. 5-3,

Sato *et al.*, 2013).

In the lower part of the peat layer, volcanic glasses condensed layer was recognized at -1.16 to -1.17 m T.P. by a content ratio analysis of volcanic ash (Sato *et al.*, 2013). Furthermore, the results of the main component analysis of this tephra sample indicate quite high coincidence with Kg tephra (Sato *et al.*, 2013). Radiocarbon ages taken from the bottom part of the peat layer, reported by Fujiwara and Sato (2012), presumed to be around 3000 cal BP and support the identification for Kg tephra (Fig. 5-3). Therefore, the peat layer began to deposit after ca. 3200 cal BP.

5-4. Results of diatom analysis

5-4-1. Inter-ridge marsh between BRs I and II (Site A)

According to the diatom assemblages, the sediments of the Site A can be divided into five zones (Fig. 5-2). The zone A-1 and A-2 belong to the humic mud layer, and the zone A-A-3 and A-4 is comparable to the lower grayish mud layer. The zone A-5 is corresponding to the overlying sediments, i. e. peat layer, upper grayish mud layer and top humic mud layer.

Zone A-1 (-1.23 to -1.76 m T.P.)

Zone A-1 is comparable to the middle to lower part of the humic mud layer. The major diatom species of Zone A-1 were fresh to brackish water species such as *Synedra tabulata*, *Synedra pluchella* and *Staurosira construens* with around 10% abundance. In addition, various fresh water species, *Aulacoseira granulata*, *Fragilaria* spp. *Eunotia* spp., were found in this

zone. Relative abundances of these fresh water species were less than 10%. A small number of brackish to marine water species such as *Cocconeis scutellum* and *Amphora ventricosa* were found to occupy around 2-3%.

Coexistence of various environments diatom indicator implies that allotropic diatom fossils were transported from various environments with sediment or flowing water. Abundance of *Synedra tabulata*, which is an indicator of aquatic plant vegetation in saline water (12-35 per mil; Kosugi, 1988), and appearance of some brackish to marine water species indicate that brackish water condition was distributed around Site A. Considering humic deposits are found commonly in this zone, the author suggests high possibility that have been a stable brackish marsh nearby a riverine mouth.

Zone A-2 (-1.07 to -1.18 m T.P.)

Zone A-2 was corresponding to the upper part of the humic mud layer. Zone A-2 was characterized by abrupt increasing of *Cyclotella striata* with abundant fresh to brackish water species. Relative abundances of *Cyclotella striata* reached up to ~20%. Some fresh to brackish water species, such as *A. granulata* and *Eunotia* spp. decreased from Zone A-1 to show ~5-10% relative abundance. Various fresh water species are found, but all of them decrease from Zone A-1 to be less than 5%.

Because *Cyclotella striata* is a brackish to marine water planktonic species, water depth and salinity probably increased from Zone A-1. This water depth and salinity increase are also suggested by depositional facies that still humic muddy and becomes finer upward than the lower sediments. On the other hand, abundant fresh and fresh to brackish water species suggests that brackish water area still developed as well as the zone A-1. Therefore, this

diatom zone suggests that water depth around a riverine mouth increased and more saline water condition developed.

Zone A-3 (-0.51 to -1.02 m T.P.)

Zone A-3 is corresponding to the most part of the lower grayish mud layer. The diatom assemblages of Zone A-3 were composed of fresh to brackish water species and fresh water species. *Rhopalodia gibberula* obviously increased from Zone A-2 and replaces other fresh to brackish water species such as *S. tabulata*, *S. pluchella* and *S. construens*. Furthermore, benthic fresh water species were abundant, e.g. *Cymbella* spp., *Gomphonema* spp. and *Pinnularia* spp. The percentage of them increased upward among the Zone A-3. On the other hand, brackish to marine water species became few.

High percentage of fresh water species indicates that salinity decreased and changed to fresh water condition. Besides, dominance of benthic species replacing brackish to marine water planktonic species suggests that water depth prominently decreased. Thus, it is suggested that environmental change from river mouth to fresh water marsh occurred.

Zone A-4 (-0.42 to -0.49 m T.P.)

Zone A-4 is corresponding to the uppermost part of the lower grayish mud layer. This zone was characterized by abundant *Pinnularia* spp. and *Hantzschia amphioxys*. Besides, *Navicula contenta*, *Diploneis ovalis* and *R. gibberula* accompanied them. The percentage of them reached up to around 20% and 15% respectively. In contrast, *Cymbella* spp. and *Synedra ulna* were few in Zone A-4.

Abundant land indicators such as *H. amphioxys* and *N. contenta* (Ando, 1990) indicated that inland environment with low water level developed. Increasing of some benthic fresh

water species supports this environmental change.

Zone A-5 (0.44 to -0.36 m T.P.)

Zone A-5 was corresponding to the peat layer, the upper grayish mud layer and the top humic mud layer. In most part of the peat layer and the upper part of the upper grayish mud layer, number of fossil diatoms was not enough to count at least 200 specimens. The main components of this zone were fresh water species. *Pinnularia* spp., were dominant and occupied around 25%. In addition, *Cymbella* spp., *Amphora* spp., *Stauroneis* spp. and *Neidium* spp., which were frequently large sized and benthic fresh water species, were abundant. In addition, *Aulacoseira ambigua* is abundant (~5-10%). In contrast, *H. amphioxys* and *N. contenta* were very few.

Large amounts of benthic fresh water species suggests that a fresh water marsh developed with shallow water depth. In addition, temporarily increasing of *A. ambigua*, because this diatom species is supposed an indicator of fresh water lake and marsh (Ando, 1990), indicates a once more water level rising.

5-4-2. Inter-ridge marsh between BRs III and IV

5-4-2-1. Site B

Sediments of Site B were divided into four diatom zones (B-1 to 4, Fig. 5-4). Zone B-1 was corresponding to the massive clay layer, Zone B-2 was the most part of the thin sand layer, Zone B-3 was the uppermost of the thin sand layer and bottom of the peat layer, and Zone B-4 was the most part of the peat layer.

Zone B-1 (-0.85 m T.P.)

Zone B-1 was recognized only at the bottommost sample of Site B. The diatom assemblage of this zone was shared mainly by *N. radiosa* and *S. tabulata*. In addition, *D. smithii*, a brackish to marine water species, were found with low percentage (~4%).

Because *Synedra tabulata* is an indicator of an aquatic plant vegetation in saline water (Kosugi, 1988), it is possible that marine plants vegetated around Site B. Appearance of brackish to marine water species including *D. smithii* support this possibility. On the other hand, salinity was suggested to be low by abundance of *N. radiosa*. Considering humic deposits are found in this zone, the author suggests high possibility that a fresh to slightly brackish area connecting to the ocean is developed.

Zone B-2 (-0.74 to -0.80 m T.P.)

Zone B-2 was comparable to the obvious thin sand layer wedging between the massive mud layers. This zone was characterized by dominance of *S. construens*. The percentage of *Staurosira construens* reached up to ~60% of total counts. Besides, a small number of fresh water species were also found, and benthic fresh water species, *Pinnularia* spp., *Frustulia rhomboides* and *Gomphonema* spp., are abundant.

Fujiwara and Sato (2012) suggested that the thin sand layers wedging among the massive mud layer and peat layer found in the IRM III/IV have possibility of a kind of event deposits such as tsunami and/or storm events, because there was no river enough to transport such sandy deposits widely to the lowland. Because the diatom assemblage of Zone B-2 was quite different from those of Zone B-1, this zone is possible to be corresponding to one of these event deposits. Appearance of benthic fresh water species in Zone B-2 indicates that sediment was supplied from inland environment associated with a kind of event.

Zone B-3 (-0.67 to -0.70 m T.P.)

Zone B-3 was characterized by abundance of *C. striata* and *S. construens*. The almost half percentage of the assemblage is composed by *S. construens* and *C. striata*. *Cyclotella striata* increased upward in Zone B-3 up to more than 20%. In addition, some planktonic species such as *Thalassiosira bramaputrae*, *Cyclotella meneghiniana*, *A. granulata* and *Aulacoseira ambigua* are found with low percentage (~5%).

Temporal increase of *Cyclotella striata* indicates that inner bay environmental developed rapidly after deposition of the thin sand layer.

Zone B-4 (-0.51 to -0.66 m T.P.)

Zone B-4 was characterized by significant dominance of planktonic and tychoplanktonic fresh water species. *Fragilaria* spp. was dominant and occupies around 15-35%. And *Aulacoseira granulata*, *Aulacoseira ambigua*, *Cyclotella praetermissa* also showed relative abundance (~5-10%). However, these fresh water species, *Fragilaria* spp., *A. granulata*, *A. ambigua*, *C. praetermissa* decreased upward in Zone B-4. On the other hand, *Staurosira construens* increased upward and becomes dominant in the upper part of Zone B-4, above -0.60 cm T.P. In the upper part of the Zone B-4, *Gomphonema* spp., *Epithemia* spp. and *Eunotia* spp. also increased from the lower part.

High percentage of fresh water planktonic and tychoplanktonic species indicates environmental change from inner bay to fresh water pond. Upward increasing of benthic species indicates that water depth became shallow with sedimentation of peaty deposit.

5-4-2-2. Site C

According to the diatom assemblages, the sediments of the Site C were able to be divided into three diatom zones (C-1 to 4, Fig. 5-5). All of the three diatom zones belonged to the peat layer.

Zone C-1 (-1.38 to -1.43 m T.P.)

Zone C-1 was distributed just above the sand layer. In Zone C-1, *Staurosira construens*, a fresh to brackish water species, was dominant of the assemblage, and *Synedra tabulata* yielded with ~5% abundance. In addition, some fresh water species such as *Epithemia* spp. and *Navicula vaneei* were found abundantly.

Dominance of *Staurosira construens* indicates that salinity was fresh to brackish slightly. Because some benthic species were abundant, water depth was presumed not to be so deep enough to stimulate growing of planktonic diatom species. Considering that *Synedra tabulata*, an indicator of an aquatic plant vegetation in saline water (Kosugi, 1988), is found abundantly, the author suggests possibility that vegetation in saline water were distributed around Site C.

Zone C-2 (-1.33 to -1.37 m T.P.)

Zone C-2 was characterized by abrupt increase of *S. construens* from Zone C-1. The percentage of *Staurosira construens* reached up to around 70%. In addition, fresh water species, *Epithemia* spp. and *N. vaneei*, decreased slightly from Zone C-1.

Quite high percentage of *S. construens* implies that salinity increase occurred in Zone C-2. Upward diminishing of benthic fresh water species supports this.

Zone C-3 (-1.00 to -1.32 m T.P.)

In Zone C-3, fresh water planktonic and tycho planktonic species were dominant. *Aulacoseira granulata* showed high percentage of total counts (around 30-40%). Other

planktonic species such as *A. ambigua* and *C. praetermissa* increased from the Zone C-2 up to 5-10%. In addition, *Fragilaria* spp., a tychoplanktonic species, was found commonly in this zone with ~15% abundance. In contrast, *Staurosira construens* decreased from Zone C-2 until ~10-20%, which was much fewer than half of percentage of that of Zone C-2.

Dominance of fresh water species indicates that fresh water pond developed in this period. In particular, abundant of *A. granulata*, which is an indicator of a fresh water lake, suggests that water depth was deeper than that of the lower zones.

Zone C-4 (-0.92 to -0.97 m T.P.)

Zone C-4 was characterized by higher percentage of *S. construens* and lower percentage of *A. granulata* than those in Zone C-3. Some fresh water planktonic species such as *A. ambigua* and *C. praetermissa* and tychoplanktonic species were found as frequently as those in Zone C-3. In addition, *Cyclotella meneghiniana* and *Thalassiosira bramaputrae* increased slightly from Zone C-3.

Decreasing of *Aulacoseira granulata* indicates that water depth became shallower than that of Zone C-3. Besides, increasing of fresh to brackish water planktonic species implies that water salinity became higher.

5-5. Discussions

5-5-1. Environmental change in the inter-ridge marsh between BRs I and II

In the IRM I/II, the Zone A-1 showed diatom assemblages composed of various diatom species, fresh to brackish water and fresh water species. Inferred from the diatom assemblage of Zone A-1 and humic depositional facies, riverine mouth (estuary) environment had formed at least

until 3200 cal BP. Based on radiocarbon ages reported by Fujiwara and Sato (2012) and Sato *et al.* (2013), the formation age of estuary environment is probably before ca. 4000 cal BP. This suggests that the BR II had developed before ca. 4000 cal BP and sheltered the IRM I/II from the outer ocean area. Since 3200 cal BP, temporal salinity increase occurred suggested by diatom assemblage in Zone A-2 indicating inner bay environment (Zone A-2). Because brackish to marine planktonic species *C. striata* showed abundant in Zone, it is suggested that water depth increased accompanying salinity increasing.

After ca. 3200 cal BP, environmental change from brackish area to fresh water marsh occurred. Timing of the formation of the fresh water marsh at Site A was estimated before the Kg tephra falling (3126-3145 cal BP; Machida and Arai, 2003). Fresh water diatoms were dominant during the Zone A-3 to Zone A-5 indicates that fresh water condition had lasted without inundation of marine water after ca. 3200 cal BP. This marsh had been buried gradually with water level fluctuation. Although water level falling and well-developed peat layer had started to form at least ca. 2600 cal BP once inferred from Zone A-4, water level increased and fresh water marsh developed again after then (Zone A-5).

5-5-2. Environmental change in the inter-ridge marsh between BRs III and IV

Before ca. 3200 cal BP, a brackish water area had been formed in the IRM III/IV. Fresh to brackish water diatom species such as *S. construens* and *S. tabulate* were often found in the massive clay layer and the lower part of the peat layer in Site B and C with some fresh water diatom species, e.g. *N. radiosa* (zone B-1 and C-1). These diatom assemblages indicate that a fresh to slightly brackish area connecting to the ocean was distributed around the IRM III/IV. Just before

ca. 3200 cal BP, temporal salinity increase was suggested by increasing of *C. striata* or *S. construens* (zone B-3 and zone C-2) than before. In Site B, because of the stratigraphy, this temporal salinity increase is implied to be accompanied the deposition of the thin sand layer (Zone B-2), which might be associated with catastrophic event such as tsunami and/or storm.

From 3200 cal BP, the Kg tephra falling, fresh water ponds were formed in the IRM III/IV. The upper part of the peaty layer was characterized by fresh water diatom species. Difference of the percentage of fresh water planktonic species, e. g. *Aulacoseira granulata*, and surface geology (Fujiwara and Sato, 2012) indicate that deepest part of this fresh water pond was located around the central part of the IRM III/IV (nearby the B-B' section). Increase of benthic species in the upper part of Zone B-4 suggests that this fresh water pond had been buried from marginal parts gradually. On the other hand, Zone C-4 showed salinity increase and water level shoaling after the formation of the fresh water pond in ca. 3200 cal BP. Considering a relative younger radiocarbon age than lower diatom zones is acquired in the upper part of Zone B-3 and Zone C-4, the author suggests possibility that artificial canal connecting between the pond and the Lake Hamana constructed, which remains as a small drain in present.

5-5-3. Features of geomorphic development of the western Hamamatsu Strand Plain

Timings of development of fresh water ponds/marshes at the two inter-ridge marshes, IRM I/II and III/IV, are recognized in ca. 3200 cal BP and indicate to be almost simultaneously. The Kg tephra and radiocarbon ages indicated that environmental change from brackish water area to fresh water area (marsh or pond) in both of lowlands occurred in ca. 3200 cal BP. Formation of the fresh water ponds in the inter-ridge marsh between BRs III and IV and wide distribution of the BR

IV suggest that development of the BR IV caused development of fresh water ponds/marshes. In addition, timings of temporal salinity increase events found in the both lowlands (IRM I/II and III/IV) before the fresh water ponds/marshes formation in ca. 3200 cal BP were also synchronous. This suggests that sea water flowed into wide area of the lowlands in the western Hamamatsu Strand Plain in ca. 3200 cal BP.

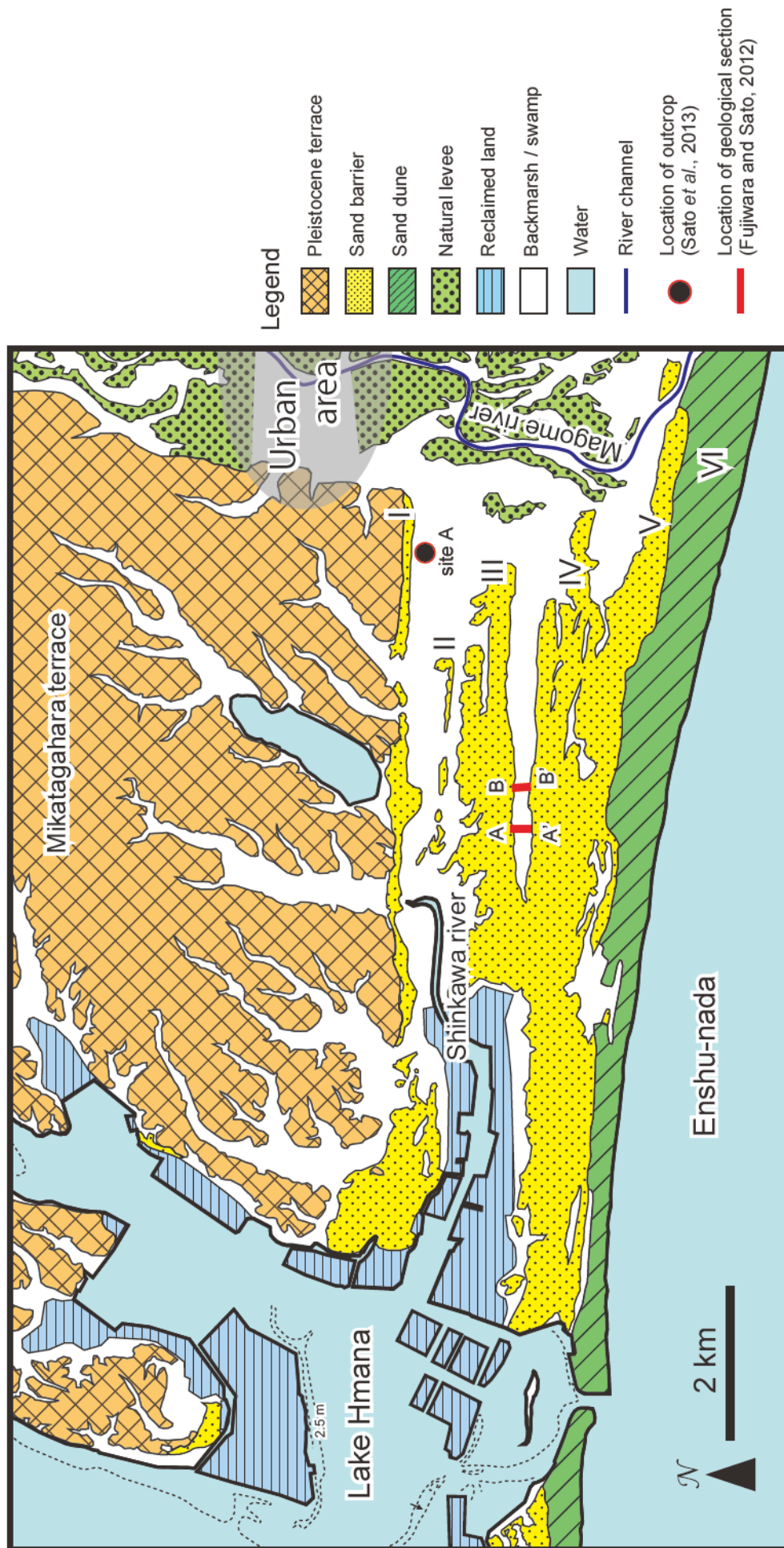


Fig. 5-1. Geological classification map of the western Hamamatsu Strand Plain and location map of the investigated site and sections. An outcrop site (Site A) of the Holocene lowland deposits was observed by Sato et al. (2013) at inter-ridge marsh between BR I and II (IRM I/II). Along two sections, A-A' and B-B' section, in inter-ridge marsh between BR III and IV (IRM III/IV), geological survey was performed by Fujiwara and Sato (2012) and Sato et al. (2013).

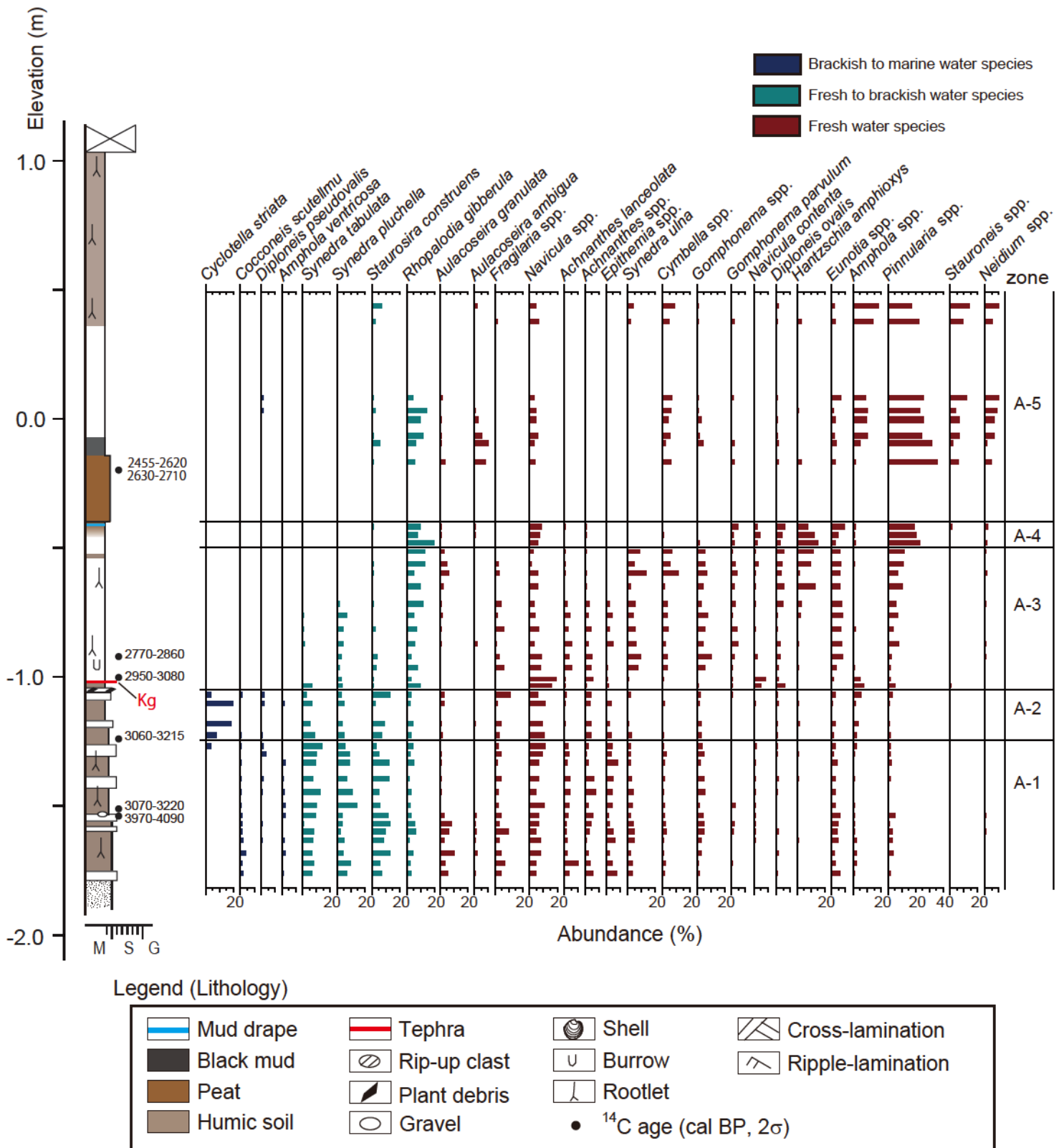


Fig.5-2. Geological columnar and diatom assemblages diagram of Site A, in the inter-ridge marsh between the BR I and II. Location of site A is shown in Fig.5-1. The radiocarbon ages is based on Sato *et al.* (2013).

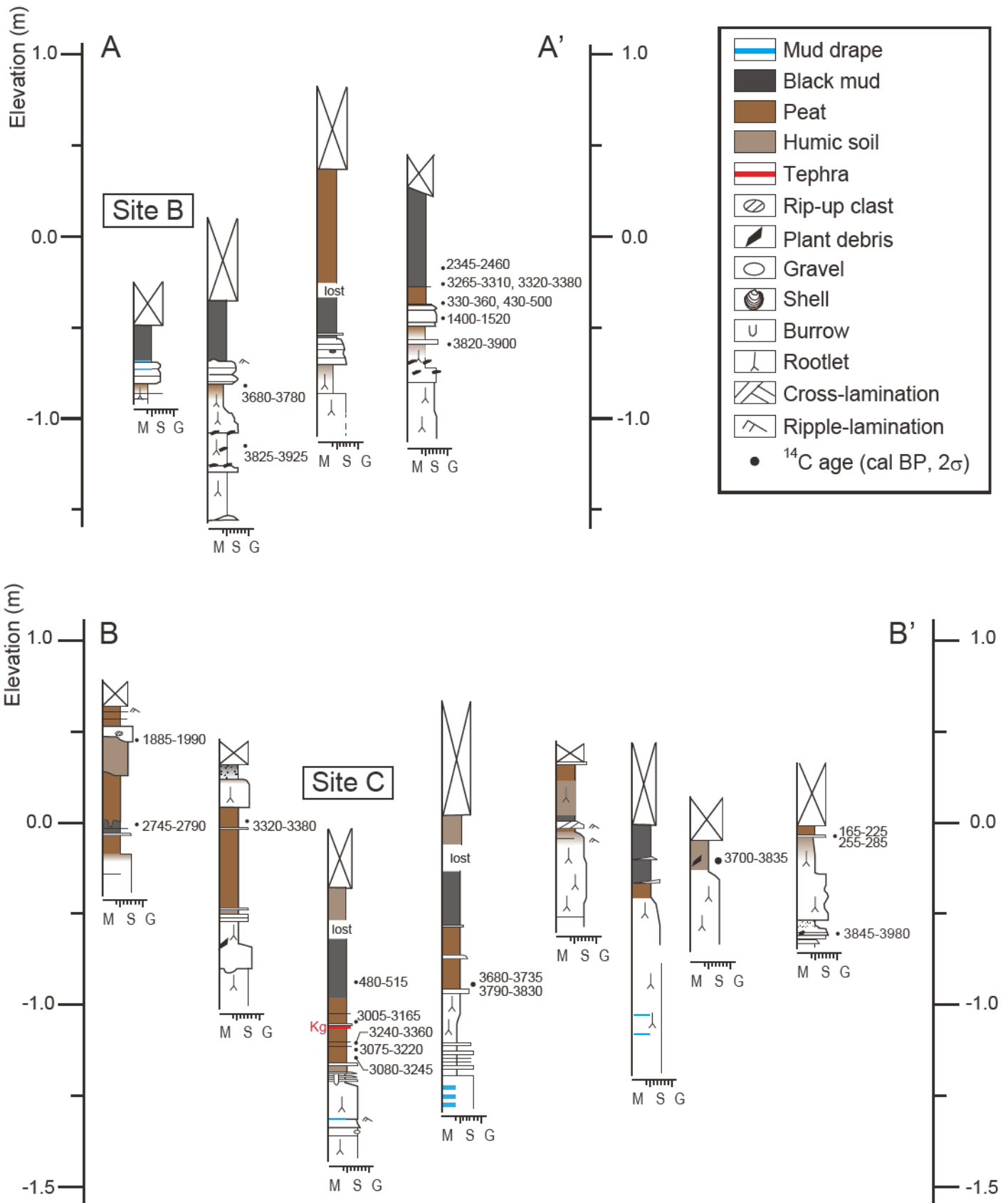


Fig. 5-3. Geological columnar sections along the A-A' and B-B' section in the inter-ridge marsh between BR III and BR IV. These are a part of sections reported by Fujiwara and Sato (2012) and Sato *et al.* (2013). Location of sections is described in Fig. 5-1.

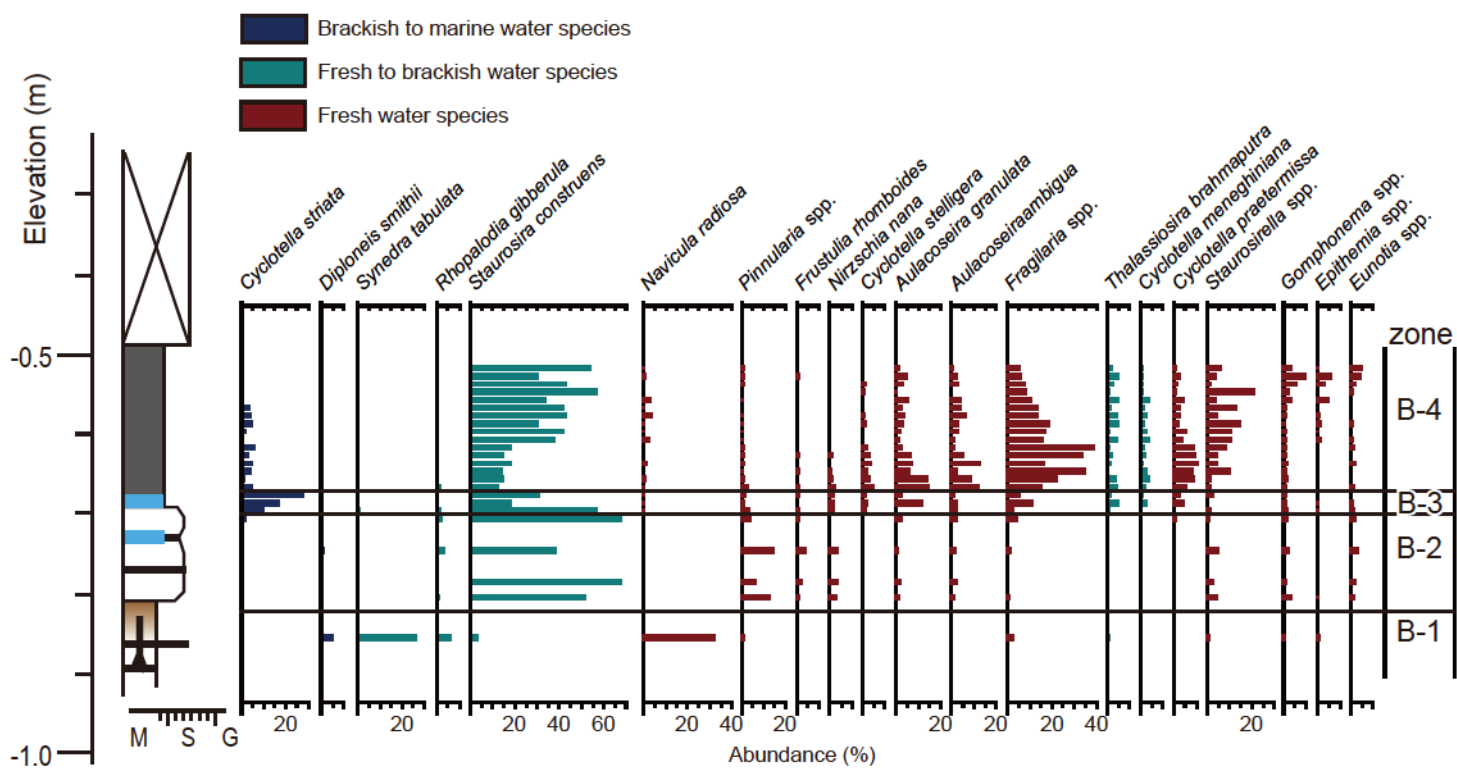


Fig. 5-4. Diatom assemblage diagram of the Site B in the inter-ridge marsh between BR III and IV.

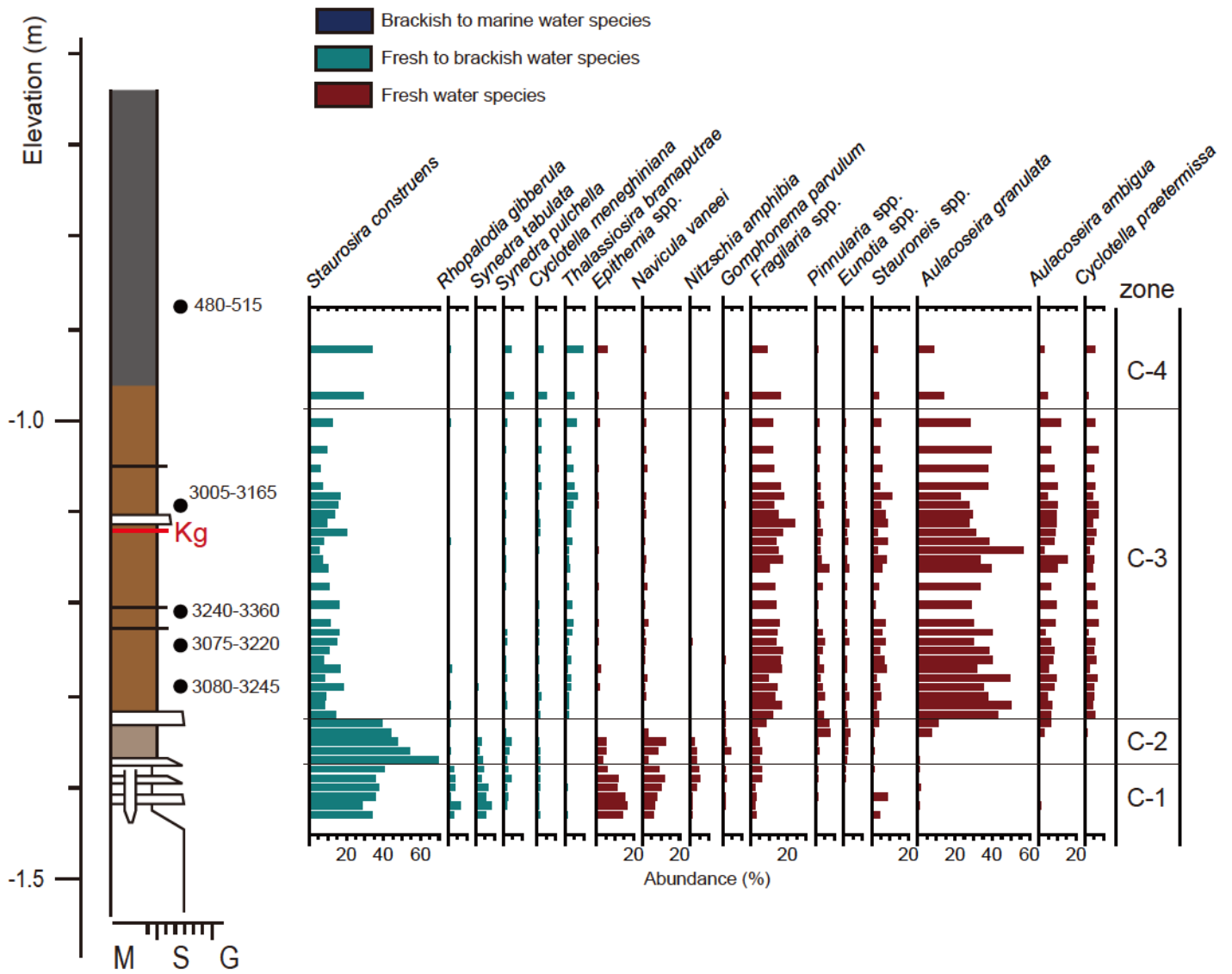


Fig. 5-5. Diatom assemblage diagram of the Site C in the inter-ridge marsh between BR III and IV.

CHAPTER VI

Synthesis for geomorphic developments of coastal sand barriers around the Lake Hamana during the middle to late Holocene

6-1. Paleo-geographical changes around the Lake Hamana

Middle to late Holocene paleo-geographic changes in and around the Lake Hamana and the western Hamamatsu Strand Plain were reconstructed in Chapter III, IV and V (Fig. 6-1). Inferred from reconstructed paleo-environmental changes, the author divided the geomorphic developments of coastal sand barriers into following five stages; Stage I (ca. 6500 cal BP); Stage II (ca. 5000 - ca. 6500 cal BP); Stage III (ca. 4500 - ca. 5000 cal BP); Stage IV (ca. 3200 - ca. 4500 cal BP); and Stage V (after ca. 3200 cal BP). Paleo-geographical maps of each stage were shown Fig.6-2.

6-1-1. Stage I (ca. 6500 cal BP)

Around the Lake Hamana, marine area expanded associated with sea-level rise during the Jomon Transgression along the incised valleys formed in the Last Glacial Maximum (Fig. 6-1). In coastal alluvial lowlands such as the Rokkengawa, Higashi-Kandagawa and Shinjo Lowlands, inner bays and/or tidal flats were formed at least before this period as mentioned in Chapter IV. In addition, marine area of the Miyakodagawa Lowland was largest in ca. 6800 cal BP, and the coastal line moved seaward after then.

Although the lake bed core in the Lake Hamana used in the present study did not reach Stage I, previous studies such as Saito (1988) and Matsubara (2001) discussed paleo-environment in

this period using lakebed cores extending to Stage I. Saito (1988) suggested brackish to marine lagoon, characterized by seawater and sediments inflow from tidal inlets, had occurred at least before Stage I based on sedimentological analysis and radiocarbon ages. In addition, Matsubara (2001) also suggested large amount of seawater inflow into the Lake Hamana during Stage I based on foraminiferal assemblages. The coastal sand barrier in the southern part of the Lake Hamana started to develop since ca. 9000 ^{14}C yr BP (Saito 1988), which led upward accumulation of sandy deposit and resulted in development of BR I at least before ca. 7000 cal BP (Matsubara, 2001).

Thus, the author suggests that dominance of diatom indicator species of inner bay environment probably indicates developing of the BR I and obstructing the alluvial lowlands and bays at the back of BRs (Fig. 6-2A). Note that the BR I was not enough developed to shut down water exchange between the Lake Hamana and the open ocean, the Enshu-nada Coast, inferred from the high percentage of brackish to marine water diatom species.

6-1-2. Stage II (from ca. 5000 to ca. 6500 cal BP)

During Stage II between ca. 5000 to ca. 6500 cal BP, fresh water ponds or marshes were formed temporarily in the alluvial lowlands such as Rokkengawa, Higashi-Kandagawa and Shinjo Lowlands. Temporal concentration of the formation of fresh water environments probably indicates that the BR I had developed much rather than those of Stage I and resulted in obstructing the lowlands strongly from the open ocean (Fig. 6-1). On the other hand, lacustrine environment during Stage II was an inner bay or brackish lagoon with continuous inflow of seawater according to previous studies such as Saito (1988), Kashima (1988), Morita *et al.* (1998), Matsubara (2000 and

2001).

These results suggest that coastal sand barriers had developed and temporarily emerged above sea-level along the southern margin of the Pleistocene terraces (Fig. 6-2B). Geomorphological arrangement of BRs implies that obstruction of alluvial lowlands was mainly caused by developed BR I. Because Matsubara (2004), however, reported that fresh water marsh was formed in ca. 6000 ¹⁴C yr BP in the inter-ridge marsh between the BR I and II, there are possibility that the BR II had already been formed until Stage II. Inferred from temporal formation of fresh water environment, these BRs were presumably not enough developed yet to shut down seawater inflow.

6-1-3. Stage III (from ca. 4500 to ca. 5000 cal BP)

Environmental changes from inner bays and tidal flats to fresh water ponds and/or marshes were estimated ca. 5000 cal BP in Higashi-Kandagawa and Shinjo Lowlands (Fig. 6-1). In Higashi-Kandagawa Lowland, major diatom species turnover was observed from brackish to marine water species to fresh water and fresh to brackish water species around 4900 cal BP, suggesting drastic salinity decline. Such turnover was also recognized in the Shinjo Lowland ca. 5150 cal BP, because thick peaty deposit including rich fresh water diatom fossils was formed since 5150 cal BP. In central part of the Lake Hamana, depositional facies and diatom assemblages in lake bed core showed stagnant inflow of seawater resulting in dysoxic environment associated with establishment of a closed brackish pond in Stage III (Fig. 6-1). This scenario is supported by Saito (1988), which suggested accumulation rate reduction around 4500 cal BP (4000 ¹⁴C yr BP) due to reduced sediments supply from the Enshu-nada Coast.

These findings suggest that addition of the BR I, II and III leads shut down of seawater inflow into the Lake Hamana during Stage III (Fig. 6-2C). Matsubara (2001) suggested that emergence of the BR I caused this environmental change. However, Matsubara (2004) reported that environmental change to freshwater marshes in the inter-ridge marsh between the BR I and II until Stage III. Considering geomorphological arrangement of the BRs in the western Hamamatsu Strand Plain, the author presumed that this environmental change was caused by emergence of the BR II or III. Thus, it is not able to eliminate the potential for the BR II and/or BR III. Because a couple of hundred years gap of the freshening events between the alluvial lowlands and the Lake Hamana, it took greater than 500 years to close off the lake inlet by gradual development of the BR I, II and III.

6-1-4. Stage IV (from ca. 4500 to ca. 3200 cal BP)

No lamina sediment in the lake bed core from the Lake Hamana was found since 4500 cal BP, suggesting mitigation of closed environment of the Lake Hamana by BRs (Fig. 6-1). In particular, high percentage of diatom species indicating of outer bay, such as *Thalassiosira* sp., environment suggests vigorous inflow of seawater from the Enshu-nada Coast since ca. 3500 cal BP. Simultaneously, seawater invasion also occurred around the alluvial lowlands around the Lake Hamana inferred from environmental changes from inner bays/tidal flats to fresh water ponds/marshes in ca. 4400 cal BP in the Higashi-Kandagawa and in ca. 3800 cal BP in the Rokkengawa Lowlands respectively (Fig. 6-1). In the Miyakodagawa Lowland, brackish to marine water planktonic diatom species increased in ca. 3500 cal BP, which indicates sea-level rise. Salinity increased in the inter-ridges marshes such as the IRM I/II and III/IV in the western

Hamamatsu Strand Plain was around 3200 cal BP (Fig. 6-1).

Therefore, obstruction by the BR I to III which had formed after ca. 5000 cal BP became weaker resulting in seawater inflow again (Fig. 6-2D). The factor of this environmental change is possibly considered morphological change including opening tidal inlets and/or sea-level rising relatively based on environmental change in the Miyakodagawa Lowland. These seemed to have induced invasion of marine water and tidal current until the inner bay and alluvial lowlands.

6-1-5. Stage V (since 3200 cal BP)

Fresh water ponds and marshes occurred in the Lake Hamana and alluvial lowlands around it (the Rokkengawa Lowland, the Higashi-Kamdagawa Lowland and the western Hamamatsu Strand Plain) since 3200 cal BP before Kg tephra falling in 3125-3146 cal BP (Fig. 6-1). In the Miyakodagawa Lowland, environmental change from inner bay to a fresh water marsh occurred in ca. 3500 cal BP. Since the freshening events, thick peat sediments were accumulated in the Rokkengawa, Higashi-Kamdagawa and Miyakodagawa Lowlands and no evidence for seawater intrusion. On the other hand, inner bay environments were maintained in the Lake Hamana after the Kg tephra falling until ca. 2250 cal BP (Fig. 6-1). A fresh water lake was established in ca. 2250 cal BP in the central part of the Lake Hamana.

Formation of fresh water lake, ponds and marshes during Stage IV suggested that the BRs developed and closed the Lake Hamana and alluvial lowlands. Because fresh water ponds/marshes in the inter-ridges marsh between the BR III and BR IV were formed during Stage V, development of the BR IV played a principal role in closing the lake and alluvial lowlands (Fig. 6-2E).

6-2. Geomorphic development trends of the Holocene coastal sand barriers

6-2-1. General trends of geomorphic development trend in ca. 3200 cal BP

Geomorphic development of coastal sand barriers around the Lake Hamana and in western Hamamatsu Strand Plain during the middle to late Holocene was generally categorized into two periods, one was transient period between ca. 6500 to ca. 3200 cal BP and the other was stable period since ca. 3200 cal BP.

The geomorphic developing process of coastal sand barriers between ca. 6500 and ca. 3200 cal BP was characterized by transient fresh water conditions (ponds and/or marshes) intermitted repeated intrusion of seawater to form inner bays or tidal flats (Fig. 6-3A). On the other hand, in the central part of the Lake Hamana, a closed inner bay environment was established during ca. 4500 to 4600 cal BP, after ca. 4500 cal BP seawater flowed again. Such repeated freshening and seawater intrusion were also found in the drowned lowlands around the Lake Hamana. In Rokkengawa Lowland, fresh water ponds/marshes were formed between ca. 3800 and ca. 4200 cal BP. In addition to this, temporal salinity reduction of water occurred at least before 4200 cal BP. In Higashi-Kandagawa Lowland, fresh water ponds/marshes were formed in ca. 5700 cal BP and between ca. 5000 cal BP and ca. 4300 cal BP. In Shinjo Lowland, fresh water ponds/marshes appeared in ca. 6500, ca. 5750 and ca. 5150 cal BP. These freshening events except for 5150 cal BP in the Shinjo Lowland were temporal events. In Miyakodagawa Lowland and the inter-ridges marshes in the western Hamamatsu Strand Plain, temporal salinity increases were observed in ca. 3200 cal BP.

Since ca. 3200 cal BP, on contrast, stable fresh water ponds or marshes developed around the Lake Hamana (Fig. 6-3B). Formations of fresh water ponds/marshes were observed in the Higashi-Kandagawa Lowland and the inter-ridges marshes in the western Hamamatsu Strand Plain. Although the timings were older, similar environmental changes were also found in Rokkengawa Lowland (ca. 3400 cal BP) and Miyakodagawa Lowland (ca. 3500 cal BP). All of these alluvial lowlands had developed thick peaty sediments deposited at fresh water conditions, indicating establishment of stable fresh water ponds and/or marshes. Lacustrine environment showed gradually salinity decline since ca. 2650 cal BP, and fresh water lake was formed in ca. 2250 cal BP. Although there is possibility that salinity increased once temporarily during ca. 2250 cal BP to the Meio earthquake in 1498 AD, continuous dominance of fresh water diatom species in the lake bed sediments indicates that the Lake Hamana had been fresh water environment from ca. 3200 cal BP to 1498 AD .

6-2-2. Trigger of short-term seawater intrusion

In the Lake Hamana and western Hamamatsu Strand Plain, repeatedly appearance of fresh water environment (ponds and/or marshes) and brackish to marine environment (inner bays and/or tidal flats) were recognized between ca. 3200 and ca. 6500 cal BP. These short-term events, which occurred in the interval of several hundred years, suggest that the BRs were not developed enough to close the Lake Hamana and the alluvial lowlands thoroughly. The BRs probably were often destroyed resulting in seawater intrusion again.

The author presents two reasons for the short-term environmental changes caused by co-seismic subsidence or tsunami events. Firstly, intervals of environmental changes were

estimated to be around 500 to 1000 years, which were much shorter than the ordinary fluctuation pattern of the relative sea-level curve in the Late Holocene in Japan (Ota *et al.*, 1990; Harima-nada Coast: Sato, 2008; Ise Bay: Umitsu, 1992; lower Yahagigawa Lowland: Sato and Masuda, 2010; Kanto Plain: Endo *et al.*, 1989 and Tanabe and Ishihara, 2013). Secondly, co-seismic subsidence had occurred at the interval of 100 to several hundred years around the study area (see Chapter II, 2-2-2). These intervals were comparable to those of short-term environmental changes. Abrupt subsidence associated with earthquakes likely led to relative sea-level rise and made saltwater wedges to invade landward along the coast easily.

Such freshening and seawater intrusion events have already been reported in western coast of the North America, for example coastal area along the Cascadia subduction zone and Alaskan Coast (Darienzo and Peterson, 1990; Hemphill-Haley, 1995; Guilbault *et al.*, 1995; Guilbault *et al.*, 1996; Nelson *et al.*, 1996; Shennan and Hamilton, 2006). Nelson *et al.* (1996) proposed five evidence for identifying co-seismic events from sediments in the case of co-seismic subsidence area, i. e., Suddenness of submergence, Amount of submergence, Lateral extent of peat-mud contacts, Tsunami concurrent with submergence and Synchronicity of submergence. These previous studies reconstructed paleo-elevation curves around lowlands for identifying co-seismic events by using statistical method on results of paleontological analyses. Thus, not only paleo-environmental data showed in the present study, it is important for evaluating affection of co-seismic events to but also reconstruct paleo-elevation around the Lake Hamana and western Hamamatsu Strand Plain by the same statistical method.

6-2-3. Controlling factors for geomorphic developing trends shift in ca. 3200 cal BP Stable and

continuous fresh water environment had established in and around the Lake Hamana since ca. 3200 cal BP, which was directly related to development of the BR IV. Therefore, continuous fresh water environment since ca. 3200 cal BP indicates that the BR IV developed more robustly than the former BRs (I to III) leading static seawater inflow.

Formation of fresh water ponds and marshes in ca. 3200 cal BP had been reported in other alluvial lowlands nearby the study area. For example, in the Seishin Plain located at ~75 km northeastern from the study area, thick peaty deposit distributed involving the Kg tephra layer (3126-3145 cal BP; Machida and Arai, 2003), which indicates stable fresh water marshes were formed before the Kg event (Shimada, 2000). And, in the lower Yahagigawa Lowland located at ~50 km eastward of the Lake Hamana, Kawase (1998) reported that fresh water marshes was formed abruptly between ca. 2500 and 3000 ^{14}C yr BP (2700-3200 cal BP) associated with emergence of deltaic topset flats. In the Kikugawa Lowland located at approximately 40 km westward of the Lake Hamana, peaty sediments started to deposit after 3000 - 3500 ^{14}C yr BP (around 3200 – 3700 cal BP) in the backmarsh of coastal sand barriers (Kashima, 1985). Therefore, timing of these freshening events in ca. 3200 cal BP were almost simultaneous in other areas, which implied that these environmental change was caused related to large-scale factors.

If amount of seismic displacement and tectonic trends around the Lake Hamana were approximately constant during the middle to late Holocene, formation of stable fresh water environments indicated that affection of seismic movement, caused short-term events, since ca. 3200 cal BP became relatively smaller than before. Currently, there is no previous study reported changing of seismic activity in Enshu-nada Coastal area in the middle to late Holocene. In the Omaezaki area located around 50 km eastward of the study area, detail discussion about

geomorphological development of the Holocene marine terraces associated with seismic movement were performed by Azuma *et al.* (2005) and Fujiwara *et al.* (2010). As the result, the seismic activity was presumed to be approximately constant through the middle to late Holocene. Therefore, following discussion is conducted on the assumption that seismic movement had been constant in the middle to late Holocene.

At present, westward coastal current is dominant along the Enshu-nada coast at the western coast from the Tenryugawa River (Aoki *et al.*, 2003). The Tenryugawa River has largest drainage basin area in the Enshu-nada Coast and presumably to be main supplier for sandy sediment to the coastal area. This is supported by present sediment transporting properties (Hattori *et al.*, 2001; Sato, 2008). Because a series of the BRs is arranged in the parallel along the coast and continuously distributed until the lower Tenryugawa Lowland, most of sediments composing the BRs are likely to be supplied from the Tenryugawa River.

Therefore, fluctuation of sediment supply of the Tenryugawa River is important factor to form BRs along the Enshu-nada Coast. The Holocene stratigraphy and geomorphological development of the lower Tenryugawa Lowland have previously been discussed by Kobayashi (1964), Kadomura (1971) and Nagasawa and Hori (2009). According to these previous studies, the lowland deposits of the lower Tenryugawa Lowland are composed by coarse deposits mainly such as sand and sandy gravels. In addition, muddy lagoon deposits are recognized at the approximately 9 km landward from the present coast line wedging among the sand and sandy gravels (Nagasawa and Hori, 2009). However, detail environmental change including transition of sediment supply of the Tenryugawa River during the middle to late Holocene has not been revealed yet. Sato and Masuda (2010) reported that r and poor-sorted sediments discharge increased in ca. 3000 cal BP in

the lower Yahagigawa Lowland, which drainage basin is neighbor that of the Tenryugawa River. In addition, Kawase (1998) suggested that drastic emergence of deltaic topset flats was caused by relative sea-level falling and increased delta front deposits in ca. 2500 - 3000 ¹⁴C yr BP (2700 - 3200 cal BP). Considering these events, the author suggests a possibility that increased sediment supply also occurred in the Tenryugawa River leading developments of the BRs along the Enshu-nada Coast since 3200 cal BP.

Timing of geomorphic trend change in ca. 3200 cal BP is synchronous to the onset of “the Yayoi Regression Period” during 2000 – 3000 ¹⁴C yr BP (Iseki, 1983; Ota *et al.*, 1990). Previous studies clarified that relative sea-level falling and riverine sediment supply increasing commonly occurred in this period in Japanese islands (Kawase, 1998; Ono, 2004; Ono, 2006; Tanabe and Ishihara, 2013). In addition, numbers of coastal sand barriers had been well developed and emerged in this period, e. g. Hokkaido Island (Ohira, 1995), Kujukuri Strand Plain (Moriwaki, 1979) and around the Suruga Bay (Matsubara, 1989; Matsubara, 2000). Geomorphic development processes clarified in this thesis is might associated with the Yoyoi Regression event.

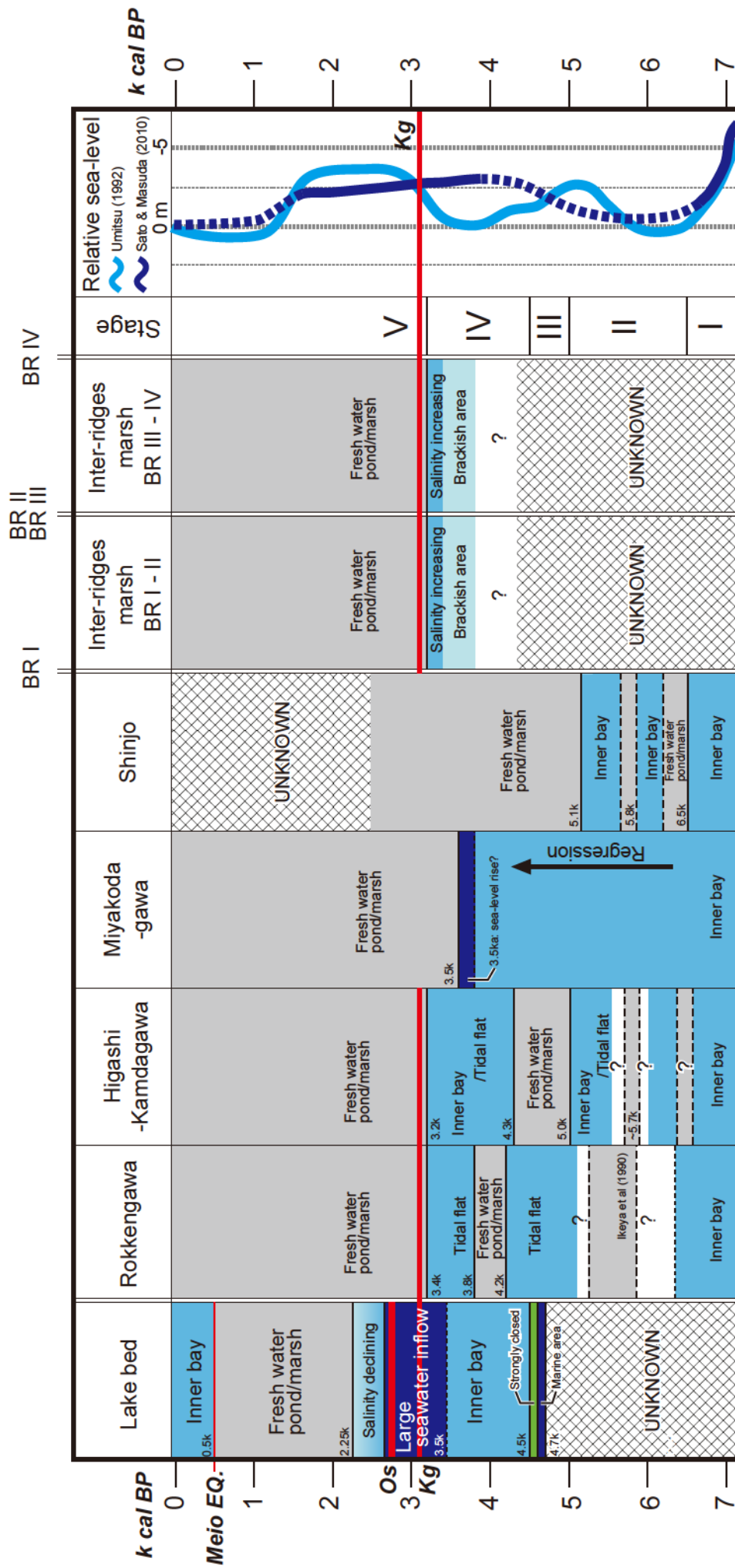


Fig. 6-1. Summary of the reconstructed middle to late Holocene environmental change around the Lake Hamana in the present study. Paleo-environmental changes in the central part of the lake based on results of diatom analysis of the lake bed core (HMT08-7) were shown in the chapter III. Environmental change in the alluvial lowlands around the Ise Bay and the lower Yahagigawa Lowland are referred from Umitsu (1992) and Sato and Masuda (2010) respectively.

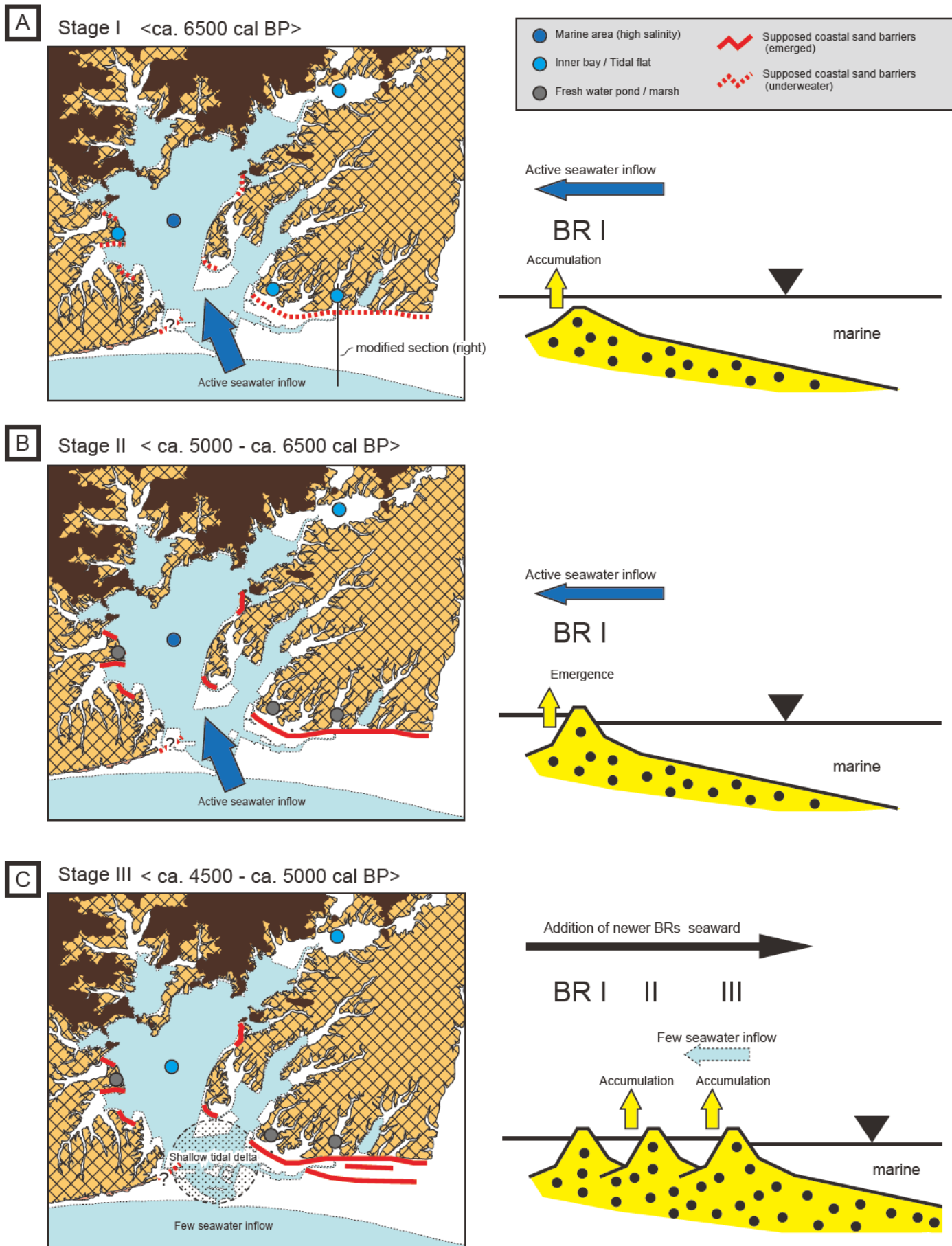
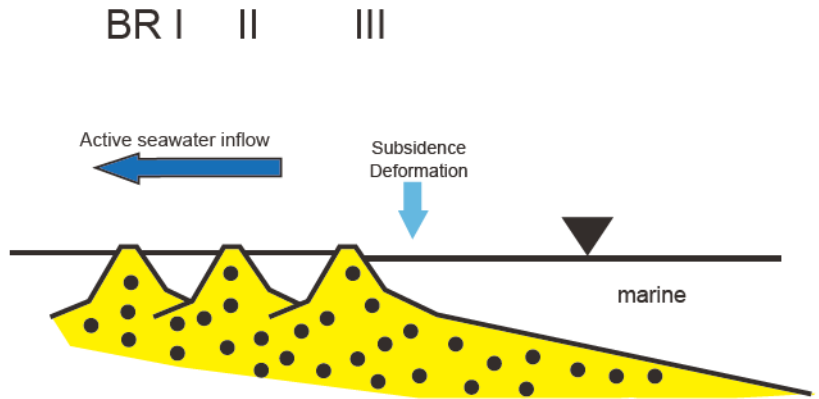
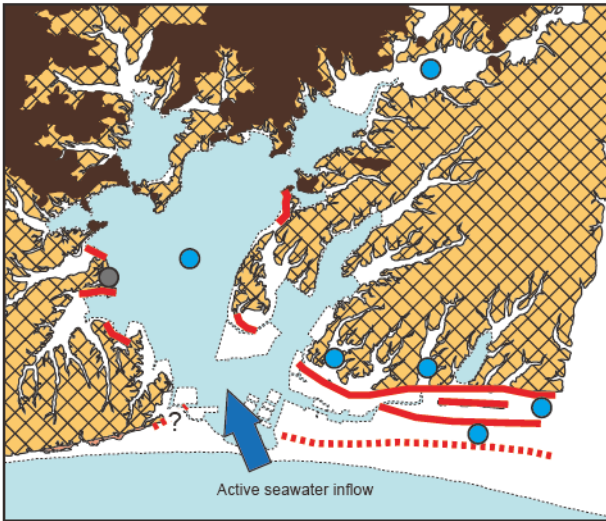


Fig.6-2. Paleo-geographic map around the Lake Hamana were reconstructed at total five stages since ca. 6500cal BP based on paleo-environmental changes in the central part of the lake and the alluvial lowlands. A: ca. 6500 cal BP, B: ca. 5000 to ca. 6500 cal BP, C: ca. 4600 to ca. 5000 cal BP, D: ca. 4500 to ca. 3200 cal BP, E: since 3200 cal BP.

D

Stage IV < ca. 3200 - ca. 4500 cal BP>



E

Stage V < since ca. 3200 cal BP>

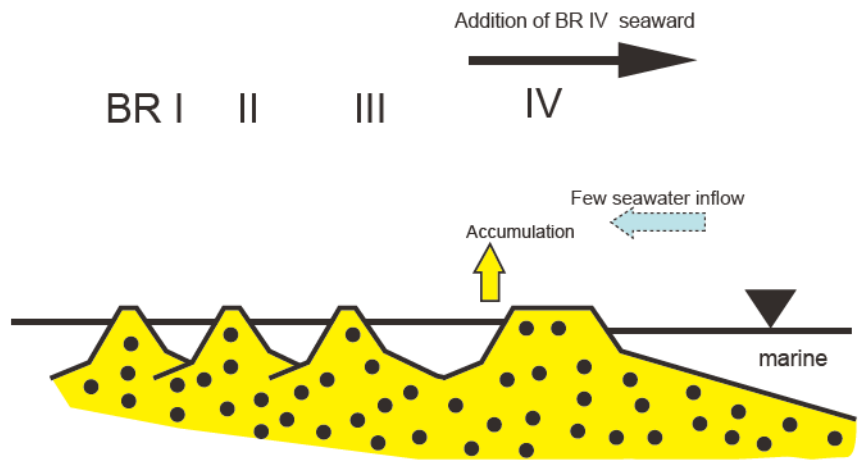
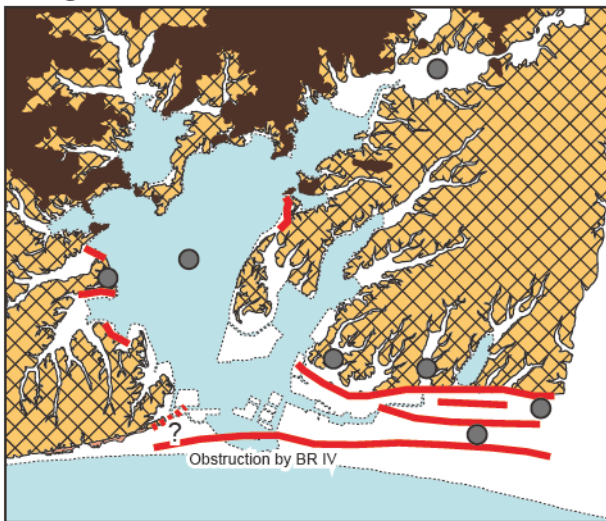
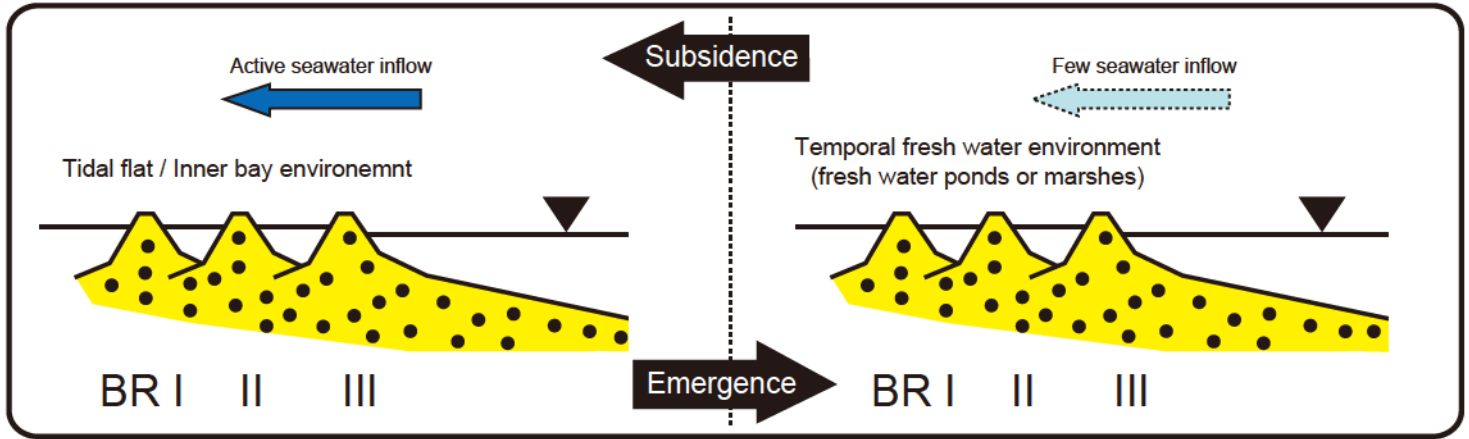


Fig. 6-2. (continued)

< ca. 3200 - ca. 6500 cal BP> Sandy deposits accumulation = Sismic activity



< since ca. 3200 cal BP> Sandy deposits accumulation > Sismic activity

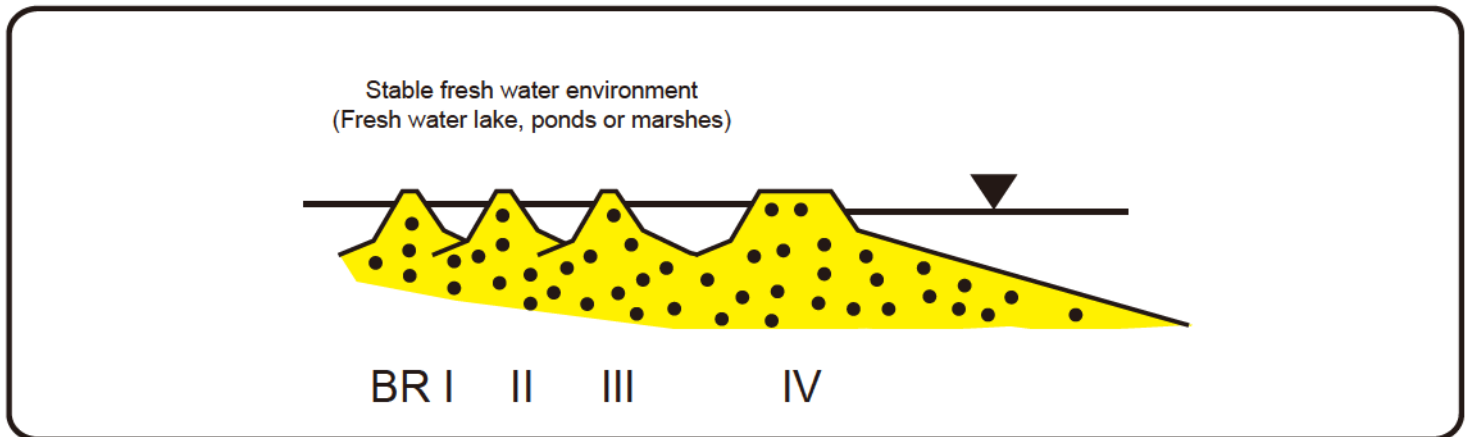


Fig. 6-3. The middle to late Holocene coastal sand barriers evolution processes around the Lake Hamana.

A: From ca. 6500 to ca. 3200 cal BP; B: since ca. 3200 cal BP.

Reference

- Ando, K. 1990. Environmental Indicators Based on Freshwater Diatom Assemblages and Its Application to Reconstruction of Paleo-environments. *Ann. Tohoku Geogr. Assoc.*: **42**, 73-88. (in Japanese with English abstract)
- Aoki, S. Kato, H. Uta, T. and Okuma H. 2003. Validation of westward floating sand developing in the western coast from Tenryugawa River and coastal line movements by them*. *Proceedings of Coastal Engineering, JSCE.*: **50**, 571-575. (in Japanese)
- Azuma, T., Ota, Y., Ishikawa, M. and Taniguchi, K. 2005. Late Quaternary Coastal Tectonics and Development of Marine Terraces in Omaezaki, Pacific Coast of Central Japan. *The Quaternary Research (Daiyonki-kenkyu)*: **44-3**, 169-176. (in Japanese with English abstract)
- Bond, G. Kromer, B., Beer, J., Muscheler, R., Evans, M. N., Showers, W., Hoffmann, S., Lotti-Bond, R., Hajdas, I. and Bonani, G. 2001. Persistent Solar Influence on North Atlantic Climate during the Holocene. *Science*: **294**, 2130-2136.
- Coastal Movements Data Center. 2013. crustal deformation estimated from tidal gauge of Japanese tidal stations. <http://cais.gsi.go.jp/cmdc/center/katoutumura.html> cited in August, 28th, 2013. (in Japanese)
- Darrienzo, M. E. and Peterson, C. D. 1990. Episodic Tectonic Subsidence of Late Holocene Salt Marshes, Northern Oregon Central Cascadia Margin. *Tectonics*: **9-1**, 1-22.
- Endo, K., Kosugi, M., Matsusita, M., Miyaji, N., Hishida, R. and Takano, T. 1989. Holocene Environmental History in and around the Paleo-Nagareyama Bay, Central Kanto Plain. *The Quaternary Research (Daiyonki-kenkyu)*: **28-2**, 61-77. (in Japanese with English abstract)

- Fujiwara, O., Hirakawa, K., Irizuki, T., Kamataki, T., Uchida, J., Abe, K., Hasegawa, S., Takada, K. and Haraguchi, T. 2006a. Progradation of Tateyama strand plain system, SW coast of Boso Peninsula, central Japan, triggered by coseismic uplifts during the historical Kanto earthquakes. *The Quaternary Research (Daiyonki-kenkyu)*: **45-3**, 235-247. (in Japanese with English abstract)
- Fujiwara, O., Komatsubara, J., Takada, K., Shishikura, M. and Kamataki, T. 2006b. Temporal development of a Late Holocene strand plain system in the Shirasuka area along Western Shizuoka Prefecture on the Pacific coast of Central Japan. *Journal of Geography (Chigaku-zasshi)*: **115-5**, 569-581. (in Japanese with English abstract)
- Fujiwara, O., Hirakawa, K., Irizuki, T., Hasegawa, S., Hase, Y., Uchida, J. and Abe K. 2010. Millennium-scale recurrent uplift inferred from beach deposits bordering the eastern Nankai Trough, Omaezaki area, central Japan. *Island Arc*: **19**, 374–388.
- Fujiwara, O. and Sato, Y. 2012. Tsunami deposits from the Takatsuka-ike, western Hamamatsu plain, Shizuoka Prefecture (a preliminary report). Meeting of the Seismological society of Japan, P2-40. (in Japanese)
- Fujiwara, O., Sato, Y., Ono, E. and Umitsu, M. 2013. Researches on Tsunami Deposits Using Sediment Cores: 3.4ka Tsunami Deposit in the Rokken-gawa Lowland near Lake Hamana, Pacific Coast of Central Japan. *Journal of Geography (Chigaku Zasshi)*: **122-2**, 308-322. (in Japanese with English abstract)
- Fujiwara, O., Ono, E., Yata, T., Umitsu, M., Sato, Y. and Heyvaert, V. M. A. Assessing the impact of 1498 Meio earthquake and tsunami along the Enshu-nada coast, central Japan using coastal geology. *Quaternary International: in Press*.

- Furusawa, A. 1995. Identification of tephra based on statistical analysis of refractive index and morphological classification of volcanic glass shards. *Jour. Geol. Soc. Japan*: **101-2**, 123-133. (in Japanese with English abstract)
- Goy, J. L. Zazo, C. and Dabrio, C. J. 2003. A beach-
- , Western Mediterranean). *Geomorphology*: **50**, 251-268.
- Guilbault, J. P., Clague J. J. and Lapointe, M. 1995. Amount of subsidence during a late Holocene earthquake –evidence from fossil tidal marsh foraminifera at Vancouver Island, west coast of Canada. *Paleogeography, Paleoclimatology, Paleoecology*: **118**, 49-71.
- Guilbault, J. P., Clague J. J. and Lapointe, M. 1996. Foraminiferal Evidence for The Amount of Coseismic Subsidence During a Late Holocene Earthquake on Vancouver Island, West Coast of Canada. *Quaternary Science Review*: **15**, 913-937.
- Habe, T. 1977. Systematics of Mollusca in Japan, Bivalvia and Scaphopoda. Hokuryukan, Tokyo. 373p. (in Japanese)
- Hattori, C. Sakao, T. Terada, T. Katano, A. and Kuroki, K. 2001. Widely sediment budget around the coastal area of Enshu and Suruga region. *Proceedings of Coastal Engineering, JSCE.*: **48**, 611-615. (in Japanese)
- Hemphill-Haley E. 1995. Diatom evidence for earthquake-induced subsidence and tsunami 300 yr ago in southern coastal Washington. *Geological Society of America Bulletin*: **107-3**, 367-378.
- Hiroki, Y. and Kimiya, K. 1990. The development of barrier-island and strand-plain systems with the glacio-eustatic sea-level change in the Pleistocene Atsumi Group, central Japan. *Jour. Geol. Soc. Japan*: **96-10**, 805-820. (in Japanese with English abstract)

- Honda, S. and Kashima, K. 1997. Paleo-environmental changes during the last 1,000 years from lake deposits at Lake Hamana, central Japan. *LAGUNA*: 4, 69-76. (in Japanese with English abstract).
- Hustedt, F. 1930a. Bacillariophyta (Diatomeae). in Die Süßwasser-Flora Mitteleuropas Heft 10 edited by Pacchers. A. Gustav Fischer.
- Hustedt, F. 1930b. Die Kieselalgen : Deutschlands, Osterreichs und der Schweiz unter Berücksichtigung der ubrigen Lander Europas sowie der angrenzenden Meeresgebiete. Dr. L. Rabenhorst's Kryptogamen-Flora von Deutschland, Osterreich und der Schweiz, VII Band, 1. Teil. (reprinted 1977). Otto Koeltz, Koenigstein, Germany. 920p.
- Hustedt, F. 1959. Die Kieselalgen : Deutschlands, Osterreichs und der Schweiz unter Berücksichtigung der ubrigen Lander Europas sowie der angrenzenden Meeresgebiete. Dr. L. Rabenhorst's Kryptogamen-Flora von Deutschland, Osterreich und der Schweiz, VII Band, 2. Teil. (reprinted 1977). Otto Koeltz, Koenigstein, Germany. 845p.
- Hustedt, F. 1961-1966. Die Kieselalgen : Deutschlands, Osterreichs und der Schweiz unter Berücksichtigung der ubrigen Lander Europas sowie der angrenzenden Meeresgebiete. Dr. L. Rabenhorst's Kryptogamen-Flora von Deutschland, Osterreich und der Schweiz, VII Band, 3. Teil. (reprinted 1977). Otto Koeltz, Koenigstein, Germany. 816p.
- Hustedt, F. 1977. Die Kieselalgen : Deutschlands, Osterreichs und der Schweiz unter Berücksichtigung der ubrigen Länder Europas sowie der angrenzenden Meeresgebiete. Teile 1, 2 und 3. Band VII. in Kryptogamen Flora Deutschland, Osterreich und der Schweiz. edited by L. Rabenhorst. Otto Koeltz, Koenigstein, Germany.
- Ikeya, N., Ohura, T., Akutsu, H. and Wada, H. 1985. A Report on Stratigraphy, Lithofacies and

- Geological Age of the Holocene Sediments along the East Coast of Hamana-ko. *Geosci. Rept. Shizuoka Univ.*: **11**, 171-179. (in Japanese with English abstract)
- Ikeya, N., Wada, H. and Ohmori, M. 1987. On the boring core sediments from Hamana Lake. *Geosci. Rept. Shizuoka Univ.*: **13**, 67-111. (in Japanese with English abstract)
- Ikeya, N., Wadam H., Akutsu, H. and Takahashi, M. 1990. A Report on Stratigraphy, Lithofacies and Geological Age of the Holocene Sediments along the East Coast of Hamana-ko. *Geosci. Repts. Shizuoka Univ.*: **11**, 171-179.
- Ikeya, N. 2000. Geological background of Lake Hamana*. *Journal of Geology on Shizuoka Prefecture**: **81**, 1-12. (in Japanese)
- Iseki, H. 1983. Alluvial Lowland *. University of Tokyo Press. 145p. (in Japanese)
- Ishibashi, K. 1984. Coseismic vertical crustal movements in the Suruga Bay region. *The Quaternary Research (Daiyonki-kenkyu)*: **23-2**, 105-110. (in Japanese with English abstract)
- Ishibashi, T., Suzuki, I., Liu, H., Takagawa, T. and Sato, S. 2009. Development Process of Hamamatsu Strand Plain Elucidated from Optically Stimulated Luminescence Dating using Feldspar. *Journal of JSCE, Division B: Hydraulic, Coastal and Environmental Engineering*: **B2-65**, 611-615. (in Japanese with English Abstract)
- Ishikawa, S., Fukumoto, Y., Sato, Y. and Kashima, K. 2011. An introduction of Diatom analysis. Kyushu University. 88p. (in Japanese)
- Isomi, H. and Inoue, M. 1972. Geology of the Hamamatsu District - Quadrangle series scale 1:50,000 Kyoto(11) No.59. Geological Survey of Japan. 40p. (in Japanese)
- Ito, A. 2003. Periods of beach ridge range formation on the Kitakami river lowlands and Late Holocene sea-level changes around Sendai bay, northeastern Japan. *Geographical Review of*

- Japan*: 76-7, 537-550. (in Japanese with English abstract).
- Ito, A. 2006. Marine regression during the historical time in Sendai coastal plain, northeastern Japan. *Bulletin of the Faculty of education, Kagoshima University, Natural science*: 57, 1-8. (in Japanese)
- Kadomura, H. 1971. Micro topography of alluvial fan and their developing processes –mainly gradual sloping fan in the Tokai-do district-*. Alluvial fan*. edited by Yazawa, D., Toya, H. and Kaiduka, S. Kokon Shoin: 55-96. (in Japanese)
- Kashima, K., Nagasawa, R. and Miyazaki, T. 1985. Data of Holocene Sea-level Change in Kikugawa-Plain, Shizuoka, Japan. *The Quaternary Research (Daiyonki-kenkyu)*: 24-1, 45-50. (in Japanese)
- Kashima, K. 1986. Holocene succession of Diatom fossil assemblages in alluvium, and those relation to paleogeographical changes. *Geographical Review of Japan*: 59A-7, 383-403. (in Japanese with English abstract)
- Kashima, K. 1988. Holocene paleo-environmental succession in Lake Hamana presumed by diatom analysis. *Jour. Res. Gr. Clas. Sed. Japan*: 5, 95-107.
- Kashima, K. 1992. Catalog of Holocene diatom fossil, part1, Tokoro Plain, Hokkaido, Noorth Japan. *Report on Earth Science, College of General Education, Kyushu University*: 29, 1-36. (in Japanese)
- Kashima, K. 2001. Salinity changes during the Late Holocenen at coastal brackish lakes in Japan. *LAGUNA*: 8, 1-14. (in Japanses with English abstract)
- Kato, T. and Tsumura, K. 1979. Vertical Land Movement in Japan as Deduced from Tidal Record, (1951-1978). *Bull. Earthq. Res. Inst.*: 54,559-628. (in Japanese with English abstract)

- Kawase, K. 1998. Late Holocene Paleoenvironmental Changes in the Yahagi River Lowlands, Central Japan. *Geographical Review of Japan*: **71A-6**, 411-435. (in Japanese with English abstract).
- Kawase, K. 2003. Geomorphic evolution of the coastal lowlands and changes in the sedimentary environment in the lower Kumozu river, Mie prefecture. *Geographical Review of Japan* **76-4**, 211-230. (in Japanese with English abstract).
- Kawase, K., et al., 2006. Japanese Diatoms Based on Electron Microscopy. Uchida Rokakuho Publishing, Tokyo (in Japanese).
- Kobayashi, K. 1964. Geology of Hamamatsu city: report of geological survey of Hamamatsu city *. 1-166. (in Japanese)
- Koike, K. and Machida, H. 2001. Atlas of quaternary marine terraces in the Japanese islands. 105p. University of Tokyo Press, Tokyo. (in Japanese)
- Kojima, N.1989. Dinoflagellate Cyst Analysis of Holocene Sediments from Lake Hamana in Central Japan. *Trans. Proc. Palaeont. Soc. Japan, N. S.*: **155**, 197-211.
- Kosugi, M. 1988. Classification of Living Diatom Assemblages as the Indicator of Environments, and Its Application to Reconstruction of Paleoenvironments. *The Quaternary Research (Daiyonki-kenkyu)*: **27-1**, 1-20. (in Japanese with English abstract)
- Kosugi, M., 1993. Diatom. In: Japan Association of Quaternary Research. A Handbook of Quaternary Research, vol. 2. University of Tokyo Press, Tokyo, pp. 245-252 (in Japanese).
- Krammer, K., Lange-Bertalot, H., 1986. Bacillariophyceae, 1. Teil: Naviculaceae. In: Ettl, H., Gerloff, J., Heynig, H., Mollenhauer, D. (Eds.), Süßwasserflora von Mitteleuropa, Band 2/1. Fischer Verlag, Stuttgart.

- Krammer, K., Lange-Bertalot, H., 1988. Bacillariophyceae, 2. Teil: Bacillariophyceae, Epithemiaceae, Surirellaceae. In: Ettl, H., Gerloff, J., Heynig, H., Mollenhauer, D. (Eds.), Süßwasserflora von Mitteleuropa, Band 2/2. Fischer Verlag, Stuttgart.
- Krammer, K., Lange-Bertalot, H., 1991a. Bacillariophyceae, 3. Teil: Centrales, Fragilariaceae, Eunotiaceae. In: Ettl, H., Gerloff, J., Heynig, H., Mollenhauer, D. (Eds.), Süßwasserflora von Mitteleuropa, Band 2/3. Fischer Verlag, Stuttgart.
- Krammer, K., Lange-Bertalot, H., 1991b. Bacillariophyceae, 4. Teil: Achnantheaceae. In: Ettl, H., Gartner, G., Gerloff, J., Heynig, H., Mollenhauer, D. (Eds.), Süßwasserflora von Mitteleuropa, Band 2/4. Fischer Verlag, Stuttgart.
- Machida, H. and Arai, F. 2003. Atlas of Tephra in and around Japan. University of Tokyo Press. 337p. (in Japanese)
- Masuda, F. 1998. Dynamic Stratigraphy Based on Highly Dense Data of 14C Ages in the Holocene. *Journal of Geography (Chigaku Zasshi)*: **107-5**, 713-727. (in Japanese with English Abstract)
- Masuda, F., Fujiwara, O., Sakai, T. and Araya, T. 2001. Relative Sea-level Changes and Co-seismic Uplifts Over Six Millennia, Preserved in Beach Deposits of the Kujukuri Strand Plain, Pacific Coast of the Boso Peninsula, Japan. *Journal of Geography (Chigaku Zasshi)*: **110-5**, 650-664. (in Japanese with English abstract)
- Matsubara, A. 1989. Geomorphic Development of Barriers in the Coastal Lowlands during the Holocene –a case study of the lowlands along the Suruga Bay, Central Japan-. *Geographical Review of Japan*: **62A-2**, 160-183. (in Japanese with English abstract).
- Matsubara, A. 2000. Holocene geomorphic development of coastal barriers in Japan. *Geographical Review of Japan*: **73A-5**, 409-434. (in Japanese with English abstract).

- Matsubara, A. 2001. Coastal barriers in Hamana Lake and the Hamamatsu lowland. *The Hiyoshi Review of Social Sciences, Keio University*: **11**, 20-32. (in Japanese)
- Matsubara, A. 2004. Sedimentary environment around archaeological sites in the Hamamatsu lowland. *The Hiyoshi Review of Social Sciences, Keio University*: **14**, 35-52. (in Japanese)
- Matsubara, A. 2005. Processes in Holocene development of coastal ridges in Japan. *The Hiyoshi Review of Social Sciences, Keio University*: **15**, 73-90.
- Matsubara, A. 2007. Relationships between geomorphic development of coastal ridges and human activities : a case study of the Hamamatsu and Haibara lowlands. *The Hiyoshi Review of Social Sciences, Keio University*: **18**, 1-13. (in Japanese)
- Matsumoto, H. 1984. Beach ridge ranges on Holocene coastal plains in Northeast Japan –the formative factors and periods-. *Geographical Review of Japan*: **57A-10**, 720-738. (in Japanese with English abstract).
- Mii, H. 1966. Evolution of coastal barriers in Japan during the Holocene. *The Quaternary Research (Daiyonki-kenkyu)*: **5-3-4**, 139-148. (in Japanese with English abstract)
- Morita, H., Kashima, K. and Takayasu, K. 1998. Paleoenvironmental changes of Lake Hamana and Lake Shinji during the Last 10,000 years, inferred by diatom assemblages from lake core sediments. *LAGUNA*: **5** 47-53. (in Japanese with English abstract).
- Moriwaki, H. 1979. The Landform Evolution of the Kujukuri Coastal Plain, Central Japan. *The Quaternary Research (Daiyonki-kenkyu)*: **18-1**, 1-16. (in Japanese with English abstract)
- Muto, T. 1987. Geology of the Mikatagahara and Iwabara Terraces, in the lower Tenryugawa River area, Japan –an interpretation from the present dissected alluvial fan-. *Jour. Geol. Soc. Japan*: **93-4**, 259-273.

- Mayewski, P. A., Rohling, E. E., Stager, J. C., Karlén, W., Maasch, K. A., Meeker, L. D., Meyerson, E. A., Gasse, F., van Kreveld, S., Holmgren, K., Lee-Thorp, J., Rosqvist, G., Rack, F., Staubwasser, M, Schneider, R. R. and Steig, E. J. 2004. Holocene climate variability. *Quaternary Research*: **62**, 243-255.
- Nagasawa, S. and Hori, K. 2009. Sedimentary Facies and Accumulation Rates of Core Sediments Obtained from the Tenryu River Alluvial Fan. (in Japanese with English abstract)
- Nakai, N., Ohishi, S. and Kuriyama, T. 1987. Application of ^{14}C -dating to sedimentary geology and climatology : Sea-level and climate change during the Holocene. *Nuc. Instr. Meth.*: **B29**, 228-231. (in Japanese with English Abstract)
- Nakajima, R., Mizuno, K. and Furusawa, A. 2008. Depositional age of the Middle Pleistocene Atsumi Group in Atsumi Peninsula, central Japan, based on tephra correlation. *Jour. Geol. Soc. Japan*: **114-2**, 70-79. (in Japanese with English abstract)
- Nelson, A. R., Shennan, I. and Long, A. J. 1996. Identifying coseismic subsidence in tidal-wetland stratigraphic sequences at the Cascadia subduction zone of western North America. *Journal of Geophysical Research*: **101**, 6115-6135.
- Ohira, A. 1995. Holocene Evolution of Peatland and Paleoenvironmental Changes in the Sarobetsu lowland, Hokkaido, Northern Japan. *Geographical Review of Japan*: **68A-10**, 695-712. (in Japanese with English abstract).
- Ohtsuka, K. and Kimiya, K. 1987. Paleolimnological environment and sedimentary processes of Hamana Lake, central Japan –Preliminary results of sedimentary facies analysis of the Lake floor boring samples-. *Geosci. Rept. Shizuoka Univ.*: **13**, 113-145. (in Japanese with English abstract)

- Okamura, M., Matsubara, H. and Furuno, H. 2009. Two-types seismic events recorded in Lake Hamana, Shizuoka Prefecture, Japan. *2009 JpGU meeting*, T225-P004. (English abstract)
- Okutani, T. 2000. Marine Mollusks in Japan. Tokai University Press, Tokyo. 1173p. (in Japanese)
- Ono, E. 2004. Factors Affecting Late Holocene Marine Regression in the Nobi Plain, Central Japan. *Geographical Review of Japan: 77-2*, 77-98. (in Japanese with English abstract).
- Ono, E., Ohira, A., Tanaka, K., Suzuki, I. and Yoshida, K. 2006. Late Holocene Landform Development and Change of Depositional Areas of Fluvial Sediment in the Central Echigo Plain, Central Japan. *The Quaternary Research (Daiyonki-kenkyu): 45-1*, 1-14. (in Japanese with English abstract)
- Ono, E. 2006. Study on geomorphological environment of Japanese coastal alluvial lowlands in the Late Holocene*. Doctoral thesis of Graduate School of Letters, Nagoya University. 141p. (in Japanese)
- Ota, Y., Matsushima, Y. and Umitsu, M. 1990. Recent Japanese research on relative sea level changes in the Holocene and related problems. Review of studies between 1980 and 1988.: Review of Studies between 1980 and 1988. *The Quaternary Research (Daiyonki-kenkyu): 29-1*, 31-48. (in Japanese with English abstract)
- Reimer, P. J., Baillie, M. G. L., Bard, E., Bayliss, A., Beck, J. W., Blackwell, P. G., Bronk Ramsay, C., Buck, C. E., Burr, G. S., Edwards, R. L., Friedrich, M., Grootes, P. M., Guilderson, T. P., Hajdas, I., Heaton, T. J., Hogg, A. G., Hughen, K. A., Kaiser, K. F., Kromer, B., McCormac, F. G., Manning, S. W., Reimer, R. W., Richards, D. A., Southon, J. R., Talamo, S., Turnery, C. S. M., van der Plicht, J. and Weyhenmeyer, C. E., 2009. IntCal09 and Marine09 radiocarbon age calibration curves, 0-50,000 years cal BP. *Radiocarbon*, **51**, 1111-1150.

- Sagiya, I. 2007. Crustal uplift in the western Shizuoka Prefecture associated with the 1944 Tonankai earthquake and a splay fault model. *JpGU* 2007, S151-006. (English abstract)
- Saito, Y. 1988 Barrier Systems as a Recorder of Holocene Sea-Level Changes and Problems on Reconstruction of their Paleogeography in the early Holocene: Example from Lake Hamana, Central Japan. *Jour. Res. Gr. Clas. Sed. Japan*: **5**, 109-132. (in Japanese with English Abstract)
- Saito, Y. 2007. Asian large river delta –affection of relative sea-level change and human activity- *. *JAQR*, Machida, H., Iwata, S. and Ono, A. (Eds.). *Quaternary Perspectives –T E ’ Present Status and Near Future-*. University of Tokyo Press. Tokyo. 55-79. 2007. (in Japanese)
- Sakakura, N. 2004. Sedimentological review of tidal environment : toward comprehension of tidal-flat environment in Japan(<Special Issue>Nature of tidal flats, its past and present). *Fossil (Kaseki)*: **76**, 48-62. (in Japanese with English abstract)
- Sato, H. 2008. Reconstruction of Holocene sea-level change along the coast of Harimanada in the eastern part of the Seto Inland Sea, western Japan. *The Quaternary Research (Daiyonki-kenkyu)*: **47-4**, 247-259. (in Japanese with English abstract)
- Sato, S. 2008. Dynamics of Sand Movement on Hamamatsu Coast Facing Enshuu-Nada. *Proceedings of Coastal Engineering, JSCE*:**B64-3**, 192-201. (in Japanese with English abstract)
- Sato, T. and Masuda, F. 2010. Temporal changes of a delta: Example from the Holocene Yahagi delta, central Japan. *Estuarine, Coastal and Shelf Science*: **86**, 415-428.
- Sato, Y., Fujiwara, O., Ono, E. and Umitsu, M. 2010a. Late Holocene environmental changes in the Rokken-gawa lowland near Lake Hamana, Pacific coast of central Japan. *JpGU* 2010, HQR010-P25. (English abstract)

- Sato, Y., Ishikawa, S., Shiomi, R., Go, Arum., Umitsu, M. and Kashima, K. 2010b. Transition of sedimentary Environment after the Middle Holocene of an alluvial lowland, Shinjo area, Kosai city, western coast of the Lake Hamana. *Proceedings of the General Meeting of the association of Japan Geographers*: **78**, 515. (Japanese abstract)
- Sato, Y., Fujiwara, O. and Ono, E. 2013. Late Holocene environmental changes of the inter-ridge marshes in the western Hamamatsu strand plain. JpGU 2013, HQR24-P13. (English abstract)
- Shennan, I. and Hamilton, S. 2006. Coseismic and pre-seismic subsidence associated with great earthquakes in Alaska. *Quaternary Science Review*: **25**, 1-8.
- Shimada, S. 2000. Eruption of the Amagi-Kawagodaira Volcano and Paleo-environments in the Late and Latest Jomon Periods around the Izu Peninsula. *The Quaternary Research (Daiyonki-kenkyu)*: **39-2**, 151-164. (in Japanese with English abstract)
- Shishikura, M., Haraguchi, T. and Miyauchi, T. 2001. Timing and recurrence interval of the Taisho-type Kanto earthquake, analyzing Holocene emerged shoreline topography in the Iwai lowland, the southwestern part of the Boso Peninsula, central Japan. *Journal of the Seismological Society of Japan. 2nd ser.*: **53**, 357-372. (in Japanese with English abstract)
- Shishikura, M., Kamataki, T., Takada, K., Suzuki, K. and Okamura, Y. 2005. Survey report of emerged beach ridges in the southwestern part of Boso Peninsula –Timing of the Taisho-type Kanto earthquake-. *Annual Report on Active Fault and Paleoequake Researches*: **5**, 51-68. (in Japanese with English abstract)
- Shishikura, M., Echigo, T. and Kaneda, H. 2007. Marine reservoir correction for the Pacific coast of central Japan using ¹⁴C ages of marine mollusks uplifted during historical earthquakes. *Quaternary Research*: **67**, 286-291.

- Shizuoka Prefecture, 1996. History of Shizuoka Prefecture, Separated. In: History of Natural Disasters, vol.2. Shizuoka Prefecture. 131p. Shizuoka. (in Japanese)
- Stuiver, M., Reimer, P. J. and Reimer, R. W. 2011, CALIB 6.0. [http://intcal/qub.ac.uk/calib/](http://intcal.qub.ac.uk/calib/) cited in June 28th, 2013.
- Sugai, T. 2012. background of development of alluvial lowlands *. Umitsu, M (eds), Geo-environment of Alluvial and Coastal Lowlands. Kokon-Shoin Pub., 13-23. (in Japanese)
- Sugiyama, Y. 1991. The Middle Pleistocene deposits in the Atsumi Peninsula and along the east coast of Lake Hamana, Tokai district -sedimentary cycles formed by the glacio-eustatic sea-level change and their correlations to the contemporaneous deposits in the Kanto and Kinki districts-. *Bull. Geol. Surv. Japan*: **42-2**, 75-109. (in Japanese with English abstract)
- Tamura T., Murakami, F. and Watanabe, K. 2010. Holocene beach deposits for assessing coastal uplift of the northeastern Boso Peninsula, Pacific coast of Japan. *Quaternary Research*: **74**, 227-234.
- Tamura, T. 2012. Beach ridges and prograded beach deposits as paleoenvironment records. *Earth-Science Reviews*: **114**, 279-297.
- Tamura, T. and Masuda, F. 2004. Recent Studies on Wave-dominated Depositional Sequences Using the High-resolution ¹⁴C Dating Analysis: The Holocene in the Kujukuri and Sendai Coastal Plains, Eastern Japan. *Journal of Geography*: **113-1**, 1-17.
- Tanabe, S. and Ishihara, Y. 2013. Evolution of the Uppermost Alluvial in the Tokyo and Nakagawa Lowlands, Kanto Plain, Japan: A Case Study of the Yamanashi River. *Jour. Geol. Soc. Japan*: **119-5**, 350-367. (in Japanese with English Abstract)
- Umitsu, M., 1992. Holocene deltaic sequence in the Kiso River delta, Central Japan. *Journal of the*

Sedimentological Society of Japan **36**, 47–56. (in Japanese with English Abstract)

Umitsu, M. 1994. Late Quaternary Environment and Landform Evolution of Riverine Coastal Lowlands. Kokon-Shoin Pub., 270p. (in Japanese)

Urabe, A., Yoshida, M. and Takahama, N. 2006. Development process of barrier-lagoon system in the Holocene sediments of the Echigo Plain, central Japan. *Mem. Geol. Soc. Japan*: **59**, 111-127. (in Japanese with English Abstract)

Yamaguchi, M., Sugai, T., Fujiwara, O., Ohmori, H., Kamataki, T. and Sugiyama, Y. 2003. Depositional Process of the Holocene Nobi Plain, Central Japan, Reconstructed from Drilling Core Analysis. *Quaternary Research (Daiyonki-kenkyu)*: **42-5**, 335-346. (in Japanese with English Abstract)

Yata, T. 2005. The damages by tsunami in Meiou-Toukai earthquake in 1498 and the suffering in Anotsu in the Middle Ages. *Historical Earthquakes (Rekishi-Jishin)*: **20**, 9-12. (in Japanese with English abstract)

Yata, T. 2009. Large Earthquakes Occurred in Medieval Period Recorded in Japanese History. Yoshikawa-kobunkan, 222p. Tokyo. (in Japanese)

Yoneda, M., Uno, H., Shibata, Y., Suzuki, R., Kumamoto, Y., Yoshida, K., Sasaki, T., Suzuki, A. and Kawahata, H. 2007. Radiocarbon marine reservoir ages in the western Pacific estimated by pre-bomb molluscan shells. *Nuclear Instruments and Methods in Physics Research Section B*: **259**, 432-437.

* English translation from the original written in Japanese.

Acknowledgement

I sincerely appreciate my thesis advisory committee members including Associate Professor Kaoru Kashima, Associate Professor Yusuke Okazaki, Professor Tasuku Akagi, Professor Haruyoshi Maeda of Graduate School of Science, Kyushu University, and Dr. Osamu Fujiwara of Active Fault and Earthquake Research Center, National Institute of Advanced Industrial Science and Technology (AIST) for their constructive reviews and suggestions for improvement of the manuscript. I am deeply grateful to Associate Professor Kaoru Kashima for his continuous encouragement and useful advises. He provided me many opportunities for studying about diatom fossils and paleo-environmental researches, participating valuable investigation and meetings and writing papers.

I express my hearty appreciation to Professor Masatomo Umitsu of Nara University, Professor Noboru Hayashi of Chubu University, Professor Tsunetoshi Mizuguchi, Professor Yasuhiro Suzuki, Professor Kohei Okamoto, Professor Satoshi Yokoyama, Professor Makoto Takahashi and Associate Professor Keiichi Okunuki of Nagoya University for their fruitful leadings when I belonged to the Department of Geography of Nagoya University. I am also grateful to Dr. Satoshi Ishiguro (National Institute for Environmental Studies), Naoyuki Yukawa, Natsuko Hayashi (Informatix Co. Ltd.), Yuta Nakamura, Ryogo Takeuchi, Tomoya Abe, Yuji Ishii and Kazutaka Arakawa (graduates of Nagoya University), Dr. Ken'ichi Yasue and Dr. Ryosuke Doke (graduates of Toyama University) and Associate Professor Daisuke Hirouchi (Shinshu University) for their considerable helps for field surveys and numerous discussion about my study.

I am deeply grateful to Professor Masatomo Umitsu for giving me the first break to study

about physical geography including geomorphological development of alluvial lowlands. I also would like to express my hearty appreciation to Dr. Osamu Fujiwara of the AIST and Associate Professor Eisuke Ono of Niigata University for providing me numerous opportunities to investigate and analysis about the paleo-environmental and paleo-geographical changed in alluvial lowlands and fruitful core samples for diatom analyses. I would like to acknowledge Project Professor Makoto Okamura and Associate Professor Hiromi Matsuoka of Kochi University for giving me valuable chance to analysis about the lake bed core samples of the Lake Hamana. I owe my gratitude to local government of the Hamamatsu City and Private Companies, the Meisei Industrial *Co. Ltd.*, the Stanley Electric *Co. Ltd.* and the Nippon-Keical *Co. Ltd.*

I would like to express my gratitude to the members of the Paleo-environmental Science Laboratory at the Graduate School of Science of Kyushu University and then-members of the Department of Geography of Nagoya University for their assistance and numerous discussions in many phases. Especially, I thank Satoshi Ishikawa and Yu Fukumoto (graduate students of Kyushu University) and Liang-Chi Wang of National Taiwan University for teaching me technique of diatom analysis kindly. I owe my gratitude to Assistant Professor Shoichi Shimoyama for his useful advices and information about tephra analysis. I acknowledge Dr. Akihiko Matsukuma and Professor Kozo Takahashi of Hokusei Gakuen University for their constructive suggestions for my research. My appreciation goes to Ms's Tomoko Koga who have done substantial amount of office work for our laboratory.

This study was partially funded by Grant-in-Aid for JSPS Fellows to me: Research Project Number 11J03774. A part of this research was supported by Professor Tatsuro Matsumoto Scholarship Funds.

Finally, I deeply appreciate my family for their understanding of my research, encouragement and invaluable support for me.